6-6-2008

Novel Insights into PKG Activation and cGMP Signaling in Response to Nitric Oxide and Atrial Natriuretic Peptide in Vascular Smooth Muscle Cells

Lydia Nausch
University of Vermont

NOVEL INSIGHTS INTO PKG ACTIVATION AND cGMP SIGNALING IN RESPONSE TO NITRIC OXIDE AND ATRIAL NATRIURETIC PEPTIDE IN VASCULAR SMOOTH MUSCLE CELLS

A Dissertation Presented

by

Lydia Waltraud Maria Nausch

to

The Faculty of the Graduate College

of

The University of Vermont

In Partial Fulfillment of the Requirements
for the Degree of Doctor of Philosophy
Specializing in Pharmacology

February, 2008

Accepted by the Faculty of the Graduate College, The University of Vermont, in partial fulfillment of the requirements for the degree of Doctor of Philosophy, specializing in Pharmacology

Dissertation Examination Committee:

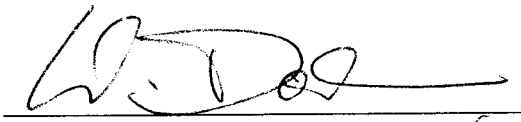

Wolfgang R. Dostmann, Ph.D — Advisor

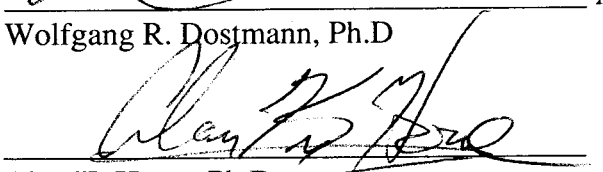

Alan K. Howe, Ph.D

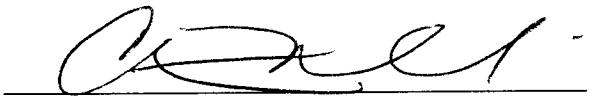

Anthony D. Morielli, Ph.D

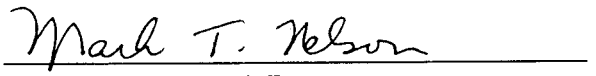

Mark T. Nelson, Ph.D

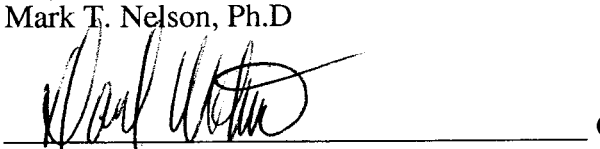

David M. Warshaw, Ph.D. — Chairperson

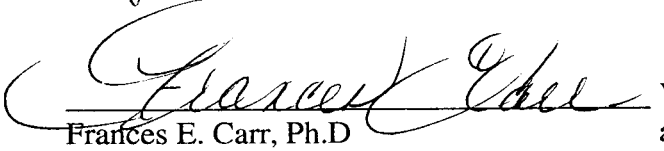

Frances E. Carr, Ph.D — Vice President for Research and Dean of Graduate Studies

Date: December 5th 2007

ABSTRACT

Cyclic 3',5'-guanosine monophosphate (cGMP) is a key signaling molecule involved in a myriad of physiological processes, including vascular smooth muscle (VSM) tone, water- and electrolyte homeostasis, platelet aggregation, airway smooth muscle tone, smooth muscle proliferation and bone formation. Increased occurrence of vascular disorders including erectile dysfunction, hypertension, stroke and coronary artery disease, have made it increasingly important to study the dynamic interplay between cGMP synthesis and hydrolysis in VSM cells. This dissertation examines the spatial distribution of intracellular cGMP, $[cGMP]_i$, in response to NO and atrial natriuretic peptide (ANP) in VSM cells. To investigate the spatial patterning of $[cGMP]_i$, we have developed a new generation of non-FRET (fluorescence resonance energy transfer) cGMP biosensors that are suitable to monitor $[cGMP]_i$ in response to physiological (low-nanomolar) NO and ANP concentrations and that qualify for real-time, confocal imaging techniques. We have termed these indicators FlincGs, for green fluorescent indicators of cGMP. For the development of FlincGs, we made use of the specific cGMP binding characteristics of PKG. We utilized site-specific mutagenesis, kinetic cGMP binding, dissociation and kinase assays, as well as crystallography, in order to investigate PKG activation and cGMP binding dynamics in greater detail. Based on these studies, our novel, non-FRET cGMP biosensors were designed by attaching cGMP binding fragments of PKG to the N-terminus of circular permutated green fluorescent protein. We applied FlincGs in cultured VSM cells as well as in intact tissue to determine whether two spatially distinct populations of guanlylyl cyclase (cytosolic versus membrane bound) underlie the generation of spatiotemporally-specific patterns of $[cGMP]_i$ formation.

CITATIONS

Material from this dissertation has been published in the following form:

Nausch LWM and Dostmann WR (2007). FlincGs: novel, non-FRET cGMP biosensors with nanomolar sensitivity for NO-induced signaling. BMC Pharmacology 7 (Suppl 1):S22.

Nausch LWM, Ledoux J, Bonev A, Nelson MT and Dostmann WR (2008). Differential patterning of cGMP in vascular smooth muscle cells revealed by single GFP-linked biosensors. Proceedings of the National Academy of Sciences. 105(1): 365-370.

Material from this dissertation is in preparation for submission to Biochemistry in the following form:

Nausch LWM, Yan X, Maier C, Nickl CK and Dostmann WR (2008). Cyclic nucleotide binding site mutations delineate the mechanism of cGMP-dependent protein kinase Iα activation.

ACKNOWLEDGEMENTS

First and foremost, I wish to express my deepest gratitude to my 'Doktorvater' (mentor) Dr. Wolfgang Dostmann, for his support, enthusiasm and encouragement has fostered my progression as a young scientist. His special sense of humor will be missed in particular. Furthermore, I would like to thank my colleague Christian Nickl for introducing me to some great techniques, such as protein expression in SF9-insect cells and biochemical kinase assays. To my fellow graduate students, Kara Held, Brent Osborne and Shiv Kumar Raidas, I extend my best wishes for their future careers. Make it magic! In particular, I am appreciative for the support, encouragement and guidance provided by the members of my Committee, Drs. Alan Howe, Tony Morielli, Mark Nelson and Dave Warshaw. They have given me the opportunity to learn from the best! In addition, I appreciate the contributions of Drs. Jonathan Ledoux, Adrian Bonev and Thomas Heppner, for they have made the confocal imaging experiments at the Andor and Noran possible. Furthermore, I would like to thank Dr. Steve Straub for fruitful scientific discussions and for proof-reading my dissertation. I owe much gratitude to Drs. Mark Nelson, Alan Howe and Christopher Berger for generously sharing their state-of-the-art imaging equipment, GFP antibodies and reagents, and stopped-flow instrumentation, respectively. The use of rat aortic smooth muscle cells has been made possible through generous tissue sharing of the Nelson, Brayden, Osol and Gokina laboratories.

Lastly, I would like to thank my family in Germany, especially my parents, who have been the best mentors and role models I could wish for. Special thanks also to my brothers Andreas and Markus, who have always kept me grounded. And last but not least,

I would like to thank my husband Bernhard for all his love, support and scientific advice throughout graduate school. He is truly one in a billion!

TABLE OF CONTENTS

LIST OF TABLES

CHAPTER ONE

CHAPTER TWO

CHAPTER FOUR

LIST OF FIGURES

CHAPTER ONE:

CHAPTER TWO:

CHAPTER THREE:

CHAPTER FOUR:

CHAPTER FIVE:

CHAPTER ONE: LITERATURE REVIEW

Introduction

Cyclic 3',5'-guanosine monophosphate (cGMP) regulates vital physiological processes through activation of cGMP-dependent protein kinases (PKGs), cyclic nucleotide gated ion channels and cGMP-specific phoshpodiesterases (PDEs) (Conti and Beavo, 2007; Francis et al., 2005; Hofmann, 2005; Hofmann et al., 2005), (Figure 1). cGMP synthesis is mediated either through soluble guanylyl cyclases (sGC) in response to nitric oxide (NO), or through particulate, membrane bound guanylyl cyclases (GC-A/B) in response to natriuretic peptides (ANP, BNP, CNP) (Kuhn, 2005). Intracellular cGMP concentration, $[cGMP]_i$, is kept in a dynamic balance through guanlylyl cyclases, that convert guanosine tri-phosphate (GTP) into cGMP and through cGMP-specific phosphodiesterases, that promote cGMP hydrolysis (Figure 2). cGMP binding to PKGs promotes phosphorylation of many downstream targets, thereby modulating a multitude of physiological processes.

(Atrial) Natriuretic Peptide production and release

Natriuretic peptides - atrial natriuretic peptide (ANP), B- and C-type natriuretic peptites (BNP, CNP) - are derived from arachidonic acid and share a common core structure consisting of a 17-member disulfide ring with a highly conserved internal sequence of (-FGXXXDRIGXXSGL-) (Kangawa and Matsuo, 1984; Sudoh et al., 1988; Sudoh et al., 1990). ANP and BNP are predominantly expressed in cardiac myocytes and act as antihypertensive and antihypervolemic factors through their actions on GC-A

expressed in peripheral tissues (such as VSM cells) and in the central nervous system. In contrast, CNP is mostly produced by vascular endothelial cells and has local effects on vascular regeneration (Komatsu et al., 1996; Tamura et al., 2004; Yamahara et al., 2003) and bone growth (Chusho et al., 2001) by binding to the specific membrane-bound guanylyl cyclase (GC) receptor GC-B (Garbers and Lowe, 1994). Most of our knowledge about the ANP/GC-A system in maintaining arterial blood pressure and blood volume has come from different genetic mouse models. Deletion of ANP or its receptor GC-A lead to arterial hypertension and cardiac hypertrophy (John et al., 1996; Kuhn et al., 2002; Lopez et al., 1995), whereas overexpression of ANP or GC-A lead to a decrease in arterial blood pressure (Oliver et al., 1998; Steinhelper et al., 1990).

Main triggers for the release of ANP from atrial secretory granules in cardiac myocytes are an increase in wall stretch, pressure and ischemia (de Bold et al., 1981; de Bold et al., 2001), but neurohumoral factors (glucocorticoids, catecholamines, arginine vasopressin, angiotensin II and endothelin) may also play a role (Ruskoaho, 1992) (Figure 3). Once in the bloodstream, ANP activates the GC-A receptor in peripheral tissues to increase $[cGMP]_i$ (Garbers and Lowe, 1994) (Figure 1) and thereby modulates blood pressure and blood volume in an endocrine fashion through vasorelaxation, diuresis and natriuresis.

Nitric Oxide synthesis and release

Besides natriuretic peptides, increasing concentrations of $[cGMP]_i$ are also mediated through the action of nitric oxide (NO) on soluble guanylyl cyclases (sGC) (Figure 1). In vascular endothelial cells, NO is produced by the endothelial nitric oxide synthase, eNOS (Palmer et al., 1988). Activation of eNOS occurs primarily through agonist-modulated increases in intracellular calcium, and binding of Ca^{2+}-calmodulin to eNOS (Figure 4). Endogenous ligands for G-protein coupled receptors that mobilize calcium and activate eNOS include acetylcholine (which signals via M_3 muscarinic receptors), histamine, adenosine, ATP/ADP, thrombin, and bradykinin (Moncada et al., 1991). Stimulation of NO-synthesis can also be initiated through shear stress (via mechanoreceptors) (Gudi et al., 1998), or through phosphorylation and de-nitrosylation of eNOS (via sphingosine 1-phosphate, VEGF or insulin) (Dimmeler et al., 1999; Erwin et al., 2005; Kou et al., 2002; Montagnani et al., 2001; Olivera and Spiegel, 1993). Catalytically active eNOS converts L-Arginine to NO and L-Citrulline. NO is then released and can freely diffuse into cells. NO has a short half-life of approximately 5 sec and is buffered in the blood stream through binding to the ferrous heme moiety of hemoglobin. The physiological effects of NO in the vasculature are mediated through increased $[cGMP]_i$ via sGC and include inhibition of leukocyte adhesion and platelet aggregation, suppression of smooth muscle cell proliferation and induction of vascular smooth muscle relaxation, leading to vasodilation (Hofmann, 2005).

Guanylyl cyclase mediated synthesis of $[cGMP]_i$

Guanine nucleotidyl (guanylyl) cyclases (GCs) are widely distributed signal-transduction enzymes that, in response to NO and natriuretic peptides, convert GTP into the second messenger cyclic GMP (Figure 2). The diffusible gas NO targets the heme containing enzyme soluble guanylyl cyclase (sGC), a protein ubiquitously expressed in mammalian cells. Studies from sGC-deficient mice have shown that NO-sGC signaling is essential for the maintenance of normal peristalsis in the gut, and for the regulation of blood pressure and vascular smooth muscle tone (Friebe et al., 2007; Mergia et al., 2006; Nimmegeers et al., 2007). sGC is a heterodimeric protein, consisting of a larger alpha-subunit and a smaller heme-binding beta-subunit (Figure 5). Four human sGC subunits exist: α_1, α_2, β_1 and β_2, of which the α_1/β_1 and α_2/β_1 heterodimers are best characterized (Mayer and Koesling, 2001; Zabel et al., 1998). The β-subunit contains a conserved amino-terminal heme-binding domain (Iyer et al., 2003; Pellicena et al., 2004), which is crucial for NO sensing. NO-induced activation of sGC depends on the presence of the reduced Fe^{2+} heme moiety (Ignarro et al., 1986). Binding of NO (10 to 100 nM; (Mo et al., 2004)) to the central ferrous iron of the prosthetic group induces conformational changes in the C-terminal catalytic domain, leading to a 400-fold increase in activity of sGC (Mayer and Koesling, 2001) and to conversion of GTP into cGMP and pyrophosphate (Figure 2). The catalytic domains of both subunits are required for the formation of a catalytically active center (Winger and Marletta, 2005). In recent years, Marletta and colleagues have reported a second NO binding site (Ballou et al., 2002; Cary et al., 2006; Zhao et al., 1999), suggesting a more complex mechanism of sGC

activation. sGC activity can be increased through commercially available compounds that act either as heme-dependent sGC stimulators (YC-1, BAY 41-2272, BAY 41-8543, CFM-1571 and A-350619) or as heme-independent sGC activators (BAY 58-2667 and HMR-1766) (Evgenov et al., 2006; Schindler et al., 2006). Oxidation of sGC inhibits cyclase activity, and is typically generated through the use of the pharmacological agents ODQ (1H-[1,2,4]oxadiazolo[4,3-a]quinoxalin-1-one), NS2028, methylene blue or ferricyanide (Hwang et al., 1998; Olesen et al., 1998; Schrammel et al., 1996; Zhao et al., 2000). Endogenously, changes in the redox state of sGC can be induced by reactive oxygen and nitrogen species such as superoxide (O^{2-}) and peroxynitrite ($ONOO^{-}$), which are generated under conditions of oxidative stress (Stasch et al., 2006). Carbon monoxide can bind to the sGC heme group, but increases sGC activity only by a factor of 4, underscoring the requirement for the particular NO-mediated conformational change (Ma et al., 2007).

In contrast to sGCs, the transmembrane particulate GCs (GC-A and GC-B) serve as a receptor for atrial, B-type (GC-A) and C-type (GC-B) natriuretic peptides. GC-A/B possess a variable N-terminal extracellular receptor domain, a transmembrane domain and an intracellular region consisting of a protein kinase–homology domain (KHD), an amphipathic alpha-helical or hinge region, and a C-terminal cyclase–homology catalytic domain (Chinkers and Garbers, 1989; Liu et al., 1997; Wilson and Chinkers, 1995) (Figure 5). Transmembrane particulate GCs exist as homodimers, and dimerization is required for full catalytic activity. Binding of natriuretic peptide to the extracellular receptor domain induces conformational changes that lead to cGMP synthesis in the

intracellular catalytic domain (Figure 2). The KHD domain modulates the enzyme activity of the C-terminal catalytic domain (Koller et al., 1992). Although the KHD domain binds ATP and contains many residues conserved in the catalytic domain of protein kinases, this domain possesses no intrinsic kinase activity. Catalytic activity of membrane GC can also be modulated through purine nucleoside analogs (P-site inhibitors) (Joubert et al., 2007).

Both families of guanylyl cyclases, sGC and GC-A, catalyze the synthesis of $[cGMP]_i$ upon stimulation. Due to their distinct cellular localization - membrane bound GC-A versus cytosolic sGC - in combination with the hydrolyzing properties of PDEs, both families of GCs may give rise to distinct pools of $[cGMP]_i$ and may differentially modulate the activity of specific target proteins such as phosphodiesterases, ion channels, cGMP-dependent protein kinases, and downstream cellular events.

Phosphodiesterase mediated hydrolysis of cGMP

In VSM cells and platelets, the GC-mediated increase in $[cGMP]_i$ is held in a dynamic balance through the hydrolyzing activity of cGMP-specific phosphodiesterases (PDEs) (Figure 2) (Cawley et al., 2007; Mullershausen et al., 2001). Based on substrate affinity, selectivity, and regulation mechanisms, PDEs have been grouped into 11 different isoenzymes (Conti and Beavo, 2007; Kass et al., 2007). Of these enzymes, PDE5, PDE6, and PDE9 are highly selective for cGMP, PDE1, PDE2, and PDE11 have dual substrate affinity, and PDE3 and PDE10 are cGMP-sensitive but cAMP-selective. In VSM cells, the primary cGMP-PDEs with known activity are PDE1 and PDE5. PDE1 is

a calcium/calmodulin-dependent enzyme while PDE5 is the first identified selective cGMP esterase. PDE3, a cAMP esterase expressed in VSM cells, can be inhibited by cGMP.

In addition to being hydrolyzed by PDEs, cGMP can modulate the catabolic activity of these enzymes by binding to tandem regulatory GAF domains, which are named for the first three classes of proteins found to contain the cGMP-binding sequence: mammalian cGMP-binding PDEs, Anabaena adenylate cyclase, and Escherichia coli Fh1A. In the case of PDE5, binding of cGMP to the two GAF sites induces a conformational change in PDE to activate its catabolic activity and to stimulate cGMP hydrolysis (Okada and Asakawa, 2002; Rybalkin et al., 2003). PDE1 does not contain any GAF sites. Another mechanism to modulate PDE activity involves phosphorylation by PKG. For PDE5, GAF binding promotes phosphorylation through PKG (at 10 x greater rates than through PKA) (Thomas et al., 1990; Turko et al., 1998). PKG phosphorylation in turn induces a conformational change that increases the cGMP-binding affinity in the regulatory GAF domain, and enhances cGMP catalytic activity by 50–70% (Corbin et al., 2000). PDE5 may also serve as an intracellular storage site by allosterically binding cGMP, thus protecting cGMP from hydrolysis and potentially releasing it when cGMP levels decline due to other signaling events (Gopal et al., 2001). A third type of functional modulation occurs via cGMP at the catalytic site. PDE3 binds both cAMP and cGMP at its catalytic site at high affinity. However, cGMP can function as a competitive inhibitor of PDE3-mediated cAMP hydrolysis (Leroy et al., 1996), and at low levels of cGMP, the effect is to enhance cAMP and its downstream effects.

PDE5 has been shown to play a key role in smooth muscle tone, for example in the corpus cavernosum and the pulmonary vasculature. Protein expression and activity are also well documented in the cerebellum, stomach, small and large intestine, bladder, and platelets (Lin et al., 2006). The recent development of highly specific inhibitors such as sildenafil, tadalafil and vardenafil for PDE5 and vinpocetine for PDE1 has greatly enhanced our understanding of PDEs. Recent studies in platelets and in aortic tissue have shown that NO triggers an initial rise and then rapid decline in $[cGMP]_i$ (Cawley et al., 2007; Mullershausen et al., 2001). These studies suggest that auto-activation of PDE5 by cGMP plays an important feedback role in NO signaling.

cGMP dependent protein kinases (PKGs)

PKG belongs to the family of Ser/Thr protein kinases and transmits changes in $[cGMP]_i$ into downstream signaling events in all eukaryotes (Figure 1). Mammals uniformly express two PKG genes, prkg1 and prkg2, that encode PKG type I and type II (Francis and Corbin, 1999; Pfeifer et al., 1999). Two alternatively spliced exons give rise to the isoforms PKG I α and β that differ only in their N-terminal 90 to 100 residues and the cGMP concentration required for kinase activation (Ruth et al., 1991).

PKG-Structure and Function

Structurally, the PKG holoenzyme exists as parallel dimer of two identical subunits, with each subunit possessing an N-terminal dimerization and autoinhibitory domain, followed by a cGMP binding regulatory domain and a catalytic domain (Figure

6) (Francis and Corbin, 1999; Pfeifer et al., 1999). PKG homodimers are held together by a parallel, alpha-helical leucine zipper present in the N terminus (Schnell et al., 2005), and are targeted to different subcellular localizations by their N-termini via G-kinase anchoring proteins (GKAPs) (Cha et al., 2005), acetylation or myristoylation (MacMillan-Crow and Lincoln, 1994; Vaandrager et al., 1997). The regulatory domain contains two in-tandem cGMP receptor sites, A and B that interact allosterically and bind cGMP with different affinities. Occupation of both binding sites induces a large change in secondary structure (Landgraf et al., 1990) to yield a more elongated molecule (Richie-Jannetta et al., 2006; Wall et al., 2003; Zhao et al., 1997). The catalytic domain includes the Mg^{2+}-ATP- and substrate recognition sites. Binding of cGMP to sites A and B in the regulatory domain releases the inhibition of the catalytic center by the N-terminal autoinhibitory/pseudosubstrate site and allows the phosphorylation of Ser/Thr residues in the N-terminal autophosphorylation site and in target proteins. Other mechanisms of PKG activation include disulfide formation through hydrogen peroxide or heavy metals (Burgoyne et al., 2007; Landgraf et al., 1991), proteolytic cleavage of an N-terminal 77-amino acid peptide (Landgraf and Hofmann, 1989; Scholten et al., 2007), or phosphorylation events in the N-terminus (Chu et al., 1998; Smith et al., 1996).

Tissue specific distribution of PKG I (α and β) and PKG II

High concentrations (> 0.1 μM) of PKG I are expressed in all smooth muscle, platelets, dorsal root ganglia, cerebellum, hippocampus, neuromuscular endplate and kidney (Geiselhoringer et al., 2004). Lower concentrations have been detected in cardiac

muscle, vascular endothelium, chondrocytes, osteoclasts and granulocytes. PKG I α is predominantly expressed in lung, heart, dorsal root ganglia and cerebellum, whereas hippocampal neurons, olfactory bulb neurons and platelets contain mainly PKG I β. Both isozymes have been identified in smooth muscle cells of the uterus, blood vessels, intestines and trachea. PKG II is expressed predominantly in the intestinal mucosa, brain nuclei, kidney, adrenal cortex, chondrocytes and lung (de Vente et al., 2001; el-Husseini et al., 1995; Vaandrager et al., 1998; Werner et al., 2004).

Physiological roles of PKG II

Most of our knowledge about the physiological roles of PKG II is derived from PKG II- deficient mice. These studies have shown that PKG II plays an important role in secretion as well as other cellular processes. PKG II is highly expressed in enterocytes of the small intestine, where it activates the cystic fibrosis transmembrane conductance regulator, thereby increasing Cl^- and water secretion (Pfeifer et al., 1996; Vaandrager et al., 2000). Furthermore, PKG II is essential for natriuretic-peptide/cGMP-mediated endochondral ossification (Miyazawa et al., 2002) and regulates autonomous bone growth. Studies with PKG II- deficient mice confirmed that PKG II is also involved in the regulation of the circadian clock (Tischkau et al., 2003). In addition, deletion of PKG II resulted in mild neurological defects, such as a moderately enhanced anxiety-like behavior and a hyposensitivity to acute alcohol intake (Werner et al., 2004).

Physiological roles of PKG I α and β

In contrast to PKG II, the major physiological roles of PKG I include regulation of vascular smooth muscle tone, smooth muscle proliferation and platelet aggregation.

Platelet Aggregation

Aggregation of platelets is initiated at areas where the endothelial cell layer has been destroyed. Endothelial cells release prostacyclin and NO, consequently raising cAMP and cGMP levels in platelets which thereby prevent clot formation. PKG I is expressed at high levels in platelets and has an anti-aggregatory function (Gambaryan et al., 2004; Marshall et al., 2004; Massberg et al., 1999). An intact platelet NO/PKG I signaling pathway is essential to prevent platelet aggregation after ischemia in vivo (Massberg et al., 1999). Platelets contain two well established PKG I substrates, VASP and IRAG. Deletion of the VASP gene in mice did not grossly affect platelet aggregation (Aszodi et al., 1999; Hauser et al., 1999), but considerably affected the interaction of platelets with the endothelium in vivo (Massberg et al., 2004). Activation of PKG I inhibited the release of Ca^{2+} from IP_3-sensitive stores in wild type and VASP-deficient platelets to similar extents (Aszodi et al., 1999). Furthermore, platelets from the IRAG mutant mice have a severe defect in the cGMP-mediated prevention of aggregation indicating that IRAG is an essential component of this pathway (Geiselhoringer et al., 2004).

Regulation of Smooth Muscle Proliferation

NO, ANP, and cGMP analogs have been shown to prevent proliferation, migration, and dedifferentiation of vascular smooth muscle cells (Calderone et al., 1998; Garg and Hassid, 1989). Recent studies suggest that PKG I modulates gene expression through the extracellular signal-regulated kinase/mitogen-activated protein kinase pathway (Hofmann et al., 2000; Pilz and Casteel, 2003). VASP, an actin-binding protein localized at the focal adhesion and cell-to-cell contacts in many cells, is differentially phosphorylated by protein kinase C, cAMP kinase, and PKG I, and might be a key player in this signaling cascade (Chen et al., 2004).

Regulation of vascular smooth muscle tone

In general, smooth muscle tone is regulated by the rise and fall of intracellular calcium, $[Ca^{2+}]_i$. The rise of $[Ca^{2+}]_i$ is initiated either by receptor-mediated generation of inositol triphosphate (IP_3) that releases Ca^{2+} from intracellular stores or by an influx of extracellular Ca^{2+} through voltage-dependent Ca^{2+} channels (Moosmang et al., 2003). This rise in $[Ca^{2+}]_i$ initiates contraction by activation of the Ca^{2+}/calmodulin-dependent myosin light chain kinase (MLCK), which phosphorylates the regulatory light chain (RLC) and, consequently, activates myosin ATPase. A decrease in $[Ca^{2+}]_i$ deactivates MLCK, allowing for dephosphorylation of RLC by myosin light chain phosphatase (MLCP) (Surks et al., 1999). Smooth muscle contraction is also modulated at constant $[Ca^{2+}]_i$ by changing the sensitivity of the contractile machinery to $[Ca^{2+}]_i$ (Somlyo and Somlyo, 2003). PKG I interferes both with the increase in $[Ca^{2+}]_i$ and with the Ca^{2+}

sensitivity through phosphorylation of IRAG, Ca^{2+}-activated maxi-K^+ (BK_{Ca}) channels, phospholamban (Koller et al., 2003; Porter et al., 1998; Robertson et al., 1993) and MLCP (Figure 1).

One mechanism to lower $[Ca^{2+}]_i$ is the PKG I-dependent phosphorylation of IRAG. IRAG is expressed at the endoplasmic reticulum membrane in smooth muscle, platelets, and some neurons, and interacts specifically with the leucine zipper of PKG I and with the IP_3 receptor type I (Ammendola et al., 2001; Geiselhoringer et al., 2004). Studies on IRAG-deficient mice revealed that PKG I-dependent phosphorylation of IRAG inhibits IP_3-induced Ca^{2+} release (Geiselhoringer et al., 2004). Additionally, PKG I lowers $[Ca^{2+}]_i$ through direct phosphorylation of BK_{Ca} channels (Robertson et al., 1993). Opening of BK_{Ca} channels hyperpolarizes the membrane and closes L-type calcium channels, thereby reducing Ca^{2+} influx. This mechanism contributes to the regulation of vascular tone, as shown in wild type and PKG I-deficient mice (Sausbier et al., 2000). An alternative mechanism to regulate smooth muscle tone is the PKG I dependent phosphorylation and activation of MLCP (Etter et al., 2001). Consequently, RLC phosphorylation is reduced and smooth muscle relaxed at constant $[Ca^{2+}]_i$.

Detection of $[cGMP]_i$ using fluorescent indicators

cGMP is a key signaling molecule for regulating vascular smooth muscle tone. In the past, $[cGMP]_i$ has been detected utilizing techniques such as guanylyl cyclase assays (Domino et al., 1991), radio-immunoassays (Brooker et al., 1979), patch cramming (Trivedi and Kramer, 1998) and patch clamping (Castro et al., 2006). However, the

dynamic rise and fall of $[cGMP]_i$ in living cells could not be monitored directly until the development of fluorescent cGMP biosensors (Honda et al., 2001; Nikolaev et al., 2006; Russwurm et al., 2007). In recent years, several fluorescence resonance energy transfer (FRET) - based indicators for cGMP have been reported, all of which utilize the general strategy of placing a conformationally sensitive cGMP binding domain between two mutants of green fluorescent protein (GFP) to modulate FRET. In 2001, Honda and colleagues were the first to report the successful development of FRET-based cGMP biosensors, called cygnets, by inserting a kinase inactive deletion fragment of cGMP-dependent protein kinase (PKG) between cyan (CFP) and yellow (YFP) mutants of green fluorescent protein (Honda et al., 2001). cGMP binding to Cygnets decreased FRET and increased the overall ratio of cyan to yellow emissions by up to 1.5-fold for recombinant protein. Recombinant cygnets are also highly selective (>100 fold) for cGMP over cAMP with apparent K_D values ranging from 0.6 to 1.9 μM (Honda et al., 2001; Honda et al., 2005), (Table 1). Cygnets have revealed transient cGMP kinetics resulting from sGC activation by NO in rat fetal lung fibroblast (RFL)-6 cells, in Purkinje neurons (Honda et al., 2001) and in cultured, unpassaged rat aortic VSM cells (Cawley et al., 2007). Reports on the next set of FRET-based cGMP indicators followed in 2006, when isolated nucleotide binding domains, such as the single cGMP-binding domain B from PKG I or the single regulatory GAF domain from PDEs, were sandwiched between CFP and YFP (Nikolaev et al., 2006). These new indicators displayed cGMP affinities in the low micromolar range (Table 1) and had moderate (100 fold; PKG/PDE2-based) to high (400 to 600 fold; PDE5-based) cGMP selectivity. In HEK cells, the sensors based on a single

PDE-GAF domain produced maximal 1.3 fold increase in FRET ratio and rapid responsiveness to NO-induced sGC activation. In 2007, Russwurm and colleagues reported the latest FRET-cGMP biosensors based on cyclic nucleotide binding sites of PKG I (Russwurm et al., 2007). Interestingly, only cGMP-binding domains arranged in tandem configuration as in their native configuration were cGMP-responsive. These new sensors produced an overall 1.6 to 1.7-fold increase in FRET ratio for recombinant protein upon cGMP binding, high cGMP affinities (0.5 to 6 μM), high cGMP selectivity and fast cGMP binding kinetics (Table 1).

While the above mentioned cGMP biosensors have advanced our understanding of cGMP signaling, they all have some intrinsic limitations. For example, in living cells, all FRET based cGMP indicators display significantly decreased FRET ratios (maximal 1.3 fold FRET ratio change), possibly due to interactions with endogenous proteins (such as PKGs and PDEs), as well as unspecific interactions caused by CFP and YFP. Due to these overall low FRET ratios, FRET-based indicators are not suitable for transgenic mouse models and hence are limited in their use to follow $[cGMP]_i$ dynamics in physiological systems. Furthermore, FRET-based indicators are unable to detect cGMP dynamics in response to physiological, low-nanomolar NO concentrations. In addition, FRET-based cGMP indicators are limited in their use for real-time, confocal imaging techniques and therefore have limited use to study real-time $[cGMP]_i$ dynamics in microdomains of living cells. These limitations prompted us to develop a new generation of non-FRET cGMP biosensors (Chapter 4), called FlincGs, suitable to monitor $[cGMP]_i$ in response to physiological (low-nanomolar) NO concentrations. In addition, FlincGs are

powerful tools to study $[cGMP]_i$ dynamics in response to various stimuli, by utilizing high-resolution, real-time confocal microscopy. FlincG-type biosensors are derived from the cGMP-receptor domains of PKG. Thus, it has been necessary to characterize the molecular mechanism and the cGMP binding dynamics underlying PKG activation (Chapters 2 and 3).

Focus of Dissertation

Regulation of vascular smooth muscle tone is one of the major functions of cGMP-dependent protein kinase I. To investigate in detail cGMP-dependent PKG activation, we introduced several site-specific mutations in the regulatory cGMP binding domain and studied their effects on cGMP binding, dissociation and kinase activity (Chapter 2). We further attempted to crystallize full-length and deletion fragments of PKG to gain more insight into PKG structure and function (Chapter 3). Based on these studies, we developed a new generation of PKG-derived, non-FRET cGMP biosensors to examine the spatial distribution of $[cGMP]_i$ in response to NO and ANP in cultured VSM cells (Chapter 4) as well as in intact cerebral arteries (Chapter 5). These novel indicators for cGMP allow for investigation of the complex cross-talk between cGMP and calcium, and in addition, might be suitable for the development of transgenic mice with tissue-specific expression of cGMP biosensors.

Table 1: Kinetic characteristics of different cGMP biosensors *in vitro* and in living cells

Sensor	Backbone	$EC_{50,cGMP}$ [µM]	$EC_{50,cAMP}$ [µM]	cGMP/cAMP[1]	$(F/F_0)_{max}$[2]	$(F/F_0)_{max}$[3]	Reference
Cygnet 2.1	PKG I α (78-671)	1.7	> 1,000	> 600	1.5	1.3	(Honda et al., 2001)
cGES-GKIB	PKG I B-site	5.0	486	97	-	1.3	(Nikolaev et al., 2006)
cGES-DE2	PDE2A GAF-B site	0.9	115	128	-	1.3	
cGES-DE5	PDE5A GAF-B site	1.5	630	420	-	1.3	
cGi-500	PKG I α (79-345)	0.5	-	-	1.7	1.3	(Russwurm et al., 2007)
cGi-3000	PKG I α (79-336)	3	-	-	1.7	1.3	
cGi-6000	PKG I α (79-328)	6	-	-	1.6	1.3	
α-FlincG	PKG I α (1-356)	0.035	40	1140	1.5	1.2	(Nausch et al, Chapter 4)
β-FlincG	PKG I β (1-372)	1.1	31	30	2.1	1.2	
δ-FlincG	PKG I α (77-356)	0.17	48	280	1.7	1.7	

1: Selectivity; 2: determined for recombinant protein; 3: determined in living cells;

Figure legends:

Figure 1: Overview of cGMP signaling in VSM cells. cGMP is synthesized by soluble guanylyl cyclases (sGC) in response to nitric oxide (NO), or by particulate, membrane bound guanylyl cyclases (GC-A/B) in response to natriuretic peptides (ANP, CNP). Physiological effects of cGMP are mediated through the action of phosphodiesterases (PDEs) and cGMP dependent protein kinases (PKGs), by phosphorylating IRAG, phospholamban (PL), myosin light chain phosphatase (MLCP) or Ca^{2+}-activated maxi-K^{+} (BK_{Ca}) channels. Adapted from (Hofmann, 2005).

Figure 2: GTP conversion into cGMP and pyrophosphate (PP_i) is catalyzed by guanylyl cyclases (GC), while cGMP hydrolysis is mediated by phosphodiesterases (PDE). Chemical structures were created with the program ChemSketch.

Figure 3: Atrial Natriuretic Peptide (ANP) secretion from the atrium. Adapted from (Dietz, 2005; Gardner et al., 2007; Ruskoaho, 1992).

Figure 4: Nitric Oxide (NO) synthesis and release from vascular endothelium. Adapted from (Albrecht et al., 2003).

Figure 5: General domain structure of dimeric receptor (rGC) and soluble (sGC) guanylyl cyclases. The receptor architecture consists of the extracellular domain (BCD), transmembrane segment (TM), kinase homology domain (KHD), coiled-coil domain

(CCD) and guanylyl cyclase domain (GC). The heterodimeric soluble guanylyl cyclase consists of a heme domain (HD), a CC and a GC domain. Adapted from (Fitzpatrick et al., 2006).

Figure 6: Domain structure of PKG I α. Inset: The alpha-helical, N-terminal dimerization region is the only domain for which a structure has been determined (Schnell et al., 2005).

Figure 1:

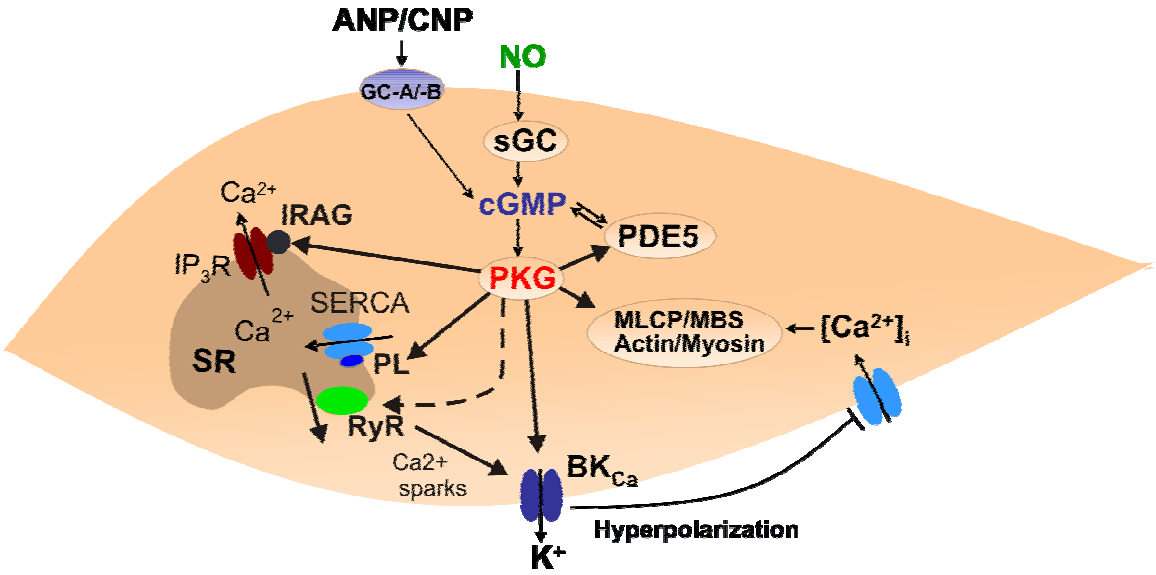
ANP/CNP
NO
GC-A/-B
sGC
cGMP
PDE5
PKG
Ca2+
IRAG
IP3R
SERCA
Ca2+
SR
PL
RyR
MLCP/MBS
Actin/Myosin
[Ca2+]i
Ca2+
sparks
BKCa
K+
Hyperpolarization

Figure 2:

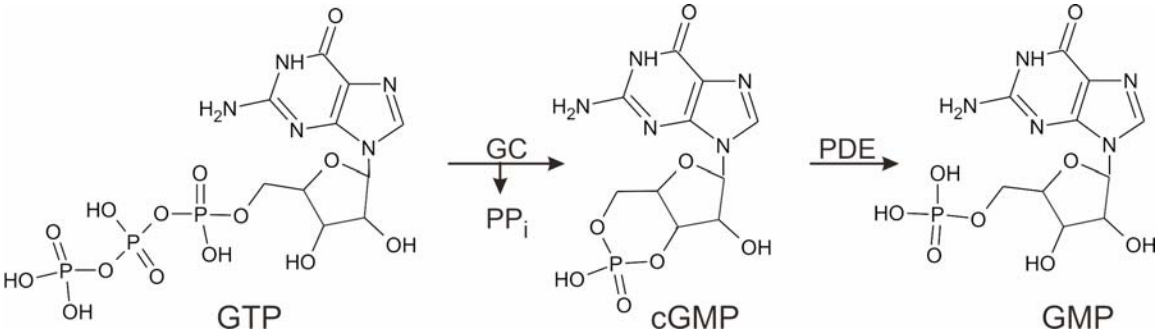

Figure 3:

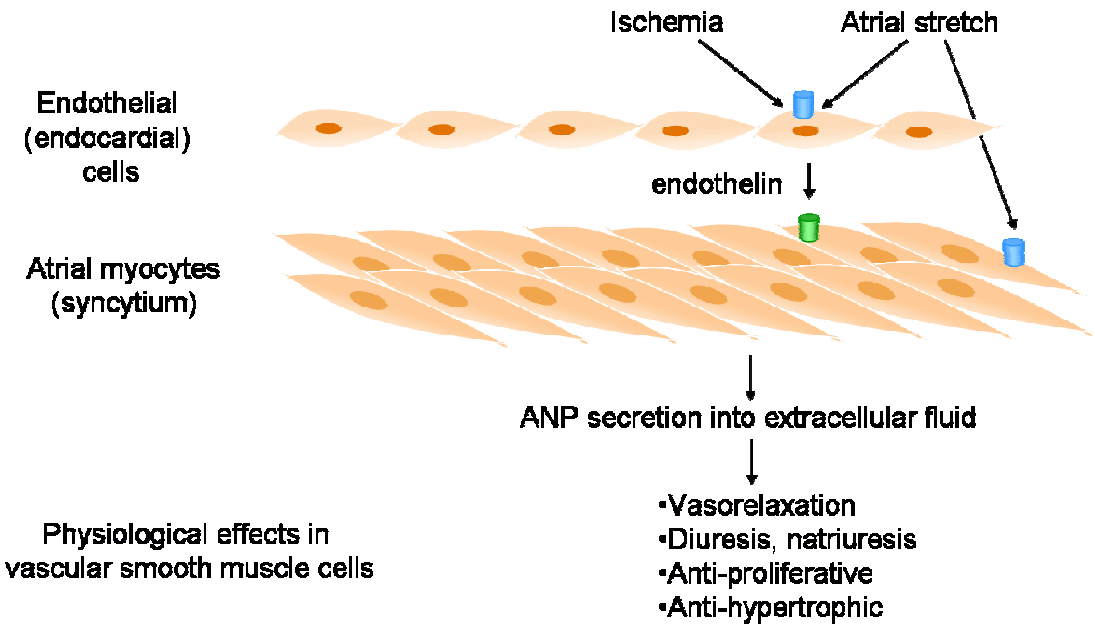
Ischemia
Atrial stretch
Endothelial (endocardial) cells
endothelin
Atrial myocytes (syncytium)
ANP secretion into extracellular fluid
•Vasorelaxation
•Diuresis, natriuresis
•Anti-proliferative
•Anti-hypertrophic
Physiological effects in vascular smooth muscle cells

Figure 4:

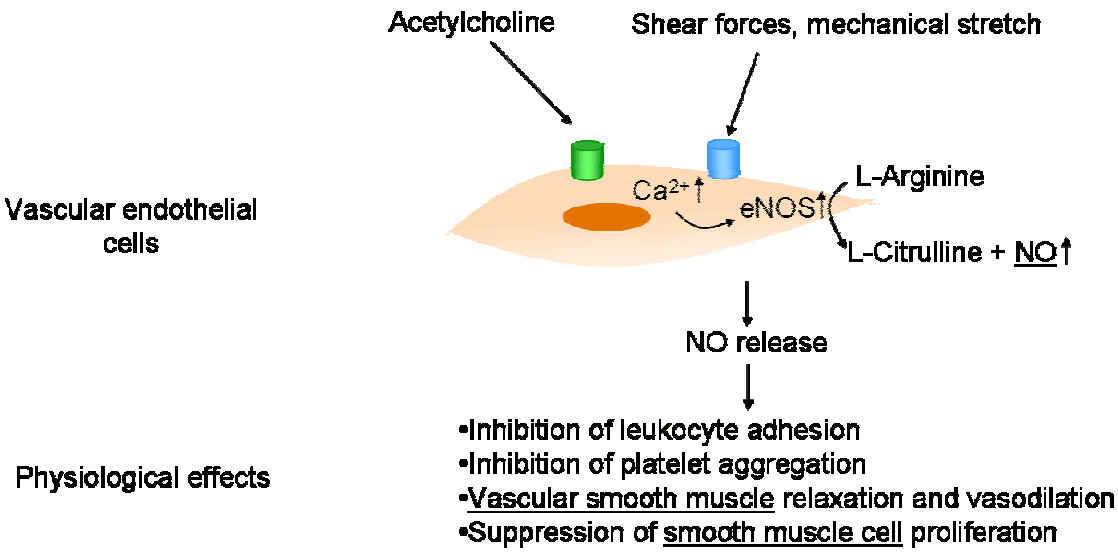
Acetylcholine
Shear forces, mechanical stretch
Vascular endothelial cells
Ca2+
eNOS
L-Arginine
L-Citrulline + NO
NO release
Physiological effects
•Inhibition of leukocyte adhesion
•Inhibition of platelet aggregation
•Vascular smooth muscle relaxation and vasodilation
•Suppression of smooth muscle cell proliferation

Figure 5:

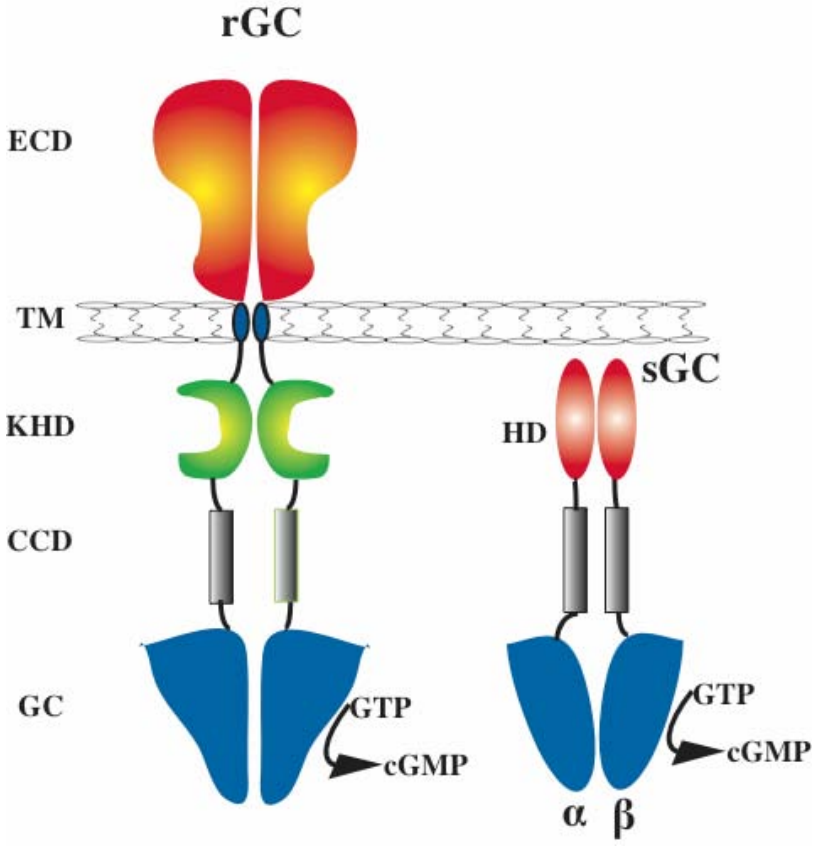

Figure 6:

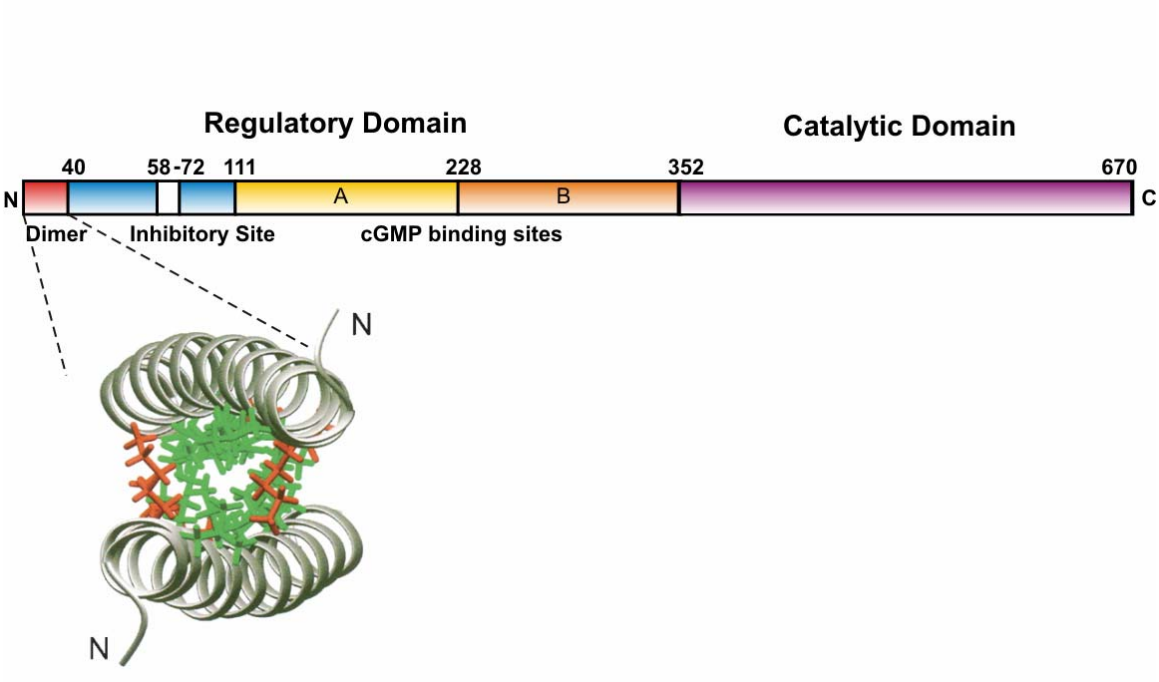
Regulatory Domain
Catalytic Domain
40
58-72
111
228
352
670
N
A
B
C
Dimer
Inhibitory Site
cGMP binding sites
N
N

References

Albrecht EW, Stegeman CA, Heeringa P, Henning RH and van Goor H. Protective role of endothelial nitric oxide synthase. *J Pathol* 199(1): 8-17, 2003.

Ammendola A, Geiselhoringer A, Hofmann F and Schlossmann J. Molecular determinants of the interaction between the inositol 1,4,5-trisphosphate receptor-associated cGMP kinase substrate (IRAG) and cGMP kinase Ibeta. *J Biol Chem* 276(26): 24153-9, 2001.

Aszodi A, Pfeifer A, Ahmad M, Glauner M, Zhou XH, Ny L, Andersson KE, Kehrel B, Offermanns S and Fassler R. The vasodilator-stimulated phosphoprotein (VASP) is involved in cGMP- and cAMP-mediated inhibition of agonist-induced platelet aggregation, but is dispensable for smooth muscle function. *Embo J* 18(1): 37-48, 1999.

Ballou DP, Zhao Y, Brandish PE and Marletta MA. Revisiting the kinetics of nitric oxide (NO) binding to soluble guanylate cyclase: the simple NO-binding model is incorrect. *Proc Natl Acad Sci U S A* 99(19): 12097-101, 2002.

Brooker G, Harper JF, Terasaki WL and Moylan RD. Radioimmunoassay of cyclic AMP and cyclic GMP. *Adv Cyclic Nucleotide Res* 10: 1-33, 1979.

Burgoyne JR, Madhani M, Cuello F, Charles RL, Brennan JP, Schroder E, Browning DD and Eaton P. Cysteine redox sensor in PKGIa enables oxidant-induced activation. *Science* 317(5843): 1393-7, 2007.

Calderone A, Thaik CM, Takahashi N, Chang DL and Colucci WS. Nitric oxide, atrial natriuretic peptide, and cyclic GMP inhibit the growth-promoting effects of norepinephrine in cardiac myocytes and fibroblasts. *J Clin Invest* 101(4): 812-8, 1998.

Cary SP, Winger JA, Derbyshire ER and Marletta MA. Nitric oxide signaling: no longer simply on or off. *Trends Biochem Sci* 31(4): 231-9, 2006.

Castro LR, Verde I, Cooper DM and Fischmeister R. Cyclic guanosine monophosphate compartmentation in rat cardiac myocytes. *Circulation* 113(18): 2221-8, 2006.

Cawley SM, Sawyer CL, Brunelle KF, van der Vliet A and Dostmann WR. Nitric oxide-evoked transient kinetics of cyclic GMP in vascular smooth muscle cells. *Cell Signal* 19(5): 1023-33, 2007.

Cha B, Kim JH, Hut H, Hogema BM, Nadarja J, Zizak M, Cavet M, Lee-Kwon W, Lohmann SM, Smolenski A, Tse CM, Yun C, de Jonge HR and Donowitz M. cGMP inhibition of Na+/H+ antiporter 3 (NHE3) requires PDZ domain adapter NHERF2, a

broad specificity protein kinase G-anchoring protein. *J Biol Chem* 280(17): 16642-50, 2005.

Chen L, Daum G, Chitaley K, Coats SA, Bowen-Pope DF, Eigenthaler M, Thumati NR, Walter U and Clowes AW. Vasodilator-stimulated phosphoprotein regulates proliferation and growth inhibition by nitric oxide in vascular smooth muscle cells. *Arterioscler Thromb Vasc Biol* 24(8): 1403-8, 2004.

Chinkers M and Garbers DL. The protein kinase domain of the ANP receptor is required for signaling. *Science* 245(4924): 1392-4, 1989.

Chu DM, Francis SH, Thomas JW, Maksymovitch EA, Fosler M and Corbin JD. Activation by autophosphorylation or cGMP binding produces a similar apparent conformational change in cGMP-dependent protein kinase. *J Biol Chem* 273(23): 14649-56, 1998.

Chusho H, Tamura N, Ogawa Y, Yasoda A, Suda M, Miyazawa T, Nakamura K, Nakao K, Kurihara T, Komatsu Y, Itoh H, Tanaka K, Saito Y, Katsuki M and Nakao K. Dwarfism and early death in mice lacking C-type natriuretic peptide. *Proc Natl Acad Sci U S A* 98(7): 4016-21, 2001.

Conti M and Beavo J. Biochemistry and physiology of cyclic nucleotide phosphodiesterases: essential components in cyclic nucleotide signaling. *Annu Rev Biochem* 76: 481-511, 2007.

Corbin JD, Turko IV, Beasley A and Francis SH. Phosphorylation of phosphodiesterase-5 by cyclic nucleotide-dependent protein kinase alters its catalytic and allosteric cGMP-binding activities. *Eur J Biochem* 267(9): 2760-7, 2000.

de Bold AJ, Borenstein HB, Veress AT and Sonnenberg H. A rapid and potent natriuretic response to intravenous injection of atrial myocardial extract in rats. *Life Sci* 28(1): 89-94, 1981.

de Bold AJ, Ma KK, Zhang Y, de Bold ML, Bensimon M and Khoshbaten A. The physiological and pathophysiological modulation of the endocrine function of the heart. *Can J Physiol Pharmacol* 79(8): 705-14, 2001.

de Vente J, Asan E, Gambaryan S, Markerink-van Ittersum M, Axer H, Gallatz K, Lohmann SM and Palkovits M. Localization of cGMP-dependent protein kinase type II in rat brain. *Neuroscience* 108(1): 27-49, 2001.

Dietz JR. Mechanisms of atrial natriuretic peptide secretion from the atrium. *Cardiovasc Res* 68(1): 8-17, 2005.

Dimmeler S, Fleming I, Fisslthaler B, Hermann C, Busse R and Zeiher AM. Activation of nitric oxide synthase in endothelial cells by Akt-dependent phosphorylation. *Nature* 399(6736): 601-5, 1999.

Domino SE, Tubb DJ and Garbers DL. Assay of guanylyl cyclase catalytic activity. *Methods Enzymol* 195: 345-55, 1991.

el-Husseini AE, Bladen C and Vincent SR. Molecular characterization of a type II cyclic GMP-dependent protein kinase expressed in the rat brain. *J Neurochem* 64(6): 2814-7, 1995.

Erwin PA, Lin AJ, Golan DE and Michel T. Receptor-regulated dynamic S-nitrosylation of endothelial nitric-oxide synthase in vascular endothelial cells. *J Biol Chem* 280(20): 19888-94, 2005.

Etter EF, Eto M, Wardle RL, Brautigan DL and Murphy RA. Activation of myosin light chain phosphatase in intact arterial smooth muscle during nitric oxide-induced relaxation. *J Biol Chem* 276(37): 34681-5, 2001.

Evgenov OV, Pacher P, Schmidt PM, Hasko G, Schmidt HH and Stasch JP. NO-independent stimulators and activators of soluble guanylate cyclase: discovery and therapeutic potential. *Nat Rev Drug Discov* 5(9): 755-68, 2006.

Fitzpatrick DA, O'Halloran DM and Burnell AM. Multiple lineage specific expansions within the guanylyl cyclase gene family. *BMC Evol Biol* 6: 26, 2006.

Francis SH, Blount MA, Zoraghi R and Corbin JD. Molecular properties of mammalian proteins that interact with cGMP: protein kinases, cation channels, phosphodiesterases, and multi-drug anion transporters. *Front Biosci* 10: 2097-117, 2005.

Francis SH and Corbin JD. Cyclic nucleotide-dependent protein kinases: intracellular receptors for cAMP and cGMP action. *Crit Rev Clin Lab Sci* 36(4): 275-328, 1999.

Friebe A, Mergia E, Dangel O, Lange A and Koesling D. Fatal gastrointestinal obstruction and hypertension in mice lacking nitric oxide-sensitive guanylyl cyclase. *Proc Natl Acad Sci U S A* 104(18): 7699-704, 2007.

Gambaryan S, Geiger J, Schwarz UR, Butt E, Begonja A, Obergfell A and Walter U. Potent inhibition of human platelets by cGMP analogs independent of cGMP-dependent protein kinase. *Blood* 103(7): 2593-600, 2004.

Garbers DL and Lowe DG. Guanylyl cyclase receptors. *J Biol Chem* 269(49): 30741-4, 1994.

Gardner DG, Chen S, Glenn DJ and Grigsby CL. Molecular biology of the natriuretic peptide system: implications for physiology and hypertension. *Hypertension* 49(3): 419-26, 2007.

Garg UC and Hassid A. Nitric oxide-generating vasodilators and 8-bromo-cyclic guanosine monophosphate inhibit mitogenesis and proliferation of cultured rat vascular smooth muscle cells. *J Clin Invest* 83(5): 1774-7, 1989.

Geiselhoringer A, Gaisa M, Hofmann F and Schlossmann J. Distribution of IRAG and cGKI-isoforms in murine tissues. *FEBS Lett* 575(1-3): 19-22, 2004.

Geiselhoringer A, Werner M, Sigl K, Smital P, Worner R, Acheo L, Stieber J, Weinmeister P, Feil R, Feil S, Wegener J, Hofmann F and Schlossmann J. IRAG is essential for relaxation of receptor-triggered smooth muscle contraction by cGMP kinase. *Embo J* 23(21): 4222-31, 2004.

Gopal VK, Francis SH and Corbin JD. Allosteric sites of phosphodiesterase-5 (PDE5). A potential role in negative feedback regulation of cGMP signaling in corpus cavernosum. *Eur J Biochem* 268(11): 3304-12, 2001.

Gudi S, Nolan JP and Frangos JA. Modulation of GTPase activity of G proteins by fluid shear stress and phospholipid composition. *Proc Natl Acad Sci U S A* 95(5): 2515-9, 1998.

Hauser W, Knobeloch KP, Eigenthaler M, Gambaryan S, Krenn V, Geiger J, Glazova M, Rohde E, Horak I, Walter U and Zimmer M. Megakaryocyte hyperplasia and enhanced agonist-induced platelet activation in vasodilator-stimulated phosphoprotein knockout mice. *Proc Natl Acad Sci U S A* 96(14): 8120-5, 1999.

Hofmann F. The biology of cyclic GMP-dependent protein kinases. *J Biol Chem* 280(1): 1-4, 2005.

Hofmann F, Ammendola A and Schlossmann J. Rising behind NO: cGMP-dependent protein kinases. *J Cell Sci* 113 (Pt 10): 1671-6, 2000.

Hofmann F, Biel M and Kaupp UB. International Union of Pharmacology. LI. Nomenclature and structure-function relationships of cyclic nucleotide-regulated channels. *Pharmacol Rev* 57(4): 455-62, 2005.

Honda A, Adams SR, Sawyer CL, Lev-Ram V, Tsien RY and Dostmann WR. Spatiotemporal dynamics of guanosine 3',5'-cyclic monophosphate revealed by a genetically encoded, fluorescent indicator. *Proc Natl Acad Sci U S A* 98(5): 2437-42, 2001.

Honda A, Sawyer CL, Cawley SM and Dostmann WR. Cygnets: in vivo characterization of novel cGMP indicators and in vivo imaging of intracellular cGMP. *Methods Mol Biol* 307: 27-43, 2005.

Hwang TL, Wu CC and Teng CM. Comparison of two soluble guanylyl cyclase inhibitors, methylene blue and ODQ, on sodium nitroprusside-induced relaxation in guinea-pig trachea. *Br J Pharmacol* 125(6): 1158-63, 1998.

Ignarro LJ, Adams JB, Horwitz PM and Wood KS. Activation of soluble guanylate cyclase by NO-hemoproteins involves NO-heme exchange. Comparison of heme-containing and heme-deficient enzyme forms. *J Biol Chem* 261(11): 4997-5002, 1986.

Iyer LM, Anantharaman V and Aravind L. Ancient conserved domains shared by animal soluble guanylyl cyclases and bacterial signaling proteins. *BMC Genomics* 4(1): 5, 2003.

John SW, Veress AT, Honrath U, Chong CK, Peng L, Smithies O and Sonnenberg H. Blood pressure and fluid-electrolyte balance in mice with reduced or absent ANP. *Am J Physiol* 271(1 Pt 2): R109-14, 1996.

Joubert S, McNicoll N and De Lean A. Biochemical and pharmacological characterization of P-site inhibitors on homodimeric guanylyl cyclase domain from natriuretic peptide receptor-A. *Biochem Pharmacol* 73(7): 954-63, 2007.

Kangawa K and Matsuo H. Purification and complete amino acid sequence of alpha-human atrial natriuretic polypeptide (alpha-hANP). *Biochem Biophys Res Commun* 118(1): 131-9, 1984.

Kass DA, Takimoto E, Nagayama T and Champion HC. Phosphodiesterase regulation of nitric oxide signaling. *Cardiovasc Res* 75(2): 303-14, 2007.

Koller A, Schlossmann J, Ashman K, Uttenweiler-Joseph S, Ruth P and Hofmann F. Association of phospholamban with a cGMP kinase signaling complex. *Biochem Biophys Res Commun* 300(1): 155-60, 2003.

Koller KJ, de Sauvage FJ, Lowe DG and Goeddel DV. Conservation of the kinaselike regulatory domain is essential for activation of the natriuretic peptide receptor guanylyl cyclases. *Mol Cell Biol* 12(6): 2581-90, 1992.

Komatsu Y, Itoh H, Suga S, Ogawa Y, Hama N, Kishimoto I, Nakagawa O, Igaki T, Doi K, Yoshimasa T and Nakao K. Regulation of endothelial production of C-type natriuretic peptide in coculture with vascular smooth muscle cells. Role of the vascular natriuretic peptide system in vascular growth inhibition. *Circ Res* 78(4): 606-14, 1996.

Kou R, Greif D and Michel T. Dephosphorylation of endothelial nitric-oxide synthase by vascular endothelial growth factor. Implications for the vascular responses to cyclosporin A. *J Biol Chem* 277(33): 29669-73, 2002.

Kuhn M. Cardiac and intestinal natriuretic peptides: insights from genetically modified mice. *Peptides* 26(6): 1078-85, 2005.

Kuhn M, Holtwick R, Baba HA, Perriard JC, Schmitz W and Ehler E. Progressive cardiac hypertrophy and dysfunction in atrial natriuretic peptide receptor (GC-A) deficient mice. *Heart* 87(4): 368-74, 2002.

Landgraf W and Hofmann F. The amino terminus regulates binding to and activation of cGMP-dependent protein kinase. *Eur J Biochem* 181(3): 643-50, 1989.

Landgraf W, Hofmann F, Pelton JT and Huggins JP. Effects of cyclic GMP on the secondary structure of cyclic GMP dependent protein kinase and analysis of the enzyme's amino-terminal domain by far-ultraviolet circular dichroism. *Biochemistry* 29(42): 9921-8, 1990.

Landgraf W, Regulla S, Meyer HE and Hofmann F. Oxidation of cysteines activates cGMP-dependent protein kinase. *J Biol Chem* 266(25): 16305-11, 1991.

Leroy MJ, Degerman E, Taira M, Murata T, Wang LH, Movsesian MA, Meacci E and Manganiello VC. Characterization of two recombinant PDE3 (cGMP-inhibited cyclic nucleotide phosphodiesterase) isoforms, RcGIP1 and HcGIP2, expressed in NIH 3006 murine fibroblasts and Sf9 insect cells. *Biochemistry* 35(31): 10194-202, 1996.

Lin CS, Lin G, Xin ZC and Lue TF. Expression, distribution and regulation of phosphodiesterase 5. *Curr Pharm Des* 12(27): 3439-57, 2006.

Liu Y, Ruoho AE, Rao VD and Hurley JH. Catalytic mechanism of the adenylyl and guanylyl cyclases: modeling and mutational analysis. *Proc Natl Acad Sci U S A* 94(25): 13414-9, 1997.

Lopez MJ, Wong SK, Kishimoto I, Dubois S, Mach V, Friesen J, Garbers DL and Beuve A. Salt-resistant hypertension in mice lacking the guanylyl cyclase-A receptor for atrial natriuretic peptide. *Nature* 378(6552): 65-8, 1995.

Ma X, Sayed N, Beuve A and van den Akker F. NO and CO differentially activate soluble guanylyl cyclase via a heme pivot-bend mechanism. *Embo J* 26(2): 578-88, 2007.

MacMillan-Crow LA and Lincoln TM. High-affinity binding and localization of the cyclic GMP-dependent protein kinase with the intermediate filament protein vimentin. *Biochemistry* 33(26): 8035-43, 1994.

Marshall SJ, Senis YA, Auger JM, Feil R, Hofmann F, Salmon G, Peterson JT, Burslem F and Watson SP. GPIb-dependent platelet activation is dependent on Src kinases but not MAP kinase or cGMP-dependent kinase. *Blood* 103(7): 2601-9, 2004.

Massberg S, Gruner S, Konrad I, Garcia Arguinzonis MI, Eigenthaler M, Hemler K, Kersting J, Schulz C, Muller I, Besta F, Nieswandt B, Heinzmann U, Walter U and Gawaz M. Enhanced in vivo platelet adhesion in vasodilator-stimulated phosphoprotein (VASP)-deficient mice. *Blood* 103(1): 136-42, 2004.

Massberg S, Sausbier M, Klatt P, Bauer M, Pfeifer A, Siess W, Fassler R, Ruth P, Krombach F and Hofmann F. Increased adhesion and aggregation of platelets lacking cyclic guanosine 3',5'-monophosphate kinase I. *J Exp Med* 189(8): 1255-64, 1999.

Mayer B and Koesling D. cGMP signalling beyond nitric oxide. *Trends Pharmacol Sci* 22(11): 546-8, 2001.

Mergia E, Friebe A, Dangel O, Russwurm M and Koesling D. Spare guanylyl cyclase NO receptors ensure high NO sensitivity in the vascular system. *J Clin Invest* 116(6): 1731-7, 2006.

Miyazawa T, Ogawa Y, Chusho H, Yasoda A, Tamura N, Komatsu Y, Pfeifer A, Hofmann F and Nakao K. Cyclic GMP-dependent protein kinase II plays a critical role in C-type natriuretic peptide-mediated endochondral ossification. *Endocrinology* 143(9): 3604-10, 2002.

Mo E, Amin H, Bianco IH and Garthwaite J. Kinetics of a cellular nitric oxide/cGMP/phosphodiesterase-5 pathway. *J Biol Chem* 279(25): 26149-58, 2004.

Moncada S, Palmer RM and Higgs EA. Nitric oxide: physiology, pathophysiology, and pharmacology. *Pharmacol Rev* 43(2): 109-42, 1991.

Montagnani M, Chen H, Barr VA and Quon MJ. Insulin-stimulated activation of eNOS is independent of Ca2+ but requires phosphorylation by Akt at Ser(1179). *J Biol Chem* 276(32): 30392-8, 2001.

Moosmang S, Schulla V, Welling A, Feil R, Feil S, Wegener JW, Hofmann F and Klugbauer N. Dominant role of smooth muscle L-type calcium channel Cav1.2 for blood pressure regulation. *Embo J* 22(22): 6027-34, 2003.

Mullershausen F, Russwurm M, Thompson WJ, Liu L, Koesling D and Friebe A. Rapid nitric oxide-induced desensitization of the cGMP response is caused by increased activity of phosphodiesterase type 5 paralleled by phosphorylation of the enzyme. *J Cell Biol* 155(2): 271-8, 2001.

Nikolaev VO, Gambaryan S and Lohse MJ. Fluorescent sensors for rapid monitoring of intracellular cGMP. *Nat Methods* 3(1): 23-5, 2006.

Nimmegeers S, Sips P, Buys E, Brouckaert P and Van de Voorde J. Functional role of the soluble guanylyl cyclase alpha(1) subunit in vascular smooth muscle relaxation. *Cardiovasc Res* 76(1): 149-59, 2007.

Okada D and Asakawa S. Allosteric activation of cGMP-specific, cGMP-binding phosphodiesterase (PDE5) by cGMP. *Biochemistry* 41(30): 9672-9, 2002.

Olesen SP, Drejer J, Axelsson O, Moldt P, Bang L, Nielsen-Kudsk JE, Busse R and Mulsch A. Characterization of NS 2028 as a specific inhibitor of soluble guanylyl cyclase. *Br J Pharmacol* 123(2): 299-309, 1998.

Oliver PM, John SW, Purdy KE, Kim R, Maeda N, Goy MF and Smithies O. Natriuretic peptide receptor 1 expression influences blood pressures of mice in a dose-dependent manner. *Proc Natl Acad Sci U S A* 95(5): 2547-51, 1998.

Olivera A and Spiegel S. Sphingosine-1-phosphate as second messenger in cell proliferation induced by PDGF and FCS mitogens. *Nature* 365(6446): 557-60, 1993.

Palmer RM, Ashton DS and Moncada S. Vascular endothelial cells synthesize nitric oxide from L-arginine. *Nature* 333(6174): 664-6, 1988.

Pellicena P, Karow DS, Boon EM, Marletta MA and Kuriyan J. Crystal structure of an oxygen-binding heme domain related to soluble guanylate cyclases. *Proc Natl Acad Sci U S A* 101(35): 12854-9, 2004.

Pfeifer A, Aszodi A, Seidler U, Ruth P, Hofmann F and Fassler R. Intestinal secretory defects and dwarfism in mice lacking cGMP-dependent protein kinase II. *Science* 274(5295): 2082-6, 1996.

Pfeifer A, Ruth P, Dostmann W, Sausbier M, Klatt P and Hofmann F. Structure and function of cGMP-dependent protein kinases. *Rev Physiol Biochem Pharmacol* 135: 105-49, 1999.

Pilz RB and Casteel DE. Regulation of gene expression by cyclic GMP. *Circ Res* 93(11): 1034-46, 2003.

Porter VA, Bonev AD, Knot HJ, Heppner TJ, Stevenson AS, Kleppisch T, Lederer WJ and Nelson MT. Frequency modulation of Ca2+ sparks is involved in regulation of arterial diameter by cyclic nucleotides. *Am J Physiol* 274(5 Pt 1): C1346-55, 1998.

Richie-Jannetta R, Busch JL, Higgins KA, Corbin JD and Francis SH. Isolated regulatory domains of cGMP-dependent protein kinase Ialpha and Ibeta retain dimerization and native cGMP-binding properties and undergo isoform-specific conformational changes. *J Biol Chem* 281(11): 6977-84, 2006.

Robertson BE, Schubert R, Hescheler J and Nelson MT. cGMP-dependent protein kinase activates Ca-activated K channels in cerebral artery smooth muscle cells. *Am J Physiol* 265(1 Pt 1): C299-303, 1993.

Ruskoaho H. Atrial natriuretic peptide: synthesis, release, and metabolism. *Pharmacol Rev* 44(4): 479-602, 1992.

Russwurm M, Mullershausen F, Friebe A, Jager R, Russwurm C and Koesling D. Design of fluorescence resonance energy transfer (FRET)-based cGMP indicators: a systematic approach. *Biochem J* 407(1): 69-77, 2007.

Ruth P, Landgraf W, Keilbach A, May B, Egleme C and Hofmann F. The activation of expressed cGMP-dependent protein kinase isozymes I alpha and I beta is determined by the different amino-termini. *Eur J Biochem* 202(3): 1339-44, 1991.

Rybalkin SD, Rybalkina IG, Shimizu-Albergine M, Tang XB and Beavo JA. PDE5 is converted to an activated state upon cGMP binding to the GAF A domain. *Embo J* 22(3): 469-78, 2003.

Sausbier M, Schubert R, Voigt V, Hirneiss C, Pfeifer A, Korth M, Kleppisch T, Ruth P and Hofmann F. Mechanisms of NO/cGMP-dependent vasorelaxation. *Circ Res* 87(9): 825-30, 2000.

Schindler U, Strobel H, Schonafinger K, Linz W, Lohn M, Martorana PA, Rutten H, Schindler PW, Busch AE, Sohn M, Topfer A, Pistorius A, Jannek C and Mulsch A. Biochemistry and pharmacology of novel anthranilic acid derivatives activating heme-oxidized soluble guanylyl cyclase. *Mol Pharmacol* 69(4): 1260-8, 2006.

Schnell JR, Zhou GP, Zweckstetter M, Rigby AC and Chou JJ. Rapid and accurate structure determination of coiled-coil domains using NMR dipolar couplings: application to cGMP-dependent protein kinase Ialpha. *Protein Sci* 14(9): 2421-8, 2005.

Scholten A, Fuss H, Heck AJ and Dostmann WR. The hinge region operates as a stability switch in cGMP-dependent protein kinase I alpha. *Febs J* 274(9): 2274-86, 2007.

Schrammel A, Behrends S, Schmidt K, Koesling D and Mayer B. Characterization of 1H-[1,2,4]oxadiazolo[4,3-a]quinoxalin-1-one as a heme-site inhibitor of nitric oxide-sensitive guanylyl cyclase. *Mol Pharmacol* 50(1): 1-5, 1996.

Smith JA, Francis SH, Walsh KA, Kumar S and Corbin JD. Autophosphorylation of type Ibeta cGMP-dependent protein kinase increases basal catalytic activity and enhances allosteric activation by cGMP or cAMP. *J Biol Chem* 271(34): 20756-62, 1996.

Somlyo AP and Somlyo AV. Ca2+ sensitivity of smooth muscle and nonmuscle myosin II: modulated by G proteins, kinases, and myosin phosphatase. *Physiol Rev* 83(4): 1325-58, 2003.

Stasch JP, Schmidt PM, Nedvetsky PI, Nedvetskaya TY, H SA, Meurer S, Deile M, Taye A, Knorr A, Lapp H, Muller H, Turgay Y, Rothkegel C, Tersteegen A, Kemp-Harper B, Muller-Esterl W and Schmidt HH. Targeting the heme-oxidized nitric oxide receptor for selective vasodilatation of diseased blood vessels. *J Clin Invest* 116(9): 2552-61, 2006.

Steinhelper ME, Cochrane KL and Field LJ. Hypotension in transgenic mice expressing atrial natriuretic factor fusion genes. *Hypertension* 16(3): 301-7, 1990.

Sudoh T, Kangawa K, Minamino N and Matsuo H. A new natriuretic peptide in porcine brain. *Nature* 332(6159): 78-81, 1988.

Sudoh T, Minamino N, Kangawa K and Matsuo H. C-type natriuretic peptide (CNP): a new member of natriuretic peptide family identified in porcine brain. *Biochem Biophys Res Commun* 168(2): 863-70, 1990.

Surks HK, Mochizuki N, Kasai Y, Georgescu SP, Tang KM, Ito M, Lincoln TM and Mendelsohn ME. Regulation of myosin phosphatase by a specific interaction with cGMP- dependent protein kinase Ialpha. *Science* 286(5444): 1583-7, 1999.

Tamura N, Doolittle LK, Hammer RE, Shelton JM, Richardson JA and Garbers DL. Critical roles of the guanylyl cyclase B receptor in endochondral ossification and development of female reproductive organs. *Proc Natl Acad Sci U S A* 101(49): 17300-5, 2004.

Thomas MK, Francis SH and Corbin JD. Substrate- and kinase-directed regulation of phosphorylation of a cGMP-binding phosphodiesterase by cGMP. *J Biol Chem* 265(25): 14971-8, 1990.

Tischkau SA, Weber ET, Abbott SM, Mitchell JW and Gillette MU. Circadian clock-controlled regulation of cGMP-protein kinase G in the nocturnal domain. *J Neurosci* 23(20): 7543-50, 2003.

Trivedi B and Kramer RH. Real-time patch-cram detection of intracellular cGMP reveals long-term suppression of responses to NO and muscarinic agonists. *Neuron* 21(4): 895-906, 1998.

Turko IV, Francis SH and Corbin JD. Binding of cGMP to both allosteric sites of cGMP-binding cGMP-specific phosphodiesterase (PDE5) is required for its phosphorylation. *Biochem J* 329 (Pt 3): 505-10, 1998.

Vaandrager AB, Bot AG, Ruth P, Pfeifer A, Hofmann F and De Jonge HR. Differential role of cyclic GMP-dependent protein kinase II in ion transport in murine small intestine and colon. *Gastroenterology* 118(1): 108-14, 2000.

Vaandrager AB, Smolenski A, Tilly BC, Houtsmuller AB, Ehlert EM, Bot AG, Edixhoven M, Boomaars WE, Lohmann SM and de Jonge HR. Membrane targeting of cGMP-dependent protein kinase is required for cystic fibrosis transmembrane conductance regulator Cl- channel activation. *Proc Natl Acad Sci U S A* 95(4): 1466-71, 1998.

Vaandrager AB, Tilly BC, Smolenski A, Schneider-Rasp S, Bot AG, Edixhoven M, Scholte BJ, Jarchau T, Walter U, Lohmann SM, Poller WC and de Jonge HR. cGMP stimulation of cystic fibrosis transmembrane conductance regulator Cl- channels co-expressed with cGMP-dependent protein kinase type II but not type Ibeta. *J Biol Chem* 272(7): 4195-200, 1997.

Wall ME, Francis SH, Corbin JD, Grimes K, Richie-Jannetta R, Kotera J, Macdonald BA, Gibson RR and Trewhella J. Mechanisms associated with cGMP binding and activation of cGMP-dependent protein kinase. *Proc Natl Acad Sci U S A* 100(5): 2380-5, 2003.

Werner C, Raivich G, Cowen M, Strekalova T, Sillaber I, Buters JT, Spanagel R and Hofmann F. Importance of NO/cGMP signalling via cGMP-dependent protein kinase II for controlling emotionality and neurobehavioural effects of alcohol. *Eur J Neurosci* 20(12): 3498-506, 2004.

Wilson EM and Chinkers M. Identification of sequences mediating guanylyl cyclase dimerization. *Biochemistry* 34(14): 4696-701, 1995.

Winger JA and Marletta MA. Expression and characterization of the catalytic domains of soluble guanylate cyclase: interaction with the heme domain. *Biochemistry* 44(10): 4083-90, 2005.

Yamahara K, Itoh H, Chun TH, Ogawa Y, Yamashita J, Sawada N, Fukunaga Y, Sone M, Yurugi-Kobayashi T, Miyashita K, Tsujimoto H, Kook H, Feil R, Garbers DL, Hofmann F and Nakao K. Significance and therapeutic potential of the natriuretic peptides/cGMP/cGMP-dependent protein kinase pathway in vascular regeneration. *Proc Natl Acad Sci U S A* 100(6): 3404-9, 2003.

Zabel U, Weeger M, La M and Schmidt HH. Human soluble guanylate cyclase: functional expression and revised isoenzyme family. *Biochem J* 335 (Pt 1): 51-7, 1998.

Zhao J, Trewhella J, Corbin J, Francis S, Mitchell R, Brushia R and Walsh D. Progressive cyclic nucleotide-induced conformational changes in the cGMP-dependent protein kinase studied by small angle X-ray scattering in solution. *J Biol Chem* 272(50): 31929-36, 1997.

Zhao Y, Brandish PE, Ballou DP and Marletta MA. A molecular basis for nitric oxide sensing by soluble guanylate cyclase. *Proc Natl Acad Sci U S A* 96(26): 14753-8, 1999.

Zhao Y, Brandish PE, DiValentin M, Schelvis JP, Babcock GT and Marletta MA. Inhibition of soluble guanylate cyclase by ODQ. *Biochemistry* 39(35): 10848-54, 2000.

CHAPTER TWO: CYCLIC NUCLEOTIDE BINDING SITE MUTATIONS DELINEATE THE MECHANISM OF cGMP-DEPENDENT PROTEIN KINASE Iα ACTIVATION

Lydia WM Nausch, Xuguang Yan*, Claudia S Maier*, Christian K Nickl and Wolfgang R Dostmann

Department of Pharmacology, University of Vermont, College of Medicine, Burlington, 05405 VT

* Department of Chemistry, Oregon State University, Corvallis, 97330 OR

Corresponding author: Wolfgang Dostmann, Ph.D, University of Vermont, Department of Pharmacology, Health Science Research Facility 330, 149 Beaumont Avenue, Burlington, VT 05405-0075, USA

Tel: (802) 656-0381, Fax: (802) 656-4523, EMail: wdostman@uvm.edu

Submitted to Biochemistry

Abstract

Binding of cGMP manifests the central allosteric mechanism of activation for the homo-dimeric cGMP-dependent protein kinase Iα (PKG). The relative contributions of the two in-tandem cGMP binding sites A and B in the enzyme's mechanism of activation are not known, however. Based on homology models derived from cAMP-dependent protein kinases (PKA), we introduced the loss-of-function mutations G167E, E168G, R177K and G291E, E292G, R301K in each cGMP binding site A and B, respectively. Surprisingly, the arginine to lysine mutations (R177K, R301K) retained cGMP binding to both sites. Their differentially shifted activation constants of 620 nM (site A) and 16 nM (site B) support a hitherto unknown dominant role of site B in modulating the phenotype of PKG activation. In accordance to the homology models, the glycine and glutamate mutations fully blocked cGMP binding to either site A or B. In contrast to PKA however, both site A loss-of-function mutants (G167E, E168G) were unexpectedly cGMP-insensitive, demonstrating constitutively elevated kinase activities. Equally unanticipated, the equivalent site B loss-of-function mutants (G291E, E292G), as well as the R301K mutant, showed intact cGMP-dependency of kinase activity characterized by decreased cGMP-sensitivities. These findings suggest a) juxtaposed orientation of low and high affinity cGMP binding sites in PKG Iα, compared to PKA Iα, and b) functional coupling between cGMP binding site A and the catalytic domain. Taken together, we propose a previously unrecognized concerted mechanism of PKG I α.

Introduction

The type Iα/Iβ and type II cGMP dependent protein kinases (PKGs) are members of the cyclic nucleotide-dependent serine/threonine protein kinases with closest sequence homologies to the type Iα/Iβ and type IIα/IIβ cyclic AMP dependent protein kinases (PKAs) (Francis and Corbin, 1994; Pfeifer et al., 1999; Scott, 1991). Although both kinase sub-families possess regulatory domains that modulate the accessibility of substrates to the catalytic domain, they differ in key architectural aspects that contribute to their respective mechanisms of activation. The tetrameric PKA holoenzymes are composed of two regulatory subunits (R_2) associated with two catalytic subunits (Brostrom et al., 1971; Gill and Garren, 1971; Reimann et al., 1971). The R_2 subunits inhibit kinase activity through the association of their autoinhibitory region with the catalytic subunit (Brostrom et al., 1971; Erlichman et al., 1973; Kemp et al., 1975; Taylor and Stafford, 1978). Binding of cAMP to the R_2 subunits causes the tetramer to dissociate and thus releases inhibition of the catalytic subunit. The PKG holoenzymes are composed differently: they consist of dimers of two identical subunits, with each subunit possessing a regulatory and catalytic domain (Gill et al., 1976; Lincoln et al., 1977; Monken and Gill, 1980; Takio et al., 1984). For each monomer, the catalytic and regulatory domains are located on one polypeptide chain and thus cGMP binding cannot induce dissociation of the catalytic domain from the holoenzyme.

Another notable characteristic for cyclic nucleotide kinases is their distinct structural order of high and low affinity cyclic nucleotide binding sites relative to the N-terminus (Doskeland et al., 1987; Ogreid and Doskeland, 1980; Ogreid and Doskeland,

1981; Ogreid et al., 1983). For PKG I β, the slow nucleotide dissociation site is closer to the N-terminus than the fast dissociation site (Reed et al., 1996), whereas for PKA I, PKA II and PKG II, the fast dissociation site is closer to the N-terminus (Bubis and Taylor, 1987; Corbin and Rannels, 1981; Taylor and Uhler, 2000; Weber et al., 1987; Woodford et al., 1989). These structural differences between PKA I and PKG I as well as PKG I and PKG II suggest different mechanisms of activation by cyclic nucleotides.

A number of approaches have been implemented to better understand the molecular events associated with activation of PKG I. Previous studies using hydrodynamic and small-angle x-ray scattering techniques have demonstrated that cGMP binding to the regulatory domain of PKG Iα and β induces substantial conformational changes (Richie-Jannetta et al., 2006; Wall et al., 2003; Zhao et al., 1997). However, the individual contributions of each cGMP-binding site still remain unknown. Our attempt to address this question is based on mutational studies in PKA that led to the development of a sequential model of type I α PKA activation (Herberg et al., 1996). Previous reports have identified six highly conserved aminoacids (Gly199, Glu200, Arg209, Gly323, Glu324 and Arg333) in the regulatory subunit of PKA I α that were critical for cAMP binding (Bubis et al., 1988; Neitzel et al., 1991; Ogreid et al., 1988; Steinberg et al., 1991; Steinberg et al., 1987). It has since been confirmed by X-ray crystallography that the highly conserved glutamate, glycine and arginine indeed coordinate cAMP in the regulatory subunit to the 2'-OH of the ribose and to the cyclic phosphate moiety, respectively (Diller et al., 2001; Su et al., 1995; Zawadzki and Taylor, 2004).

To gain more insight into the actual cGMP binding mechanism in PKG I α and the molecular mechanism of kinase activation, we have introduced single point mutations (G167E, E168G, R177K, G291E, E292G and R301K) and have analyzed their kinetic characteristics with respect to kinase activity depending on cGMP and substrate, as well as for cGMP binding and dissociation. These mutants allowed us to gain insight into: (1) the specific sites of communication between regulatory and catalytic domains of PKG, (2) conformational changes associated with cGMP binding, (3) greatly expand our current knowledge about the molecular mechanism of PKG activation and also allude to (4) fundamental differences in the molecular mechanism of activation between PKG I α and PKA I α.

Results:

Allosteric binding site mutants of PKG I α

Aminoacid-sequence alignment of cyclic nucleotide binding sites A and B revealed two highly conserved regions, FGE…RTA for PKG I α and FGE…RAA for PKA I α respectively (Figure 1A) (Francis and Corbin, 1994; Weber et al., 1989). Both sequence motifs flank the cyclic-phosphate binding cassette critical for the riboside moiety and phosphate-diester recognition (Berman et al., 2005; Diller et al., 2001; Wu et al., 2004). The charged residues as well as the glycine residue in each binding cassette of PKA I α were of special interest since alterations of these amino acids led to a complete loss of cyclic nucleotide binding to that site (Gorman and Steinberg, 1994; Murphy and Steinberg, 1985; Ogreid et al., 1988; Steinberg et al., 1991; Steinberg et al., 1987). Further studies have demonstrated that the loss-of-function glycine, glutamate and arginine mutations in the regulatory subunits RIα and RIIβ were particularly useful to aid our understanding of the mechanism of PKA activation (Bubis et al., 1988; Dostmann and Taylor, 1991; Neitzel et al., 1991; Wu et al., 2004; Zawadzki and Taylor, 2004). The goal of this study was to determine if the glycine, glutamate or arginine residues present in each of the PKG I α binding site pockets modulate (1) cGMP binding to site A and/or B of the PKG regulatory domain and (2) cGMP specific activation of the kinase catalytic domain (Figure 1 B). Therefore in analogy to PKA, we selected the following PKG I α mutants: G167E, E168G, R177K, G291E, E292G and R301K (Figure 1 A). To assess their kinetic characteristics, all PKG I α mutant and wildtype proteins were expressed in

SF9-cells and purified to apparent homogeneity using cAMP-affinity chromatography (Figure 1 C; see Methods).

Stoichiometry of PKG I α cGMP-binding site mutants

First, we conducted binding studies using [^{3}H]-labeled cGMP (Doskeland and Ogreid, 1988; Dostmann et al., 1996; Ogreid and Doskeland, 1981) to determine the influence of the point mutations on the overall cGMP binding capacity (Figure 1 D; Table 1). Replacement of either glycine or glutamate residues in site A (G167E, E168G) or site B (G291E, E292G) was sufficient to reduce the stoichiometry of cGMP binding to one ligand per PKG regulatory domain. In contrast to the type Iα regulatory subunit of PKA, the arginine to lysine mutants (R177K and R301K) fully retained cGMP binding to both sites A and B (Figure 1 D and Table 1).

To verify the reduced cGMP binding capacity in the glutamate to glycine mutants (E168G, E292G), we utilized electrospray ionization mass spectrometry (ESI) under non-denaturing conditions (Figures 2 A-F). In agreement with previously published reports, PKG wildtype gave rise to intense charge state distribution ranging from 23+ to 29+ and yielding a mass charge envelope of 5,000 to 6,500 m/z (Pinkse et al., 2004; Scholten et al., 2007) (Figure 2 A). Deconvolution spectra indicate that dimeric native PKG bound in average two molecules cyclic nucleotides (Figure 2 A, inset), and possibly residual cAMP from eluting the protein from affinity column or cyclic nucleotides endogenously present in SF9 cells. Incubation of wildtype PKG with cGMP (20 μM) predicts binding of four cGMP molecules per dimeric wildtype PKG (measured mass 154.3 kDa) in

accordance to the number of expected nucleotide binding sites in the dimeric kinase PKG (Figure 2 B). Both PKG mutants E168G and E292G co-eluted with other (unidentified) proteins from the affinity columns, however, both PKG mutants gave rise to charge state distributions of sufficient intensities and qualities to observe and analyze distinct PKG species (Figures 2 C to F). Deconvolution of the complex charge state distribution of PKG E292G indicated the presence of dimeric PKG E292G with no cyclic nucleotide, one and two cyclic nucleotides with approximate contributions of 20%, 38% and 42%, respectively, as estimated from the deconvoluted mass spectrum (Figure 2 C, inset). Incubation with 20 μM cGMP gave rise to a stoichiometry of two cGMP molecules per dimeric PKG E292G (with a measured mass of 153.6 kDa) (Figure 2 D). A minor fraction (< 20%) of E292G dimer containing three cGMP (measured mass 153.9 kDa) was also observed. Similarly, nano-electrospray mass spectrometry revealed dimeric PKG E168G bound to one or two residual cyclic nucleotides (15 and 85 % contribution, respectively), (Figure 2 E). After incubation with 20 μM cGMP, the predominating species observed were again dimeric E168G bound to two or three cyclic nucleotides (with contribution of 80-85 % and 15-20 %, respectively), (Figure 2 F). Therefore, ESI mass spectrometry supports the [^{3}H]-cGMP binding assays suggesting loss of cGMP binding in the mutated cGMP binding sites (E168G, E292G).

Kinetic characterization of site A loss-of-function mutants of PKG I α

To gain insight into specific cGMP binding sites of PKG I α, all identified single site binding mutants (G167E, E168G, G291E, E292G) were tested for their cGMP

binding, dissociation and activation kinetics. First, we studied the kinetic behavior of the N-terminal binding site A mutants G167E and E168G (Figure 3). In contrast to PKG wildtype (K_D = 40 nM), both PKG mutants displayed increased cGMP binding constants (K_D) of 385 nM and 195 nM for G167E and E168G, respectively (Figure 3 A; Table 1). Skatchard analysis confirmed binding of a single cGMP molecule to the functional, low affinity site B (K_D = 327 nM and 197 nM for G167E and E168G, respectively; Table 1; Figure 3 B). Based on their Hill coefficients, G167E (n_H = 0.6) and E168G (n_H = 0.8) exhibited non-cooperative cGMP binding behavior, further indicating the presence of a single cGMP binding site in both mutants. In contrast, PKG wildtype displayed highly cooperative cGMP binding (n_H = 1.5), indicating positive cooperativity and cross-talk between sites A and B under native conditions, as reported previously (Wolfe et al., 1989). In agreement with cGMP binding studies, cGMP dissociation kinetics attested monophasic, fast dissociation from the isolated, cGMP binding site B in G167E and E168G (k_{-1} = 11.8 and 22.2 min^{-1}, respectively; Table 2; Figures 3 D, E). Dissociation as well as binding assays confirmed impaired cGMP binding to site A, and intact cGMP binding to site B, thereby identifying site A as high affinity, and site B as low affinity binding sites in PKG I α. Surprisingly, kinase activation of mutants G167E and E168G did not reveal higher activation constants K_a, indicative of lower cGMP binding affinity (Figure 3 F, Table 3). Instead, site A knock-out mutants exhibited basal, cGMP-independent catalytic activity (10 to 20 %; Figure 3 F) but could not be fully activated in presence of increasing cGMP concentrations. Therefore, glycine 167 and glutamate 168

are not only critical for cGMP binding to site A but also reveal that cGMP binding to a functional cGMP binding site A is essential for kinase activation (Figure 3 G).

Kinetic characterization of site B loss-of-function mutants of PKG I α

Next, we investigated cGMP binding, dissociation and kinase activity of the C-terminal, low affinity binding site B mutants G291E and E292G (Figure 4). Replacement of glycine 291 or glutamate 292 led to monophasic, non-cooperative cGMP binding with slightly lower K_D-values of 26 nM and 18 nM for G291E and E292G, respectively, compared to PKG wildtype (Table 1; Figure 4 A). Skatchard analysis confirmed binding of a single cGMP molecule to the functional high affinity site A (K_D = 29 nM and 21 nM for G291E and E292G, respectively; Table 1; Figure 4 B). Similar to site A knock-out mutants, Hill coefficients for G291E (n_H = 0.9) and E292G (n_H = 0.9) indicated non-cooperative cGMP binding (Figure 4 C). In addition, cGMP dissociation kinetics verified slow, monophasic dissociation from site A for mutants G291E (k_{-1} = 0.01 min^{-1}; $\tau_{1/2}$ = 80 min) and E292G (k_{-1} = 0.01 min^{-1}; $\tau_{1/2}$ = 90 min) (Table 2; Figures 4 D, E). In agreement with site A knock-out mutants (Figure 3), dissociation and association kinetics of site B knock-out mutants confirm that site A and B are high- and low- affinity binding sites for cGMP, respectively. In contrast to site A knock-out mutants, site B mutants clearly demonstrated cGMP-dependent activation (Figure 4 F) with maximal kinase activity comparable to wildtype PKG. However, apparent activation constants (K_a) revealed that mutants G291E (K_a = 18 nM) and E292G (K_a = 37 nM) bound cGMP with an even higher affinity than wildtype (K_a = 53 nM), reflecting cGMP binding and kinase

activation through the higher affinity, intact site A (Figure 4 G, Table 3). Hence, glycine 291 and glutamate 292 are critical for cGMP binding to site B (Figure 4 G), but cGMP binding to site B is not essential for PKG activation. In the absence of cooperativity, cGMP binding to a functional site A is sufficient and promotes full PKG activation.

To further investigate the cross-talk between regulatory and catalytic domains of PKG I α, we tested the PKG mutants E168G and E292G for maximal catalytic activity depending on substrate concentration and for Michaelis-Menten constants (K_M) in comparison to PKG wildtype catalytic activity (Figure 5, Table 3). When probing E168G for catalytic activity depending on substrate concentration, this mutant showed an overall decreased reaction velocity (v_{max} = 3 ± 0.2 μmol/(mg x min)) and K_M value (310 ± 5 nM) as compared to wildtype (K_M = 705 ± 20 nM) (Table 3). In contrast, impaired cGMP binding to site B had no influence on catalytic velocity, since E292G showed K_M (968 ± 26 nM) and v_{max} values (v_{max} = 8.9 ± 0.3 μmol/(mg x min)) similar to wildtype PKG I α (v_{max} = 10.5 ± 0.4 μmol/(mg x min)). These findings further support our hypothesis that a dysfunctional site A directly impacts kinase fidelity, thus a fully functional cGMP-binding site A appears to be vital for full PKG activity and seemingly independent of the cGMP binding site B.

Kinetic characterization of R301K and R177K mutants of PKG I α

Next, we studied the kinetic behavior of PKG mutants R177K and R301K (Figure 6). In contrast to previous studies utilizing PKA (Bubis et al., 1988; Zawadzki and Taylor, 2004), both arginine to lysine mutants fully retained cGMP binding to both sites

A and B (Figures 2 A, 6 A). Despite full cGMP binding capacity, R177K and R301K displayed slightly shifted cGMP activation (Figure 6 A) and binding constants (Figure 6 B) towards higher (R301K) and lower (R177K) cGMP affinity as compared to PKG wildtype (Tables 1 and 3). This suggests that the arginine to lysine mutations modulate, but not diminish, cGMP binding to the mutated cGMP binding site. Hill analysis revealed diminished cGMP-cooperativity (n_H = 1.1) as compared to PKG wildtype (n_H = 1.5), indicating that the communication between sites A and B is impaired (Figure 6 C; Table 1). In agreement with kinase activation and cGMP binding studies, cGMP dissociation kinetics attested biphasic dissociation for both mutants (Figures 6 D; Table 2). Dissociation kinetics were faster as compared to wildtype and might be a reflection of reduced cooperativity between cGMP binding sites A and B. These results suggest that both sites A and B need to be functional and cooperative, in order to achieve cGMP binding and kinase activation as seen under native, wildtype conditions.

Discussion:

In the past, extensive mutational analysis has helped to identify six highly conserved aminoacids (Gly199, Glu200, Arg209, Gly323, Glu324 and Arg333) in the regulatory subunit of PKA I α that were critical for cAMP binding (Bubis et al., 1988; Ogreid et al., 1988; Steinberg et al., 1991; Steinberg et al., 1987). It has since been confirmed by X-ray crystallography that the highly conserved glutamate, glycine, arginine indeed coordinate cAMP in the regulatory subunit with hydrogen bonds (Su et al., 1995; Zawadzki and Taylor, 2004). In PKA I α, glutamate 200 has been shown to coordinate the ribosyl-hydroxy-group of cAMP in the regulatory subunit. Furthermore, arginine 209 has been identified to stabilize cAMP by interacting with the negatively charged, axial oxygen of the cAMP-phosphate group (Dostmann and Taylor, 1991; Dostmann et al., 1990; Su et al., 1995). In our studies, however, only the homologous glutamate (E168, E292), but not the arginine (R177, R301), was crucial for cGMP binding to the regulatory domain of PKG I α. Both site A and B knock-out mutants (E168G, E292G) in PKG I α confirm that the highly conserved glutamate is essential for cGMP binding. Replacement of glycine (G167, G291) with glutamate might interfere with cGMP binding due to charge-repulsion caused by the sterically large, charged glutamate, and therefore, conclusions about glycine-cGMP interactions cannot be drawn. In this study, abolishing cGMP binding to site A or site B has proven to be an invaluable tool to gain insight into the molecular mechanism of PKG activation.

For site A knock out mutants, cGMP binding to lower affinity site B is still functional but not sufficient to fully activate PKG I α (Figures 3 and 7 A). This suggests

that coupling between a functional site A and the catalytic domain (A-C coupling) is necessary to fully activate PKG. Site B knock-out mutations further support the hypothesis, that the catalytic domain is activated directly through site A (Figure 4 and 7 B). In absence of a functional site B, cGMP binding to site A leads to A-C coupling and to full PKG activation. Besides A-C coupling, the interactions between cGMP binding sites A and B also play a crucial part in PKG activation. Loss of binding to either one of the cGMP binding sites consequentially results in loss of cooperativity, as shown by Hill analysis (Table 1). Due to lack of cooperativity, activation and binding curves for site B knock-out mutants are shifted towards higher affinities, reflecting the influence of only one cGMP site, the high affinity site A. The modulatory influence of site B on site A is lost, and therefore, activation and binding constants are very similar and shifted towards higher affinities for site B knock-out mutants (e.g. for E291G: K_a = 18 nM; K_D = 26 nM) (Tables 1 and 3). In contrast, the activation constant (K_a = 53 nM) for PKG wildtype represents a combination of binding constants for both sites A and B and is significantly higher than the binding constant for PKG wildtype site A (K_D = 6/110 nM for site A/B; Table 1; (Hofmann et al., 1985)), indicating the modulatory effect of site B on site A. The un-coupling of both cGMP binding sites G291E and E292G allows kinase activation through site A, since the modulatory (negative) influence of site B on site A is lost.

Based on these results, we present the following mechanism of activation for PKG wildtype (Figure 7 C): both cGMP binding sites A and B are equally accessible to bind cGMP. At low cGMP concentrations, site A is fully occupied (K_D = 6 nM; Table 1), but site B (K_D = 110 nM; Table 1) prevents site A from activating the catalytic domain

(A-C coupling interrupted) due to cooperative, (negative-) modulatory effects (n_H = 1.5; Table 1). Only when both sites A and B are fully occupied with cGMP, site A can communicate to the catalytic domain and initiate the release of the autoinhibitory domain, hence making the catalytic domain accessible for substrates (Figure 7 C).

Several conclusions can be drawn from the proposed concerted mechanism of PKG activation: this activation mechanism reveals that site B plays a pivotal role in modulating responsiveness of PKG to a broader range of $[cGMP]_i$. Therefore, the mechanism for PKG activation might have developed during evolution in order to allow PKG to react in response to raising $[cGMP]_i$ levels and not to basal cGMP levels in cells (Francis et al., 1988; Kotera et al., 2003). In addition, the concerted mechanism of activation for PKG is significantly different from the sequential mechanism of PKA activation. Biochemical data as well as the recently published crystal structure of PKA holoenzyme propose a highly ordered and sequential pathway of cAMP binding to the type I α PKA holoenzyme in which domain B serves as a ‘‘gatekeeper’’ for cAMP access to domain A (Herberg et al., 1996; Kim et al., 2007; Kim et al., 2005).

Besides being very useful tools to decipher the mechanism of PKG activation, site A and B knock-out mutants also determine for the first time the distinct structural order of fast and slow cyclic nucleotide binding sites relative to the NH_2 terminus in PKG I α. For PKG I β, the slow nucleotide dissociation site is closer to the NH_2 terminus than the fast dissociation site (Reed, RB, Corbin JD JBC 1996), whereas for PKA I and PKG II, the fast dissociation site is closer to the NH_2 terminus (Bubis and Taylor, 1987; Corbin and Rannels, 1981; Taylor and Uhler, 2000; Weber et al., 1987; Woodford et al., 1989).

Similar to PKG I β, the slow nucleotide dissociation site is closer to the NH_2 terminus than the fast dissociation site for PKG I α.

In conclusion, our data suggest an overall concerted mechanism of activation for PKG I α that is significantly different from the sequential mechanism of PKA activation (Kim et al., 2007; Kim et al., 2005). Our results support coupling between both cGMP binding sites A and B, as well as coupling between cGMP binding site A and the catalytic domain. Furthermore, the structural order of high and low affinity binding sites for PKG I α is similar to PKG I β, since the high affinity binding site A is closer to the NH_2 terminus. Structural insights into PKG would greatly advance our understanding of cGMP coordination in the regulatory domain and the complexity involved in kinase activation.

Methods

Mutagenesis, expression and purification

cGMP-binding mutants were constructed by introducing single site specific mutations in the regulatory domain of bovine PKG I α at positions G167E, E168G, R177K, G291E, E292G and R301K. PKG constructs were preceded by a BamHI site and a start codon (ATG), and followed by a stop codon and an EcoRI site. The entire PKG coding sequences were inserted into the BamHI and EcoRI sites of pFAST-BAC vector (invitrogen) and transected into SF9 cells for expression.

PKG wildtype and mutants were expressed in SF9 cells using the Bac-to-Bac system and purified utilizing cyclic nucleotide affinity chromatography as described previously (Feil et al., 1993).

Kinase activity

K_M and v_{max} values were determined according to Ruth and colleagues (Ruth et al., 1991) by measuring the kinase activity for 1.5 min at 30°C in a final volume of 100 µl containing 20 µl buffer (250 mM MES pH 6.9; 2 mM EGTA; 5 mM Mg-Acetate; 50 mM NaCl), 10 µl BSA (10 mg/ml); 10 µl DTT (100 mM); 10 µl [γ-^{32}P] ATP (1 mM; specific activity 300-400 cpm/pmol), 10 µl cGMP (1 mM) or water, 10 µl appropriate peptide solution, and 20 µl PKG (5 mM MES, pH 7.0; 0.2 mM EDTA; 0.5 mg/ml BSA) to a final concentration of 2.6 nM. Fifty five-microliter aliquots were spotted on 2 x 2 cm phospho-cellulose paper strips (P-81 Whatman), extensively washed in 75 mM phosphoric acid, and the dried strips were subjected to scintillation counting. Peptide

(TQAKRKKSLAMA, (Dostmann et al., 2000)) concentrations ranged from 125 nM to saturating levels, and all assays were run in duplicate. Similar procedures were used to determine the K_a values. Ten-microliter aliquots of peptide (200 µM) were added to each assay, and the cGMP concentrations varied from 1 nM to saturating levels.

cGMP binding and dissociation

cGMP binding was assayed by incubating PKG enzyme (25 nM) for 90 minutes at 4°C with various concentrations of [^{3}H]-GMP, before precipitating and filtering as described previously (Dostmann et al., 1996; Ruth et al., 1991). Similar procedures were used to follow cGMP dissociation. Proteins were incubated at 4°C for 90 min in the presence of 250 nM [^{3}H]-cGMP and dissociation was initiated by the addition of 10 µM cold cGMP. Hill analysis was performed to determine Hill coefficients (n_H) with the $\log[b/(b_{max}-b)]$ plotted against the log of the cyclic nucleotide concentration [M], where b indicates fractional cGMP binding. Skatchard analysis was used to determine single binding site affinities by plotting [cGMP (bound/free)] against bound cGMP.

Electrospray ionization mass spectrometry (ESI)

Mass spectra of intact protein or cGMP-protein complexes were recorded on a time-of-flight (TOF) mass spectrometer (Micromass LCT classic model, Waters, Manchester, UK), fitted with a nano-electrospray source (Waters, Manchester, UK). Samples were introduced by means of Au/Pd coated borosilicate capillaries (Cat. No. ES380, Proxeon Biosystems, Odense, Denmark). Data were recorded in the positive ion mode between

m/z 3000 - 8000 under conditions of increased pressure in the source and intermediate pressure regions measured by built-in gauges in the mass spectrometer (Pirani gauge 7 mBar and Penning gauge 9 x 10^{-7} mBar) (Pinkse et al., 2004; Tahallah et al., 2001) and processed using the MassLynx 4.0 software (Waters, Manchester, UK). Nanoflow electrospray voltages were optimized for transmission of larger multimer protein assemblies (capillary voltage 1800 -1900 V and cone voltage 120-140 V). For sample preparation, PKG was buffer exchanged to a volatile buffer containing 200 mM ammonium acetate (pH 6.7) with Ultrafree-0.4 centrifugal filter units (5000 NMWL, Millipore, Bedford, MA, USA) and concentrated to 5 μM final. cGMP (20 μM final concentration), when applied, was also dissolved in this buffer and preincubated with PKG on ice for 5 min before analysis by ESI.

Acknowledgement

We thank Dr. Kathleen Trybus for providing SF9-insect cells. This work was supported by grants from the NIH (HL68891) and the NSF (MCB-9983097) to WRD.

Table 1: cGMP binding kinetics and stoichiometry of PKG mutants and wildtype

PKG	N[1]	K_D[2] [nM]	K_D[3] [nM]		n_H[4]
			Site A	Site B	
WT	1.6 ± 0.2	40	6	110	1.5
G167E	0.8 ± 0.1	382	-	327	0.6
E168G	0.6 ± 0.05	195	-	197	0.8
G291E	0.8 ± 0.1	26	29	-	0.9
E292G	0.7 ± 0.1	18	21	-	0.9
R177K	1.5 ± 0.2	172	-	-	1.1
R301K	1.7 ± 0.2	12	-	-	1.1

[1] N = Stoichiometry; [2]: from [^{3}H]-cGMP binding assays; [3]: from Skatchard analysis;

[4] Hill coefficient; the values represent the mean ± SEM of 6 to 9 experiments.

Table 2: Dissociation kinetics of PKG mutants and wildtype

PKG	k_{-1} [min^{-1}]		$\tau_{1/2}$ [min]	
	Site A	Site B	Site A	Site B
WT	0.01 ± 0.005	5.5 ± 0.3	110	0.18
G167E	-	11.8 ± 0.1	-	0.09
E168G	-	22.2 ± 0.1	-	0.05
G291E	0.01 ± 0.003	-	80	-
E292G	0.01 ± 0.001	-	90	-
R177K	0.02 ± 0.003	6.7 ± 0.2.	55	0.15
R301K	0.07 ± 0.002	8.5 ± 0.2	15	0.12

The values represent the mean ± SEM of 6 to 9 experiments.

Table 3: Catalytic activity of PKG mutants and wildtype

PKG	Activation		Substrate turn-over	
	K_a [nM]	v_{max} [μmol x mg^{-1} x min^{-1}]	K_M [nM]	v_{max} [μmol x mg^{-1} x min^{-1}]
WT	53 ± 4	9.7 ± 0.2	705 ± 20	10.5 ± 1.3
G167E	-	1.6 ± 0.3	150 ± 4	2.9 ± 0.3
E168G	-	2.7 ± 0.1	310 ± 5	3.0 ± 0.3
G291E	18 ± 3	10.4 ± 0.2	654 ± 21	9.7 ± 1.0
E292G	37 ± 5	10.2 ± 0.4	968 ± 26	8.9 ± 0.3
R177K	620 ± 10	12.1 ± 0.1	653 ± 15	11.6 ± 0.2
R301K	16 ± 2	11.7 ± 0.5	890 ± 33	11.1 ± 0.5

The values represent the mean ± SEM of 6 to 9 experiments.

Figure legends

Figure 1: (A) Sequence alignment of PKG I α and PKA I α cyclic nucleotide binding sites; asterixes denote identical amino-acids, and residues targeted for site specific mutagenesis for this study are indicated with arrows. (B) Domain composition of PKG I α. (C) 10% SDS-PAGE of PKG I α wildtype (WT) and all affinity-purified mutants (1-5 µg protein per lane). (D) Stoichiometry of wild type and single-site cyclic nucleotide binding mutants using [^{3}H]-cGMP binding assays (see Methods).

Figure 2: Native electrospray ionization mass spectra of PKG wildtype (A, B) and mutants E292G (C, D) and E168G (E, F) in the absence (left) and presence (right) of 20 µM cGMP. The mass spectra indicate distribution of charge state, the corresponding insets show the respective de-convoluted mass spectra. Peaks marked with asterixes indicate unidentified proteins.

Figure 3: Kinetic characterization of PKG mutants G167E (Δ) and E168G (▼) in comparison to PKG wildtype (■). (A) [^{3}H]-cGMP binding studies with (B) Skatchard and (C) Hill analysis. (D, E) [^{3}H]-cGMP dissociation from (D) slow and (E) fast cGMP binding sites A and B, respectively. (F) cGMP dependent kinase activation of (G) PKG site A mutants.

Figure 4: Kinetic characterization of PKG mutants G291E (▲) and E292G (□) in comparison to PKG wildtype (■). (A) [^{3}H]-cGMP binding studies with (B) Skatchard and

(C) Hill analysis. (D, E) [^{3}H]-cGMP dissociation from (D) slow and (E) fast cGMP binding sites A and B, respectively. (F) cGMP dependent kinase activation of (G) PKG site B mutants.

Figure 5: Substrate (LAMA, see Methods)-dependent kinase activity of PKG wildtype (■), E168G (▼) and E292G (◆).

Figure 6: Kinetic characterization of PKG mutants R177K (x) and R301K (●)) in comparison to PKG wildtype (■). (A) cGMP dependent kinase activation (B) [^{3}H]-cGMP binding studies with (C) Hill analysis. (D) [^{3}H]-cGMP dissociation from (D) slow and fast sites A and B, respectively.

Figure 7: Model for activation of (A) site A knock-out mutants, (B) site B knock-out mutants and (C) PKG wildtype.

Figure 1:

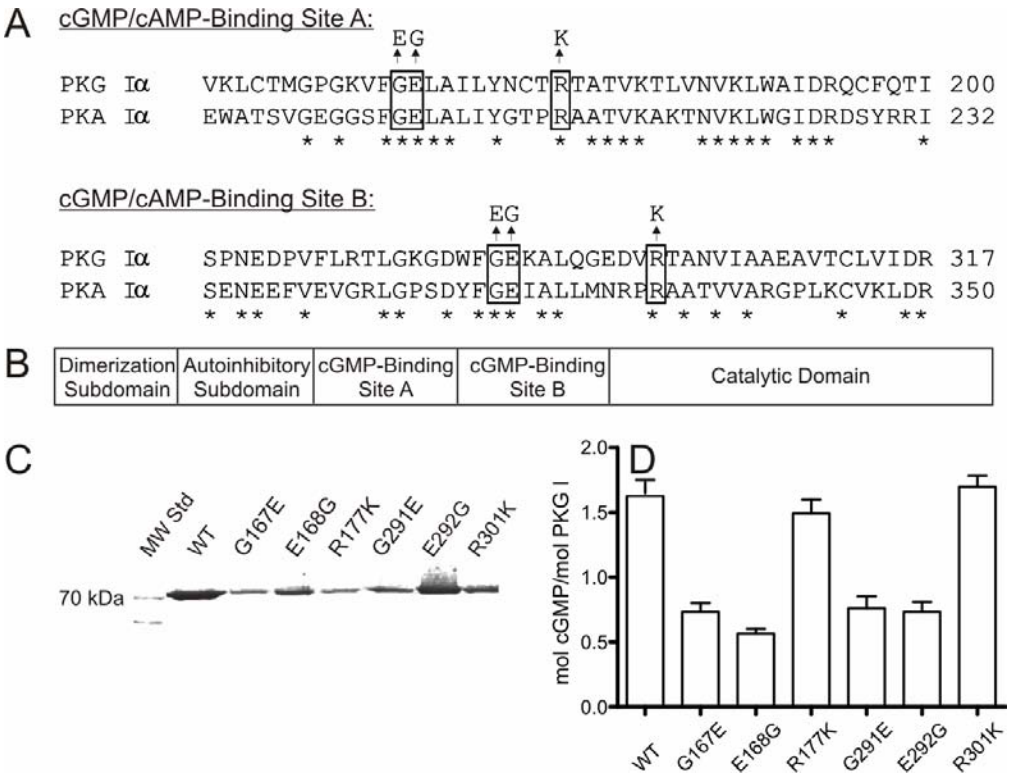
A
cGMP/cAMP-Binding Site A:
EG
K
PKG Iα VKLCTMGPGKVFGELAILYNCTRTATVKTLVNVKLWAIDRQCFQTI 200
PKA Iα EWATSVGEGGSFGELALIYGTPRAATVKAKTNVKLWGIDRDSYRRI 232
cGMP/cAMP-Binding Site B:
EG
K
PKG Iα SPNEDPVFLRTLGKGDWFGEKALQGEDVRTANVIAAEAVTCLVIDR 317
PKA Iα SENEEFVEVGRLGPSDYFGEIALLMNRPRAATVVARGPLKCVKLDR 350
B
Dimerization Subdomain
Autoinhibitory Subdomain
cGMP-Binding Site A
cGMP-Binding Site B
Catalytic Domain
C
MW Std
WT
G167E
E168G
R177K
G291E
E292G
R301K
70 kDa
D
mol cGMP/mol PKG I
2.0
1.5
1.0
0.5
0.0
WT
G167E
E168G
R177K
G291E
E292G
R301K

Figure 2:

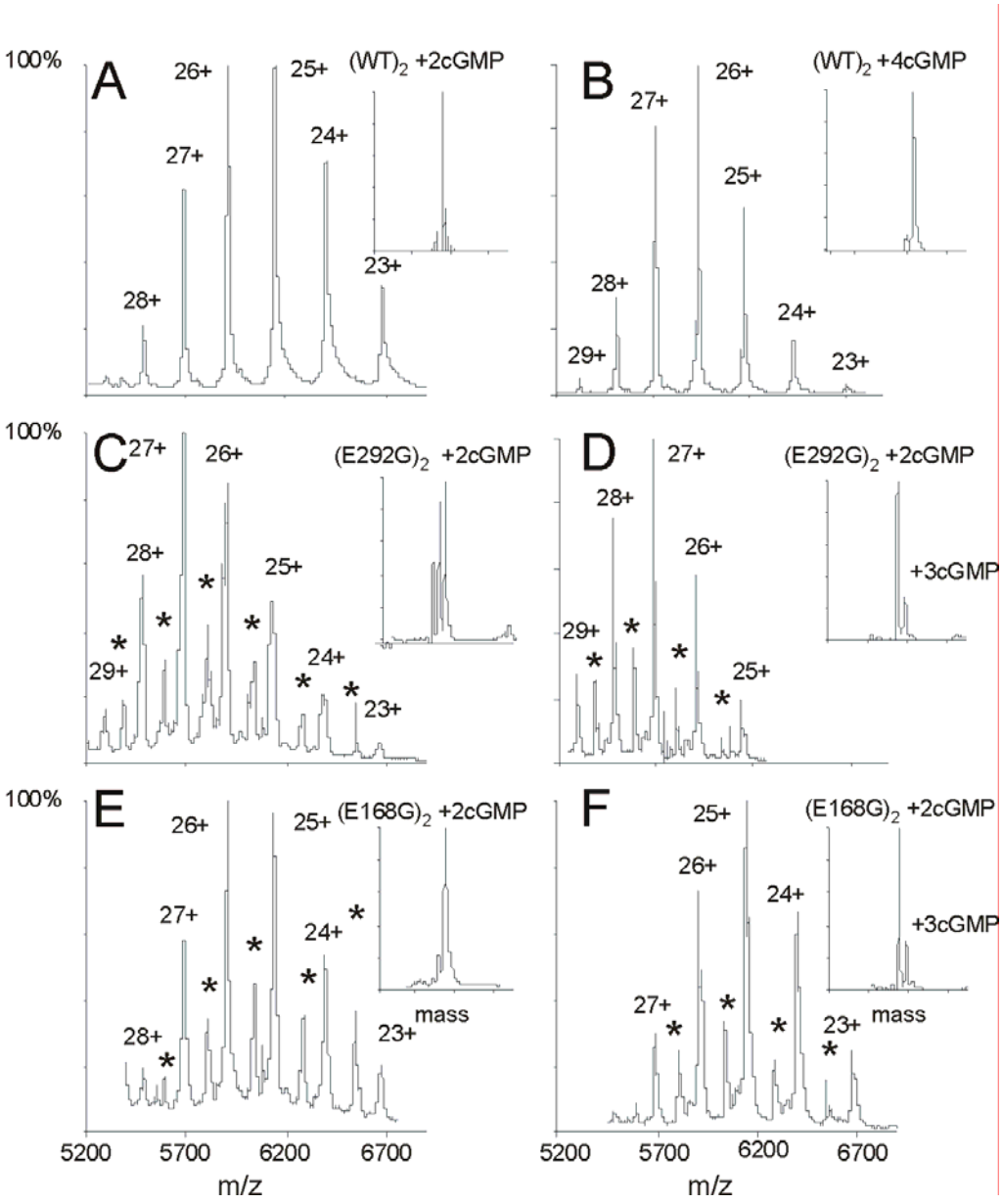
100%
A
26+
25+
(WT)2 +2cGMP
27+
24+
28+
23+
B
27+
26+
(WT)2 +4cGMP
25+
28+
24+
29+
23+
100%
C
27+
26+
(E292G)2 +2cGMP
28+
25+
29+
24+
23+
D
27+
(E292G)2 +2cGMP
28+
26+
+3cGMP
29+
25+
100%
E
26+
25+
(E168G)2 +2cGMP
27+
24+
mass
28+
23+
F
25+
(E168G)2 +2cGMP
26+
24+
+3cGMP
27+
23+
mass
5200
5700
6200
6700
m/z
5200
5700
6200
6700
m/z

Figure 3:

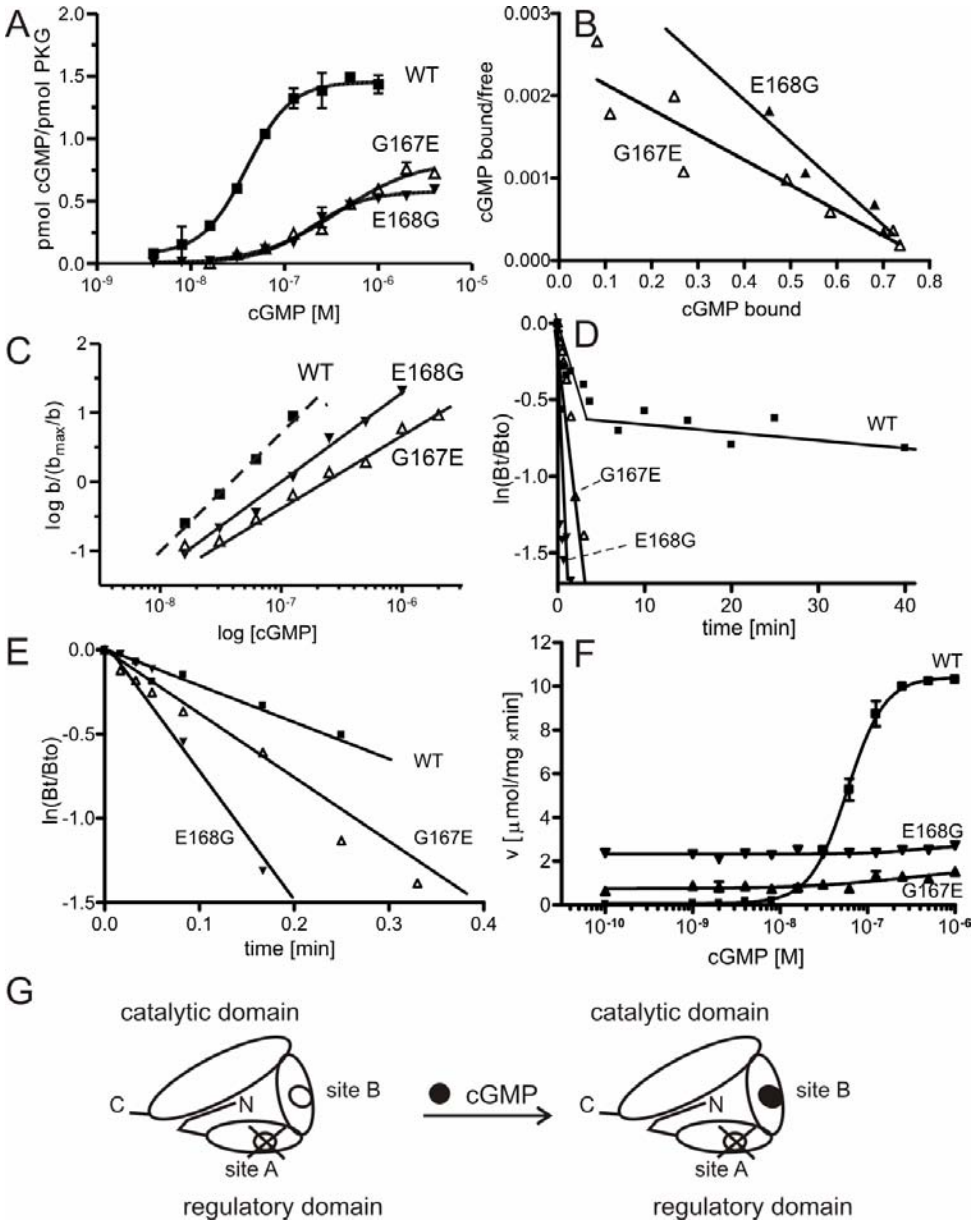
A
pmol cGMP/pmol PKG
cGMP [M]
WT
G167E
E168G
B
cGMP bound/free
cGMP bound
E168G
G167E
C
log b/(b_max/b)
log [cGMP]
WT
E168G
G167E
D
ln(Bt/Bto)
time [min]
WT
G167E
E168G
E
ln(Bt/Bto)
time [min]
WT
E168G
G167E
F
v [µmol/mg x min]
cGMP [M]
WT
E168G
G167E
G
catalytic domain
C
N
site B
site A
regulatory domain
cGMP
catalytic domain
C
N
site B
site A
regulatory domain

Figure 4:

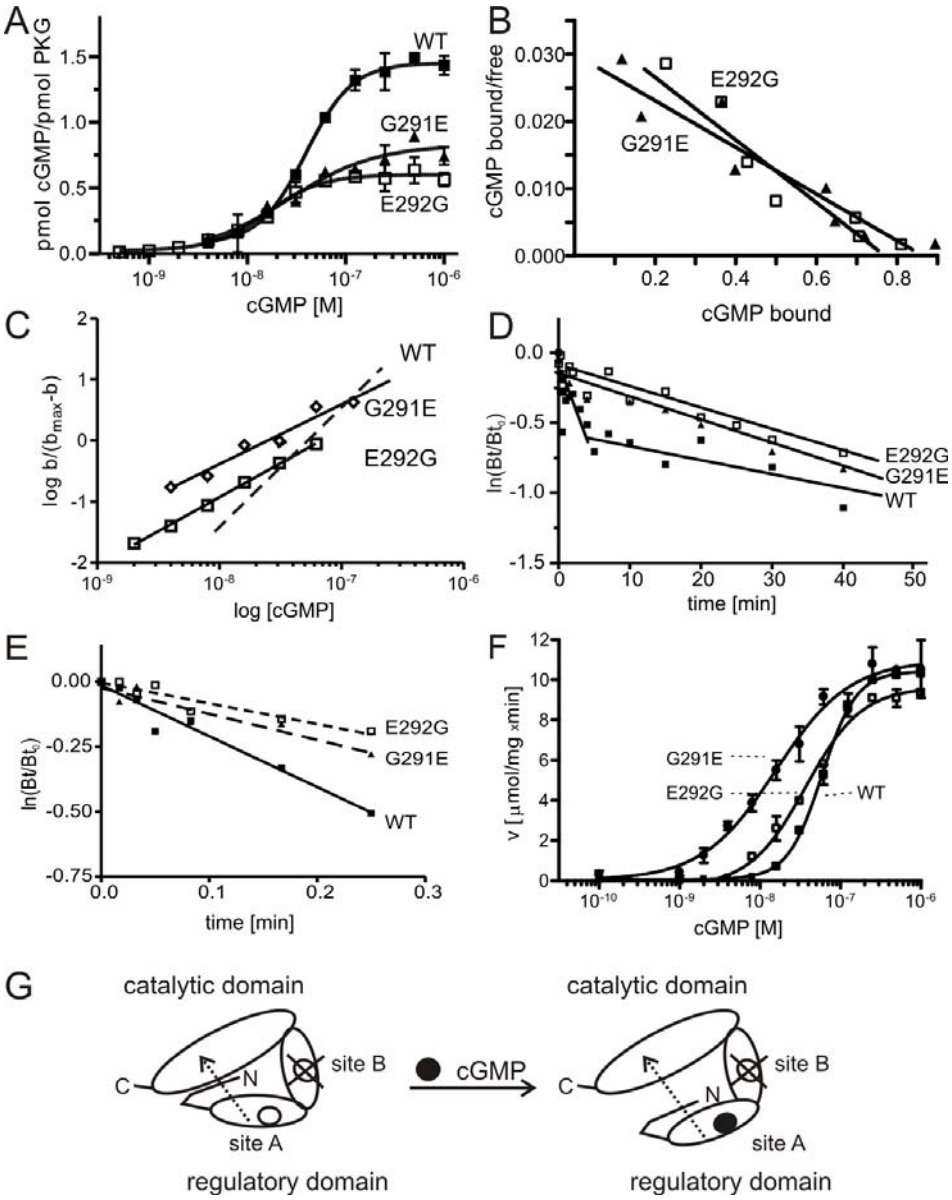
A
pmol cGMP/pmol PKG
WT
G291E
E292G
cGMP [M]
B
cGMP bound/free
E292G
G291E
cGMP bound
C
log b/(b_max-b)
WT
G291E
E292G
log [cGMP]
D
ln(Bt/Bt0)
E292G
G291E
WT
time [min]
E
ln(Bt/Bt0)
E292G
G291E
WT
time [min]
F
v [µmol/mg xmin]
G291E
E292G
WT
cGMP [M]
G
catalytic domain
site B
C
N
site A
regulatory domain
cGMP
catalytic domain
site B
C
N
site A
regulatory domain

Figure 5:

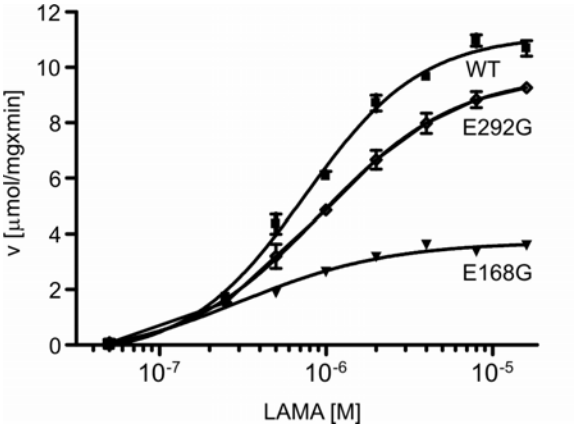

Figure 6:

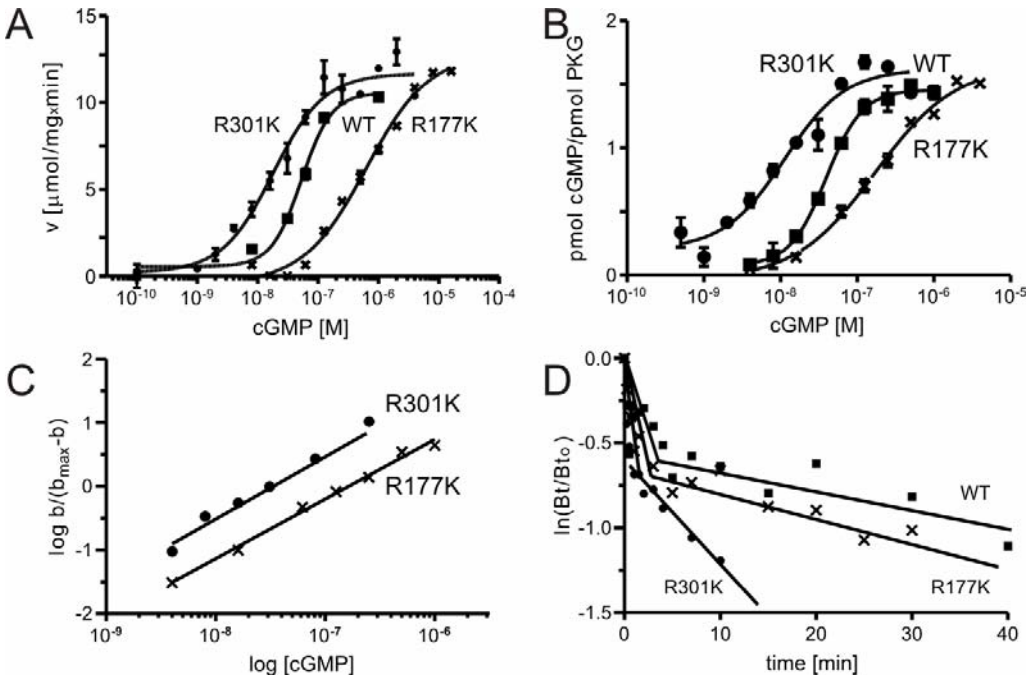
A
v [µmol/mg x min]
R301K
WT
R177K
cGMP [M]
B
pmol cGMP/pmol PKG
R301K
WT
R177K
cGMP [M]
C
log b/(b_max-b)
R301K
R177K
log [cGMP]
D
ln(Bt/Bt0)
WT
R301K
R177K
time [min]

Figure 7:

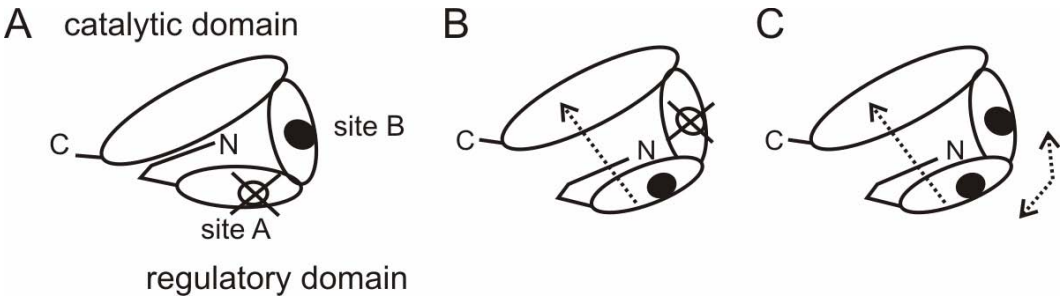
A
catalytic domain
C
N
site B
site A
regulatory domain
B
C
N
C
C
N

References:

Berman HM, Ten Eyck LF, Goodsell DS, Haste NM, Kornev A and Taylor SS. The cAMP binding domain: an ancient signaling module. *Proc Natl Acad Sci U S A* 102(1): 45-50, 2005.

Brostrom CO, Corbin JD, King CA and Krebs EG. Interaction of the subunits of adenosine 3':5'-cyclic monophosphate-dependent protein kinase of muscle. *Proc Natl Acad Sci U S A* 68(10): 2444-7, 1971.

Bubis J, Neitzel JJ, Saraswat LD and Taylor SS. A point mutation abolishes binding of cAMP to site A in the regulatory subunit of cAMP-dependent protein kinase. *J Biol Chem* 263(20): 9668-73, 1988.

Bubis J and Taylor SS. Correlation of photolabeling with occupancy of cAMP binding sites in the regulatory subunit of cAMP-dependent protein kinase I. *Biochemistry* 26(12): 3478-86, 1987.

Corbin JD and Rannels SR. Perturbation and structural organization of the two intrachain cAMP binding sites of cAMP-dependent protein kinase II. *J Biol Chem* 256(22): 11671-6, 1981.

Diller TC, Madhusudan, Xuong NH and Taylor SS. Molecular basis for regulatory subunit diversity in cAMP-dependent protein kinase: crystal structure of the type II beta regulatory subunit. *Structure* 9(1): 73-82, 2001.

Doskeland SO and Ogreid D. Ammonium sulfate precipitation assay for the study of cyclic nucleotide binding to proteins. *Methods Enzymol* 159: 147-50, 1988.

Doskeland SO, Vintermyr OK, Corbin JD and Ogreid D. Studies on the interactions between the cyclic nucleotide-binding sites of cGMP-dependent protein kinase. *J Biol Chem* 262(8): 3534-40, 1987.

Dostmann WR, Koep N and Endres R. The catalytic domain of the cGMP-dependent protein kinase Ialpha modulates the cGMP-binding characteristics of its regulatory domain. *FEBS Lett* 398(2-3): 206-10, 1996.

Dostmann WR, Taylor MS, Nickl CK, Brayden JE, Frank R and Tegge WJ. Highly specific, membrane-permeant peptide blockers of cGMP-dependent protein kinase Ialpha inhibit NO-induced cerebral dilation. *Proc Natl Acad Sci U S A* 97(26): 14772-7, 2000.

Dostmann WR and Taylor SS. Identifying the molecular switches that determine whether (Rp)-cAMPS functions as an antagonist or an agonist in the activation of cAMP-dependent protein kinase I. *Biochemistry* 30(35): 8710-6, 1991.

Dostmann WR, Taylor SS, Genieser HG, Jastorff B, Doskeland SO and Ogreid D. Probing the cyclic nucleotide binding sites of cAMP-dependent protein kinases I and II with analogs of adenosine 3',5'-cyclic phosphorothioates. *J Biol Chem* 265(18): 10484-91, 1990.

Erlichman J, Rubin CS and Rosen OM. Physical properties of a purified cyclic adenosine 3':5'-monophosphate-dependent protein kinase from bovine heart muscle. *J Biol Chem* 248(21): 7607-9, 1973.

Feil R, Muller S and Hofmann F. High-level expression of functional cGMP-dependent protein kinase using the baculovirus system. *FEBS Lett* 336(1): 163-7, 1993.

Francis SH and Corbin JD. Structure and function of cyclic nucleotide-dependent protein kinases. *Annu Rev Physiol* 56: 237-72, 1994.

Francis SH, Noblett BD, Todd BW, Wells JN and Corbin JD. Relaxation of vascular and tracheal smooth muscle by cyclic nucleotide analogs that preferentially activate purified cGMP-dependent protein kinase. *Mol Pharmacol* 34(4): 506-17, 1988.

Gill GN and Garren LD. Role of the receptor in the mechanism of action of adenosine 3':5'-cyclic monophosphate. *Proc Natl Acad Sci U S A* 68(4): 786-90, 1971.

Gill GN, Holdy KE, Walton GM and Kanstein CB. Purification and characterization of 3':5'-cyclic GMP-dependent protein kinase. *Proc Natl Acad Sci U S A* 73(11): 3918-22, 1976.

Gorman KB and Steinberg RA. Spectrum of spontaneous missense mutations causing cyclic AMP-resistance phenotypes in cultured S49 mouse lymphoma cells differs markedly from those of mutations induced by alkylating mutagens. *Somat Cell Mol Genet* 20(4): 301-11, 1994.

Herberg FW, Taylor SS and Dostmann WR. Active site mutations define the pathway for the cooperative activation of cAMP-dependent protein kinase. *Biochemistry* 35(9): 2934-42, 1996.

Hofmann F, Gensheimer HP and Gobel C. cGMP-dependent protein kinase. Autophosphorylation changes the characteristics of binding site 1. *Eur J Biochem* 147(2): 361-5, 1985.

Kemp BE, Bylund DB, Huang TS and Krebs EG. Substrate specificity of the cyclic AMP-dependent protein kinase. *Proc Natl Acad Sci U S A* 72(9): 3448-52, 1975.

Kim C, Cheng CY, Saldanha SA and Taylor SS. PKA-I holoenzyme structure reveals a mechanism for cAMP-dependent activation. *Cell* 130(6): 1032-43, 2007.

Kim C, Xuong NH and Taylor SS. Crystal structure of a complex between the catalytic and regulatory (RIalpha) subunits of PKA. *Science* 307(5710): 690-6, 2005.

Kotera J, Grimes KA, Corbin JD and Francis SH. cGMP-dependent protein kinase protects cGMP from hydrolysis by phosphodiesterase-5. *Biochem J* 372(Pt 2): 419-26, 2003.

Lincoln TM, Dills WL, Jr. and Corbin JD. Purification and subunit composition of guanosine 3':5'-monophosphate-dependent protein kinase from bovine lung. *J Biol Chem* 252(12): 4269-75, 1977.

Monken CE and Gill GN. Structural analysis of cGMP-dependent protein kinase using limited proteolysis. *J Biol Chem* 255(15): 7067-70, 1980.

Murphy CS and Steinberg RA. Hotspots for spontaneous and mutagen-induced lesions in regulatory subunit of cyclic AMP-dependent protein kinase in S49 mouse lymphoma cells. *Somat Cell Mol Genet* 11(6): 605-15, 1985.

Neitzel JJ, Dostmann WR and Taylor SS. Role of MgATP in the activation and reassociation of cAMP-dependent protein kinase I: consequences of replacing the essential arginine in cAMP binding site A. *Biochemistry* 30(3): 733-9, 1991.

Ogreid D and Doskeland SO. Protein kinase II has two distinct binding sites for cyclic AMP, only one of which is detectable by the conventional membrane-filtration method. *FEBS Lett* 121(2): 340-4, 1980.

Ogreid D and Doskeland SO. The kinetics of association of cyclic AMP to the two types of binding sites associated with protein kinase II from bovine myocardium. *FEBS Lett* 129(2): 287-92, 1981.

Ogreid D, Doskeland SO, Gorman KB and Steinberg RA. Mutations that prevent cyclic nucleotide binding to binding sites A or B of type I cyclic AMP-dependent protein kinase. *J Biol Chem* 263(33): 17397-404, 1988.

Ogreid D, Doskeland SO and Miller JP. Evidence that cyclic nucleotides activating rabbit muscle protein kinase I interact with both types of cAMP binding sites associated with the enzyme. *J Biol Chem* 258(2): 1041-9, 1983.

Pfeifer A, Ruth P, Dostmann W, Sausbier M, Klatt P and Hofmann F. Structure and function of cGMP-dependent protein kinases. *Rev Physiol Biochem Pharmacol* 135: 105-49, 1999.

Pinkse MW, Heck AJ, Rumpel K and Pullen F. Probing noncovalent protein-ligand interactions of the cGMP-dependent protein kinase using electrospray ionization time of flight mass spectrometry. *J Am Soc Mass Spectrom* 15(10): 1392-9, 2004.

Reed RB, Sandberg M, Jahnsen T, Lohmann SM, Francis SH and Corbin JD. Fast and slow cyclic nucleotide-dissociation sites in cAMP-dependent protein kinase are transposed in type Ibeta cGMP-dependent protein kinase. *J Biol Chem* 271(29): 17570-5, 1996.

Reimann EM, Brostrom CO, Corbin JD, King CA and Krebs EG. Separation of regulatory and catalytic subunits of the cyclic 3',5'-adenosine monophosphate-dependent protein kinase(s) of rabbit skeletal muscle. *Biochem Biophys Res Commun* 42(2): 187-94, 1971.

Richie-Jannetta R, Busch JL, Higgins KA, Corbin JD and Francis SH. Isolated regulatory domains of cGMP-dependent protein kinase Ialpha and Ibeta retain dimerization and native cGMP-binding properties and undergo isoform-specific conformational changes. *J Biol Chem* 281(11): 6977-84, 2006.

Ruth P, Landgraf W, Keilbach A, May B, Egleme C and Hofmann F. The activation of expressed cGMP-dependent protein kinase isozymes I alpha and I beta is determined by the different amino-termini. *Eur J Biochem* 202(3): 1339-44, 1991.

Scholten A, Fuss H, Heck AJ and Dostmann WR. The hinge region operates as a stability switch in cGMP-dependent protein kinase I alpha. *Febs J* 274(9): 2274-86, 2007.

Scott JD. Cyclic nucleotide-dependent protein kinases. *Pharmacol Ther* 50(1): 123-45, 1991.

Steinberg RA, Gorman KB, Ogreid D, Doskeland SO and Weber IT. Mutations that alter the charge of type I regulatory subunit and modify activation properties of cyclic AMP-dependent protein kinase from S49 mouse lymphoma cells. *J Biol Chem* 266(6): 3547-53, 1991.

Steinberg RA, Russell JL, Murphy CS and Yphantis DA. Activation of type I cyclic AMP-dependent protein kinases with defective cyclic AMP-binding sites. *J Biol Chem* 262(6): 2664-71, 1987.

Su Y, Dostmann WR, Herberg FW, Durick K, Xuong NH, Ten Eyck L, Taylor SS and Varughese KI. Regulatory subunit of protein kinase A: structure of deletion mutant with cAMP binding domains. *Science* 269(5225): 807-13, 1995.

Tahallah N, Pinkse M, Maier CS and Heck AJ. The effect of the source pressure on the abundance of ions of noncovalent protein assemblies in an electrospray ionization orthogonal time-of-flight instrument. *Rapid Commun Mass Spectrom* 15(8): 596-601, 2001.

Takio K, Wade RD, Smith SB, Krebs EG, Walsh KA and Titani K. Guanosine cyclic 3',5'-phosphate dependent protein kinase, a chimeric protein homologous with two separate protein families. *Biochemistry* 23(18): 4207-18, 1984.

Taylor MK and Uhler MD. The amino-terminal cyclic nucleotide binding site of the type II cGMP-dependent protein kinase is essential for full cyclic nucleotide-dependent activation. *J Biol Chem* 275(36): 28053-62, 2000.

Taylor SS and Stafford PH. Characterization of adenosine 3':5'-monophosphate-dependent protein kinase and its dissociated subunits from porcine skeletal muscle. *J Biol Chem* 253(7): 2284-7, 1978.

Wall ME, Francis SH, Corbin JD, Grimes K, Richie-Jannetta R, Kotera J, Macdonald BA, Gibson RR and Trewhella J. Mechanisms associated with cGMP binding and activation of cGMP-dependent protein kinase. *Proc Natl Acad Sci U S A* 100(5): 2380-5, 2003.

Weber IT, Shabb JB and Corbin JD. Predicted structures of the cGMP binding domains of the cGMP-dependent protein kinase: a key alanine/threonine difference in evolutionary divergence of cAMP and cGMP binding sites. *Biochemistry* 28(14): 6122-7, 1989.

Weber IT, Steitz TA, Bubis J and Taylor SS. Predicted structures of cAMP binding domains of type I and II regulatory subunits of cAMP-dependent protein kinase. *Biochemistry* 26(2): 343-51, 1987.

Wolfe L, Francis SH and Corbin JD. Properties of a cGMP-dependent monomeric protein kinase from bovine aorta. *J Biol Chem* 264(7): 4157-62, 1989.

Woodford TA, Correll LA, McKnight GS and Corbin JD. Expression and characterization of mutant forms of the type I regulatory subunit of cAMP-dependent protein kinase. The effect of defective cAMP binding on holoenzyme activation. *J Biol Chem* 264(22): 13321-8, 1989.

Wu J, Jones JM, Nguyen-Huu X, Ten Eyck LF and Taylor SS. Crystal structures of RIalpha subunit of cyclic adenosine 5'-monophosphate (cAMP)-dependent protein kinase complexed with (Rp)-adenosine 3',5'-cyclic monophosphothioate and (Sp)-adenosine 3',5'-cyclic monophosphothioate, the phosphothioate analogues of cAMP. *Biochemistry* 43(21): 6620-9, 2004.

Zawadzki KM and Taylor SS. cAMP-dependent protein kinase regulatory subunit type IIbeta: active site mutations define an isoform-specific network for allosteric signaling by cAMP. *J Biol Chem* 279(8): 7029-36, 2004.

Zhao J, Trewhella J, Corbin J, Francis S, Mitchell R, Brushia R and Walsh D. Progressive cyclic nucleotide-induced conformational changes in the cGMP-dependent protein kinase studied by small angle X-ray scattering in solution. *J Biol Chem* 272(50): 31929-36, 1997.

CHAPTER THREE: STRUCTURAL CHARACTERIZATION OF PKG USING CRYSTALLOGRAPHY

Introduction

Within the family of cyclic nucleotide-dependent Ser/Thr protein kinases, PKG shares the closest sequence homology and domain structure with PKA (Figures 1 A, 2 A). In the past, X-ray crystallographic and NMR studies have proven invaluable to characterize the structure of PKA. The crystal structure of the catalytic subunit of PKA established for the first time the conserved structural features of the protein kinase superfamily (Knighton et al., 1991). The catalytic subunit is a globular protein consisting of two lobes - a highly dynamic small lobe that serves as an ATP binding site, and a large lobe that serves as a framework for the catalytic machinery and also as a docking scaffold for target proteins (substrates or inhibitors). The regulatory (R) subunit is highly dynamic and functions primarily as a cAMP receptor (Figure 1 C) (Su et al., 1995). The parallel, helical dimerization/docking (D/D) domain interacts with scaffold proteins, called A-kinase anchoring proteins (AKAPs) (Kinderman et al., 2006; Newlon et al., 2001). Following this domain is a variable and flexible linker region containing an inhibitor site that docks to the active-site cleft of the catalytic (C) subunit and two in-tandem cAMP-binding domains (A and B). The phosphate-binding cassette (PBC), a helix-loop region where cAMP binds, is the most conserved domain among all cyclic nucleotide binding proteins, which include PKA/PKG, catabolite activator protein, hyperpolarization-activated cyclic nucleotide-modulated channel, and exchange protein directly activated

by cAMP. The crystal structure of the PKA holoenzyme (Figure 1 D), recently published by Kim and colleagues (Kim et al., 2007; Kim et al., 2005), reveals in molecular detail the highly dynamic processes and conformational changes that need to occur during PKA activation.

In contrast, the mechanism of PKG activation is not very well described structurally. Hydrodynamic and small-angle x-ray scattering techniques have confirmed that cGMP binding induces significant conformational changes in the regulatory PKG domain (Richie-Jannetta et al., 2006; Wall et al., 2003; Zhao et al., 1997). The parallel, alpha-helical interactions of the N-terminal domains (Schnell et al., 2005) have been revealed using NMR and support an overall parallel orientation of the dimeric PKG holoenzyme (Figures 2 A, B). The structure of other functional domains, such as the cGMP binding sites and the catalytic domain, have not been characterized using crystallography or NMR.

Large quantities of protein are generally a pre-requisite for crystallographic screens. Since PKA can be easily expressed in bacteria, sufficient quantities can be generated for crystallographic studies. Conversely, PKG can only be over-expressed in a soluble form in a mammalian expression system (e.g. SF 9 insect cells), which generally results in lower protein yields compared to a bacterial expression system. The goal of this study was to develop a bacterial expression system for PKG deletion fragments in order to yield sufficient quantities of protein for crystallographic studies and in order to simplify the existing expression protocol. In addition, full-length PKG as well as deletion fragments were tested for crystallization.

Results

Crystallization of full-length PKG

First, highly concentrated PKG (5 mg/ml; Figure 3 A) was utilized to screen various crystallization conditions (Hampton Screen # 1 and #2). Out of several hundred conditions, four gave rise to crystals or crystal-like structures (Figures 3 B to E). Mixing of full-length PKG with Hampton Screen #1, condition #24 (HS-1/24) (0.2 M Calcium chloride dihydrate, 0.1 M Sodium acetate trihydrate pH 4.6, 20% v/v 2-Propanol) resulted in 3-dimensional, bi-refringent crystals that were 50 x 30 x 20 µm in size (Figure 3 B). The same type of crystals appeared when the enzyme storage buffer (without protein) was mixed with buffer #24 (Figure 3 B, insertion). Therefore, these crystals were comprised of salt, not protein. In Figure 3 C, full-length PKG was combined with HS-1/17 (0.2 M Lithium sulfate monohydrate, 0.1 M Tris hydrochloride pH 8.5 and 30% w/v Polyethylene glycol 4,000). After several days of incubation, granula and spherulites (50-80 µm diameter) appeared. These micro-structures were indicative of protein-crystals, since the control-drop with enzyme storage buffer produced a different form of salt precipitation (Figure 3 C, insertion). Similarly, addition of PKG to HS-1/16 (0.1 M HEPES sodium pH 7.5 and 1.5 M Lithium sulfate monohydrate) gave rise to a mixture of protein precipitation and 30-50 µm crystals (Figure 3 D). These crystals most likely consist of protein, because the control drop without protein produced a differently shaped salt precipitation. When full-length PKG was combined and incubated with HS-1/13 (0.2 M Sodium citrate tribasic dihydrate, 0.1 M Tris hydrochloride pH 8.5, 30% v/v Polyethylene glycol 400), 2-dimensional crystal-plates (50 x 30 µm in size (Figure 3E))

grew after several days. These crystals were most promising, since the control drop was lacking any (salt-) crystal formation (Figure 3 E, insertion). Therefore, the crystal-plates in Figure 3 E can be attributed to PKG protein.

Deletion fragments of PKG are suitable for bacterial expression and form the basis for crystallization

For X-ray crystallographic studies, vast amounts of protein are necessary to screen numerous crystallization conditions. So far, the amount of PKG protein has been a limiting factor for crystallization, since PKG can only be expressed in highly sophisticated insect cell expression systems (e.g. SF 9). Since it is more challenging to produce sufficient amounts of protein in SF9 cells, our goal was to establish a bacterial expression system for PKG deletion fragments, focusing on the regulatory domain of PKG. These PKG deletion mutants would then form the basis for crystallographic studies.

We first focused on the cGMP-binding site B (Figure 4 A) and cloned three different size constructs into the bacterial expression vector pET19b: construct B1 (E227-G327), B2 (E227-Y336) and B3 (E227-K342). The different constructs were tested for expression in E.coli BLR (Figure 4 B). Comparison to non-induced cells revealed that constructs B1-B3 could be successfully over-expressed in bacteria with high yields (approximately 5 mg per 50 ml E.coli).

After successfully establishing a bacterial expression system for a single cGMP binding site, we attempted to clone both cGMP binding sites into the bacterial vector pET

19b (Figure 5 A) and over-express it in bacteria. Two different size constructs have been designed, RS3 (Q110-G327) and RS4 (Q110-K342), and both constructs were tested for expression and solubility. As shown in Figure 5 B, RS3 and RS4 could both be over-expressed in E.coli BLR after induction with 0.4 mM IPTG. Comparing samples of homogenate, supernatant and pellet of RS4 revealed that it is only partly expressed in a soluble form in bacteria (Figure 5 C). About 30% of protein was detected in the pellet and could not be recovered. Construct RS4 was over-expressed in bacteria and purified to 2.5 mg/ml final concentration. Next, RS4 was screened for crystallization using Hampton Research Screens #1 and #2. Crystal-clusters were only seen for RS4 in combination with 0.2 M Calcium chloride dihydrate, 0.1 M Sodium acetate trihydrate pH 4.6 and 20% v/v 2-Propanol (Figure 5 D). To increase the likelihood of crystal formation in future studies, crystallization screens should be repeated using higher protein concentrations. In addition, the crystallization condition that resulted in RS4 crystals (Figure 5 D) should be refined in varying pH, incubation temperature, salt- and precipitant concentrations.

Discussion

Site-specific mutagenesis, hydrodynamic studies, as well as small angle x-ray scattering approaches have been used extensively to gain insight into PKG folding (Richie-Jannetta et al., 2006; Wall et al., 2003; Zhao et al., 1997). In this study, we attempted to address this question by crystallizing full-length PKG as well as PKG-derived deletion fragments. As shown in Figures 3 B to E, we were able to obtain PKG crystals and crystal-like structures. The crystallization conditions that produced PKG crystals (Figure 3 E) or crystal-like structures (Figures 3 C, D) need to be refined in future studies by varying pH, incubation temperature, salt- and precipitant concentrations. Fine-tuning these conditions and utilizing macro- or micro- seeding may result in enlarged PKG crystals that qualify for diffraction and ultimately reveal a structural model for PKG. There are still some challenges associated with crystallizing full-length PKG, such as protein availability through production in SF9 cells, as generation of well-diffracting crystals. Therefore, having smaller fragments of PKG serves multiple purposes: smaller deletion fragments are more likely to be successfully expressed in bacteria, and smaller proteins are also more likely to form crystals that are diffracting to high resolution. In addition, removal of the N-terminal domain in the deletion fragments prevents PKG-dimer formation as well as autophosphorylation events. The molecular structure of the cGMP binding sites could elucidate very elegantly the mechanism of cGMP binding and PKG activation. Furthermore, crystals of either full-length PKG or smaller PKG fragments could be used for soaking in PKG-inhibitors such as DT2 (Dostmann et al., 2000; Taylor et al., 2004) and PKG-activators. This would not only

extend our knowledge about the detailed molecular structure of PKG, but also answer fundamental physiological questions about PKG activation and inhibition.

The static crystal structures will provide essential clues as to the conformational versatility of PKG. However, complementary solution methods will be necessary to study the dynamics of PKG in a more physiological environment. To meet this challenge, we have used a variety of techniques, in addition to crystallography, to probe the structure and function of PKG. We have used single point mutants to study cGMP binding and kinase activation in vitro (Chapter 2), and non-FRET based indicators to monitor PKG activity and cGMP signaling in living cells and in intact tissue (Chapters 4 and 5). Such strategies are designed to unravel the complexity of PKG and cGMP signaling networks.

Materials and Methods

Plasmid construction and bacterial expression

PKG deletion fragments were constructed by inserting different size constructs of cGMP binding site B (B1: E227-G327; B2: E227-Y336; B3: E227-K342) or different size constructs of the regulatory domain (RS3: Q110-G327; RS4: Q110-K342) of bovine PKG I α into the bacterial expression vector pET19b (Novagen). All constructs were inserted into the BamHI and EcoRI sites of pET19b, multiplied in E.coli DH5α, and expressed in E.coli BLR (invitrogen). To test for bacterial expression, E.Coli BLR transformed with PKG-containing pET19b vectors were cultured at 37°C for 12h after protein induction with 0.4 mM isopropyl-β-D-thiogalactoside (IPTG). After centrifugation, PKG deletion fragment RS4 was purified using cyclic nucleotide affinity chromatography as described previously (Feil et al., 1993). Purified PKG deletion fragment RS4 (RS 4: 6 mg per 500 ml E.coli) was concentrated using Pall-Filtron concentrators to 2.5 mg/ml final concentration and applied for crystallization screens.

Expression in SF9 cells

Full-length PKG was cloned into the pFAST-BAC mammalian expression vector (invitrogen), over-expressed in SF 9 cells and purified using cyclic nucleotide affinity chromatography as described previously (Feil et al., 1993). Purified protein (5 mg per 750 ml SF9-cells) was concentrated using Pall-Filtron concentrators to 5 mg/ml final concentration and utilized for crystallization screens.

Crystallization

Hampton Screens # 1 and #2 (Hampton Research, (Jancarik and Kim, 1991)) were used to screen various crystallization conditions, mixing protein and buffer in a 1:1 ratio and incubating at room temperature for several days using the hanging drop method. As control, enzyme storage buffer was mixed with the crystallization buffer, in order to distinguish between salt crystals and protein crystals.

Figure Legends

Figure 1: Structural characterization of cAMP-dependent protein kinase (PKA). (A) Schematic representation of PKA. (B) Catalytic subunit with small (white) and large lobe (tan) bound to inhibitor peptide and ATP (red) (Taylor et al., 2005). The consensus site peptide RRGAI docks to the active site cleft. (C) Model of the dimeric RIα subunits showing the structured domains and the flexible linker (Taylor et al., 2005). The D/D domain structure was solved by NMR and the cyclic nucleotide binding domains (CNB (A) and (B)) were solved by crystallography. The flexibility of the linker was demonstrated by fluorescence anisotropy where the red dots indicate sites where the fluorescent probes are attached. (D) Crystal structure of a complex between the regulatory (RIα) and catalytic subunits of PKA (Kim et al., 2005).

Figure 2: Domain structure of cGMP-dependent protein kinase (PKG). (A) Schematic representation of PKG. (B) Structure of N-terminal dimerization sites (Schnell et al., 2005).

Figure 3: Crystallization of full-length PKG. (A) 5-20 µg PKG were loaded on 10% SDS-PAGE. Crystallization of PKG (5 mg/ml) using Hampton Research Screen condition 24 (B), condition 17 (C), condition 16 (D) and 13 (E). Insertions in the upper left depict a mixture of enzyme storage buffer with the screened condition from Hampton Research.

Figure 4: Bacterial expression of cGMP binding site B. (A) Schematic representation of PKG highlighting cGMP binding site B (boxed area in green). (B) Comparison of non-induced (lane 2) and IPTG-induced E.coli BLR cells that were transformed with pET19b-B1 (lane 3), pET19b-B2 (lane 4) or pET19b-B3 (lane 5).

Figure 5: Crystallization of PKG regulatory domain. (A) Schematic representation of PKG highlighting the regulatory domain (boxed area in green). (B) Comparison of non-induced and IPTG-induced E.coli BLR cells that were transformed with empty pET19b vector (lanes 2-3), pET19b-RS3 (lanes 4-5) or pET19b-RS4 (lanes 6-7). (C) Protein expression of RS4 was tested for solubility by comparing samples from homogenate (lane 2), supernatant (lane 3) and pellet (lane 4). (D) Crystallization of RS4 (2.5 mg/ml) using condition 24 of Hampton Screen.

Figure 1:

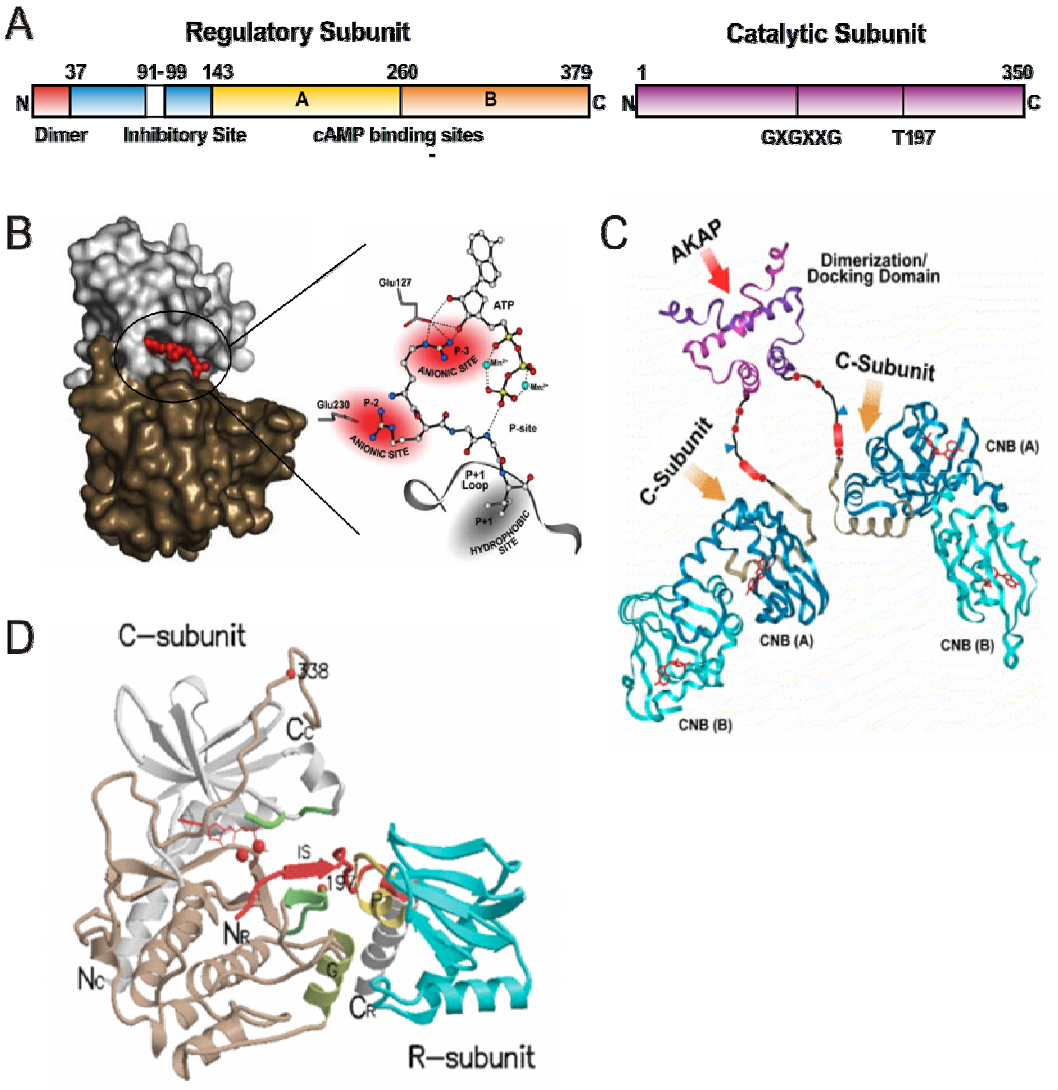
A
Regulatory Subunit
37
91-99
143
260
379
N
A
B
C
Dimer
Inhibitory Site
cAMP binding sites
Catalytic Subunit
1
350
N
C
GXGXXG
T197
B
Glu127
ATP
P-3
ANIONIC SITE
Glu230
P-2
ANIONIC SITE
P-site
P+1 Loop
P+1
HYDROPHOBIC SITE
C
AKAP
Dimerization/ Docking Domain
C-Subunit
C-Subunit
CNB (A)
CNB (A)
CNB (B)
CNB (B)
D
C–subunit
338
CC
IS
199
PB
NR
NC
CR
R–subunit

Figure 2:

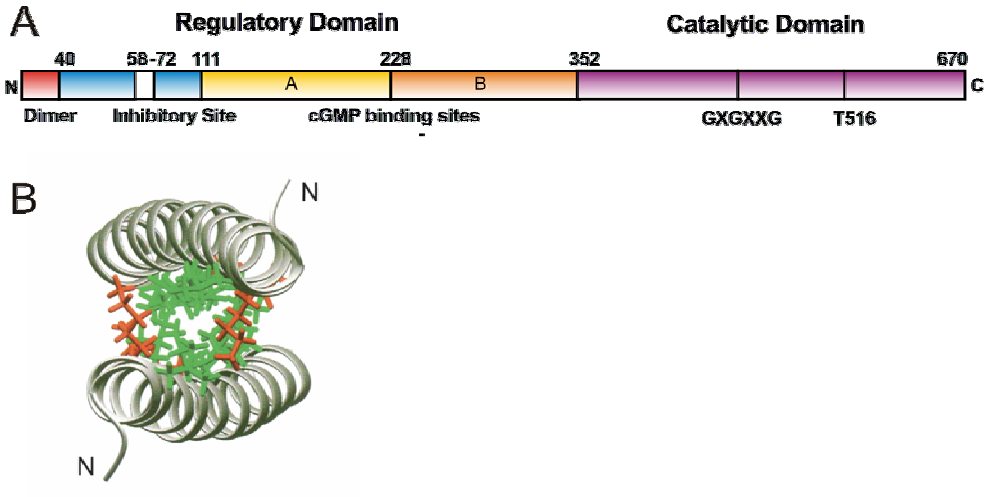
A
Regulatory Domain
Catalytic Domain
40
58-72
111
228
352
670
N
A
B
C
Dimer
Inhibitory Site
cGMP binding sites
GXGXXG
T516
B
N
N

Figure 3:

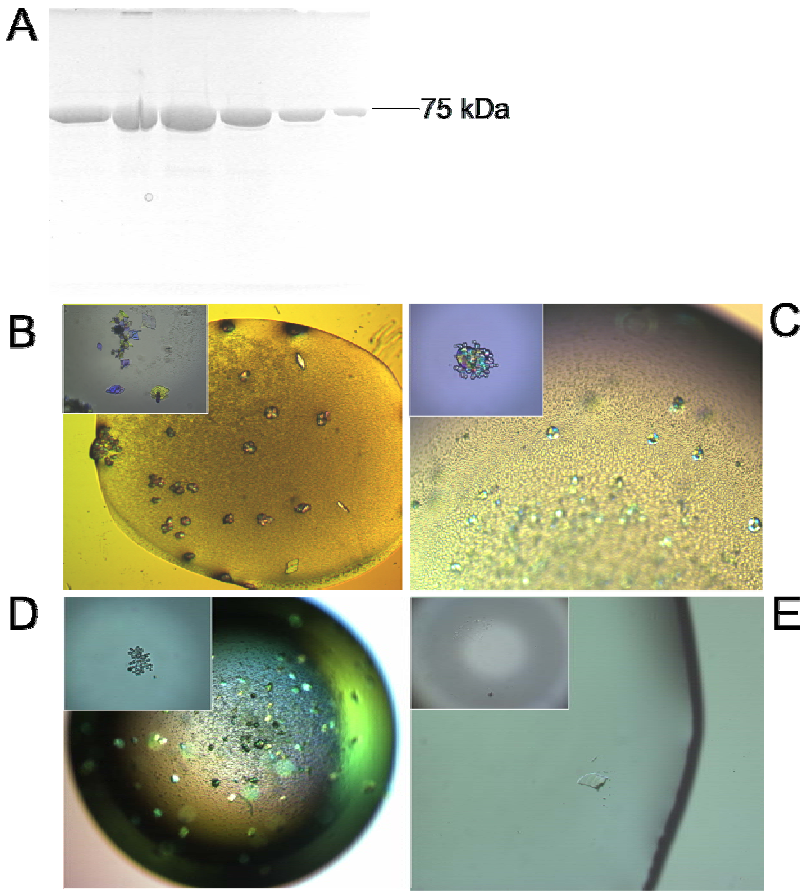

Figure 4:

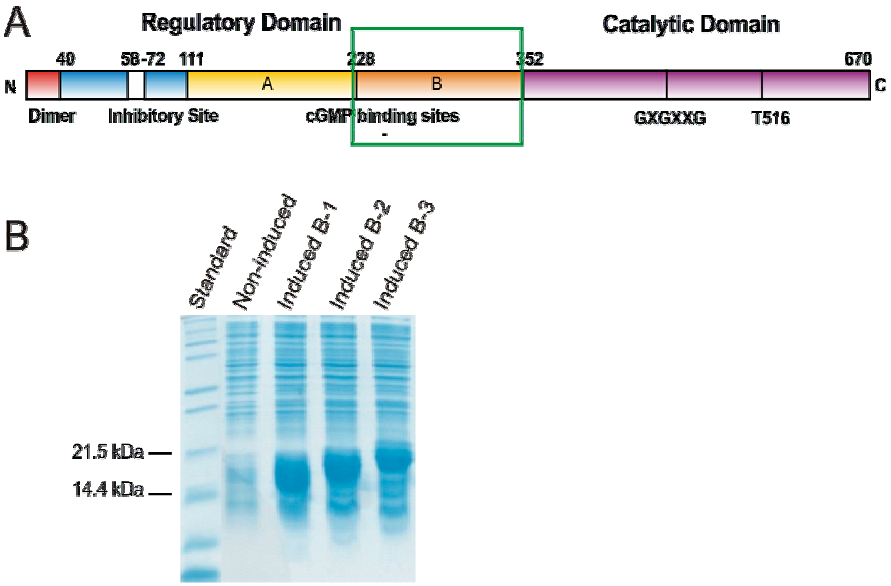
A
Regulatory Domain
Catalytic Domain
40
58-72
111
228
352
670
N
A
B
C
Dimer
Inhibitory Site
cGMP binding sites
GXGXXG
T516
B
Standard
Non-induced
Induced B-1
Induced B-2
Induced B-3
21.5 kDa
14.4 kDa

Figure 5:

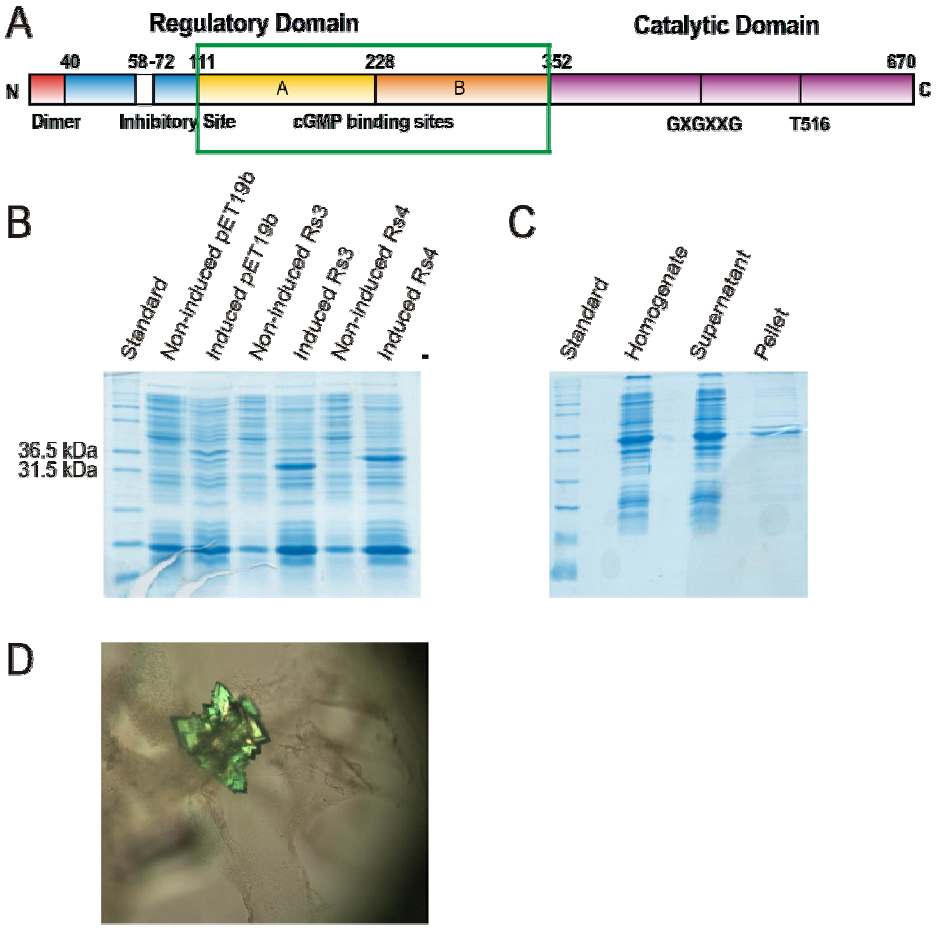
A
Regulatory Domain
Catalytic Domain
40
58-72
111
228
352
670
N
A
B
C
Dimer
Inhibitory Site
cGMP binding sites
GXGXXG
T516
B
Standard
Non-induced pET19b
Induced pET19b
Non-induced Rs3
Induced Rs3
Non-induced Rs4
Induced Rs4
36.5 kDa
31.5 kDa
C
Standard
Homogenate
Supernatant
Pellet
D

References

Dostmann WR, Taylor MS, Nickl CK, Brayden JE, Frank R and Tegge WJ. Highly specific, membrane-permeant peptide blockers of cGMP-dependent protein kinase Ialpha inhibit NO-induced cerebral dilation. *Proc Natl Acad Sci U S A* 97(26): 14772-7, 2000.

Feil R, Muller S and Hofmann F. High-level expression of functional cGMP-dependent protein kinase using the baculovirus system. *FEBS Lett* 336(1): 163-7, 1993.

Jancarik J and Kim SH. Sparse matrix sampling: a screening method for crystallization of proteins. *J Appl Cryst* 24: 409-411, 1991.

Kim C, Cheng CY, Saldanha SA and Taylor SS. PKA-I holoenzyme structure reveals a mechanism for cAMP-dependent activation. *Cell* 130(6): 1032-43, 2007.

Kim C, Xuong NH and Taylor SS. Crystal structure of a complex between the catalytic and regulatory (RIalpha) subunits of PKA. *Science* 307(5710): 690-6, 2005.

Kinderman FS, Kim C, von Daake S, Ma Y, Pham BQ, Spraggon G, Xuong NH, Jennings PA and Taylor SS. A dynamic mechanism for AKAP binding to RII isoforms of cAMP-dependent protein kinase. *Mol Cell* 24(3): 397-408, 2006.

Knighton DR, Zheng JH, Ten Eyck LF, Ashford VA, Xuong NH, Taylor SS and Sowadski JM. Crystal structure of the catalytic subunit of cyclic adenosine monophosphate-dependent protein kinase. *Science* 253(5018): 407-14, 1991.

Newlon MG, Roy M, Morikis D, Carr DW, Westphal R, Scott JD and Jennings PA. A novel mechanism of PKA anchoring revealed by solution structures of anchoring complexes. *Embo J* 20(7): 1651-62, 2001.

Richie-Jannetta R, Busch JL, Higgins KA, Corbin JD and Francis SH. Isolated regulatory domains of cGMP-dependent protein kinase Ialpha and Ibeta retain dimerization and native cGMP-binding properties and undergo isoform-specific conformational changes. *J Biol Chem* 281(11): 6977-84, 2006.

Schnell JR, Zhou GP, Zweckstetter M, Rigby AC and Chou JJ. Rapid and accurate structure determination of coiled-coil domains using NMR dipolar couplings: application to cGMP-dependent protein kinase Ialpha. *Protein Sci* 14(9): 2421-8, 2005.

Su Y, Dostmann WR, Herberg FW, Durick K, Xuong NH, Ten Eyck L, Taylor SS and Varughese KI. Regulatory subunit of protein kinase A: structure of deletion mutant with cAMP binding domains. *Science* 269(5225): 807-13, 1995.

Taylor MS, Okwuchukwuasanya C, Nickl CK, Tegge W, Brayden JE and Dostmann WR. Inhibition of cGMP-dependent protein kinase by the cell-permeable peptide DT-2 reveals a novel mechanism of vasoregulation. *Mol Pharmacol* 65(5): 1111-9, 2004.

Taylor SS, Kim C, Vigil D, Haste NM, Yang J, Wu J and Anand GS. Dynamics of signaling by PKA. *Biochim Biophys Acta* 1754(1-2): 25-37, 2005.

Wall ME, Francis SH, Corbin JD, Grimes K, Richie-Jannetta R, Kotera J, Macdonald BA, Gibson RR and Trewhella J. Mechanisms associated with cGMP binding and activation of cGMP-dependent protein kinase. *Proc Natl Acad Sci U S A* 100(5): 2380-5, 2003.

Zhao J, Trewhella J, Corbin J, Francis S, Mitchell R, Brushia R and Walsh D. Progressive cyclic nucleotide-induced conformational changes in the cGMP-dependent protein kinase studied by small angle X-ray scattering in solution. *J Biol Chem* 272(50): 31929-36, 1997.

CHAPTER FOUR: DIFFERENTIAL PATTERNING OF cGMP IN VASCULAR SMOOTH MUSCLE CELLS REVEALED BY SINGLE GFP-LINKED BIOSENSORS

Lydia WM Nausch, Jonathan Ledoux, Adrian D. Bonev, Mark T Nelson and Wolfgang R Dostmann

Department of Pharmacology, University of Vermont, College of Medicine, Burlington, 05405 VT

Corresponding author: Wolfgang Dostmann, Ph.D, University of Vermont, Department of Pharmacology, Health Science Research Facility 330, 149 Beaumont Avenue, Burlington, VT 05405-0075, USA

Tel: (802) 656-0381, Fax: (802) 656-4523, EMail: wdostman@uvm.edu

Text: 34 pages; 5 Figures, 3 Tables, 1 supporting information, 4 supporting Figures, 4 supporting movies. Word and character count: 47,692

Proceedings of the National Academy of Sciences. Jan 8, 105(1): 365-370, 2008.

Abbreviations footnote: cGMP, cyclic-3',5'-guanosine monophosphate; $[cGMP]_i$, intracellular cGMP; cAMP, cyclic-3',5'-adenosine monophosphate; VSM, vascular smooth muscle; PDE, phosphodiesterase; PKG, cGMP dependent protein kinase; pGC, particular guanylyl cyclase; sGC, soluble guanylyl cyclase; NO, nitric oxide; ANP, atrial natriuretic peptide; FRET, fluorescence resonance energy transfer; cpEGFP, circular permutated EGFP; FlincG, fluorescent indicator of cGMP; DEA-NO, Diethylamine NONOate; PROLI-NO, 1-[2-(carboxylato)pyrrolidin-1-yl]diazen-1-ium-1,2-diolate

Abstract

Here we report the design of unprecedented, non-FRET based cGMP-biosensors, named FlincGs, to assess the dynamics of nitric oxide (NO) and atrial natriuretic peptide (ANP) induced synthesis of intracellular cGMP, $[cGMP]_i$. Regulatory fragments of PKG I α, PKG I β, and an N-terminal deletion mutant of PKG I α were fused to circular permutated EGFP to generate α-, β-, and δ-FlincG, with high dynamic ranges and apparent $K_{D,cGMP}$ values of 35 nM, 1.1 μM and 170 nM, respectively. All indicators displayed significant selectivity for cGMP over cAMP, and 1.5 to 2.1 fold increases in fluorescence intensity at 510 nm when excited at 480 nm. Surprisingly, FlincGs displayed an additional excitation peak at 410 nm. δ-FlincG permitted ratiometric (480/410 nm) measurements, with a cGMP specific 3.5 fold ratio change. In addition, δ-FlincG presented cGMP association and dissociation kinetics sufficiently fast to monitor rapid changes of $[cGMP]_i$ in intact cells. In unpassaged, adenoviral transfected vascular smooth muscle (VSM) cells, δ-FlincG had an $EC_{50,cGMP}$ of 150 nM, and revealed transient global cGMP elevations to sustained physiological NO ($EC_{50,\ DEA/NO}$ = 4 nM), and the decay phase was dependent on the activity of PDE-5. In contrast, ANP elicited sustained sub-membrane elevations in $[cGMP]_i$, which were converted to global cGMP elevations by inhibition of PDE-5 by sildenafil. These results indicate that FlincG is an innovative tool to elucidate the dynamics of a central biological signal –cGMP-, and that NO and natriuretic peptides induce distinct cGMP patterning under the regulation of PDE-5, and hence likely differentially engage cGMP targets.

Introduction

Cyclic 3',5'-guanosine monophosphate (cGMP) has profound effects on cell function through actions on cGMP-specific phosphodiesterases (PDEs) and cGMP-dependent protein kinases (PKGs), as well as through several types of cyclic nucleotide-activated ion channels (CNGs) (Conti and Beavo, 2007; Francis et al., 2005; Hofmann, 2005; Hofmann et al., 2005). cGMP is synthesized by two distinct families of guanylyl cyclases: i) the natriuretic peptide-specific, plasma membrane associated guanylyl cyclases (pGC), and (ii) the nitric oxide (NO) activated, cytosolic soluble guanylyl cyclases (sGC) (Cary et al., 2006; Garthwaite, 2005; Kuhn, 2005; Mullershausen et al., 2005). Intracellular cGMP levels are terminated through the hydrolyzing activities of cGMP-specific phosphodiesterases (Conti and Beavo, 2007).

In recent years, several FRET-based cGMP indicators have been developed in an effort to monitor spatio-temporal dynamics of $[cGMP]_i$ (Honda et al., 2001; Nikolaev et al., 2006; Russwurm et al., 2007). Particularly, Cygnet-type cGMP indicators have significantly advanced our understanding of cGMP dynamics in VSM and other cell types (Cawley et al., 2007; Honda et al., 2001; Honda et al., 2005; Honda et al., 2005; Mongillo et al., 2006; Takimoto et al., 2005). However, FRET-based cGMP indicators have limitations. They require a technically laborious dual emission detection system and generally show overall low cyan/yellow emission ratio changes in intact cells. Furthermore, at low, physiological NO-concentrations (< 10 nM), FRET-based cGMP indicators are limited in their use to detect fluctuations in $[cGMP]_i$ (Cawley et al., 2007). However, recent studies using purified cyclase, intact platelets and cerebellar cells have

shown that sGC is activated at low-nanomolar NO concentrations (1 to 10 nM) (Mo et al., 2004; Roy and Garthwaite, 2006). FRET-based cGMP indicators are also limited in resolving possible compartmentalized intracellular cGMP signaling events using confocal microscopy. It was recently suggested that in VSM cells and cardiac myocytes cGMP signaling may be spatially segregated and that this functional compartmentalization may be the cause of the unique actions of ANP and NO (Castro et al., 2006; Fischmeister et al., 2006; Kass et al., 2007; Piggott et al., 2006; Takimoto et al., 2007). The goal of this study was to develop previously undescribed, non-FRET biosensors suitable to monitor the temporal changes of $[cGMP]_i$ in response to low-nanomolar NO or ANP, and to investigate the spatial patterning of $[cGMP]_i$, using real-time, confocal imaging techniques.

The concept of non-FRET based biosensors, containing a single GFP-based fluorescence unit was first described by Tsien and colleagues with the development of Ca^{2+}-sensitive 'camgaroos', by placing calmodulin at an insertion-permissive site within the β sheets of GFP (Baird et al., 1999). Subsequently, circularly permutated EGFP (cpEGFP) advanced non-FRET based biosensors even further and gave rise to the development of 'GCaMP'-type Ca^{2+} indicators, in which the Ca^{2+}-dependent interaction between calmodulin and its specific binding protein M13 was directly translated into conformational changes and an increase in fluorescence intensity of the single fluorescent molecule cpEGFP (Nakai et al., 2001; Tallini et al., 2006). We adopted this concept of non-FRET biosensors to design cGMP indicators, called FlincGs (fluorescent indicators of cGMP). FlincG indicators are composed of cpEGFP, N-terminally fused to regulatory

domain fragments of PKG. The overall favorable kinetic and spectroscopic characteristics of this single emission detection system permits for the first time the direct examination of local cGMP dynamics in response to low-nanomolar NO or ANP in VSM cells in real-time.

Results and Discussion

Bioengineering FlincG biosensors from type I PKG.

FlincGs are composed of two in-tandem, PKG derived cGMP binding sites fused to the N-terminus of cpEGFP (Figure 1 A). In contrast to GCaMP-type calcium indicators (Nakai et al., 2001), FlincGs do not require intramolecular protein-protein interactions between separate domains. Instead, dose-dependent binding of cGMP to both receptor domains was sufficient to increase fluorescence intensity in cpEGFP (Figure 1 C, inset). Previous studies using hydrodynamic and small-angle x-ray scattering techniques support our findings that cGMP binding to the regulatory domain of PKG I induces substantial conformational changes (Richie-Jannetta et al., 2006; Wall et al., 2003; Zhao et al., 1997). α-FlincG was developed by attaching the entire regulatory domain of PKG I α (residues 1-356) to cpEGFP (Figure 1 B). cGMP increased fluorescence intensity of this construct by up to 1.5-fold, with an apparent K_D of 35 nM (Figure 1 C) and with an approximately 1,100 fold selectivity for cGMP over cAMP (Table 1).

To increase the dynamic range of $[cGMP]_i$ detection, we took advantage of the fact that the activation constants of PKG I α and I β shift from 75 nM to approximately 1.0 to 1.8 μM (Ruth et al., 1991; Ruth et al., 1997; Wolfe et al., 1989). PKG I α and I β are genetic splice-variants and consist of different N-termini, but are virtually identical within their cGMP binding and catalytic domains (Ruth et al., 1991). Thus, we developed β-FlincG, by connecting the regulatory domain of PKG I β to the N-terminus of cpEGFP (Figure 1 B). As predicted, this FlincG variant demonstrated a shifted cGMP binding constant of 1.1 μM (Figure 1 C, Table 1), indicating the significance of the N-terminus

for modulating cGMP binding affinities. Interestingly, removal of the entire N-terminal domain (Δ1-77) of PKG I α resulted in δ-FlincG, which exhibited an apparent K_D of 170 nM. This result is in accordance to an analogous PKG I α deletion fragment, Δ1-77/352-670 for which a similar cGMP binding constant (K_D = 218 nM) has been reported (Dostmann et al., 1996). This finding further supports the concept that the N-terminal domain of PKG, not the catalytic domain, primarily modulates cGMP binding affinities of the FlincG indicators. Interestingly, the C-terminus of FlincGs did not affect fluorescence intensity changes. Neither the linker sequence shown in Figure 1 B, which was the product of a randomized cloning approach, nor attachment of the PKG catalytic domain, or complete removal of any C-terminal appendage had any effect on overall fluorescence intensity changes (data not shown).

Under cell-free conditions, α- and β-FlincG exhibited maximal 1.5 and 2.1-fold intensity changes, respectively (Figure 1 C, Table 1). When expressed in VSM cells, the maximal fluorescence increases of α- and β-FlincG were reduced to about 1.2-fold, although these indicators retained high NO-sensitivity ($EC_{50,\ DEA\text{-}NO}$ = 0.3 and 12 nM, respectively) (Table 2; Figure 1 D). Both biosensors contain their respective N-terminal PKG dimerization sequences, which may give rise to interactions with endogenous PKG and thus decreases their observed maximal intensity changes (Figure 1 D, Table 2). In support of this idea, co-immunoprecipitation experiments demonstrated formation of mixed dimers between wild-type PKG and α-, or β-FlincG (supp. Figure 1). However, δ-FlincG did not display any interaction with wildtype PKG, because it lacks the N-terminal dimerization domain (supp. Figure 1). Hence, we did not observe a reduction of

maximal fluorescence intensity when comparing purified δ-FlincG to indicator expressed in intact VSM cells (Figures 1 C, E), whilst retaining high NO sensitivity ($EC_{50,\ DEA\text{-}NO}$ = 4 nM; Figure 1 E). This indicator was also highly selective for cGMP over cAMP (> 280 fold, Table 1).

Recently published FRET cGMP-sensors by Russwurm and colleagues (Russwurm et al., 2007) display a comparable maximal FRET ratio change of 75 % for recombinant protein. In living cells however, all FRET-indicators published so far, exhibit a significant decrease in maximal FRET ratio change, ranging from 35 to 45 % (Cawley et al., 2007; Honda et al., 2001; Nikolaev et al., 2006; Russwurm et al., 2007). In contrast, FlincG cGMP biosensors have been designed to minimize interactions with endogenous proteins and to maintain maximal fluorescence intensity changes in living cells while retaining nanomolar NO sensitivity. Since δ-FlincG exhibits all these favorable characteristics in living cells, we selected δ-FlincG as indicator suitable for studying intracellular cGMP dynamics.

Kinetic, spectral analysis and environmental stability of δ-FlincG

A more refined spectral analysis revealed that in addition to the 491 excitation maximum, δ-FlincG displayed a second, blue-shifted excitation peak at 410 nm (Figure 2 A). Furthermore, these excitation maxima at 410 and 491 nm respond differentially in response to 1 μM cGMP. It should be noted, that all FlincG indicators possessed this secondary 410 nm excitation maximum (data not shown), but only for δ-FlincG cGMP decreased the emission intensity at 410 nm 0.5-fold, with a corresponding emission

maximum at 507 nm (Figure 2 B). In addition, excitation at 480 nm yielded an emission maximum at 511 nm (Figure 2 C) with an overall 1.75-fold fluorescence intensity increase. Thus, our results are in contrast to the excitation emission spectra of EGFP and previous cpEGFP based indicators, such as camgaroos and GCaMPs, which display only one excitation maximum at 489 nm (Baird et al., 1999; Griesbeck et al., 2001; Nakai et al., 2001).

Based on its dual excitation spectrum, δ-FlincG offers several technical alternatives to previous FRET-based cGMP imaging techniques. First, the two excitation wavelengths may be combined and analyzed ratiometrically (480/410 nm excitation), similar to the Ca^{2+} indicator Fura (Grynkiewicz et al., 1985). As a result, the overall ratio change increased up to 3.5 fold *in vitro*, and the overall apparent $K_{D,cGMP}$ was 488 nM, with approximately 100-fold selectivity for cGMP over cAMP (Figure 2 D, Table 1). Second, a single wavelength excitation system could be utilized by employing a 410/510 nm excitation/emission detection profile. However, for the initial experiments with δ-FlincG, the single wavelength approach (480/510 nm excitation/emission) was used, because it is faster, has decreased risk of photo-bleaching, superior cGMP/cAMP selectivity, and an advantageous apparent cGMP binding constant of 170 nM (Figure 1 C and Table 1). Nonetheless, in future studies, the ratiometric approach (Figure 2 D) would present a number of significant inherent advantages, including the determination of $[cGMP]_i$.

To examine further δ-FlincG's utility as a $[cGMP]_i$-biosensor, we investigated its environmental stability under varying pH conditions (supp. Figure 2). Previously reported

cpGFP based biosensors, such as camgaroos and GCaMPs, have displayed significant pH sensitivity under physiological conditions with pK_a values of 8.9 and 7.1, respectively (Baird et al., 1999; Nakai et al., 2001). Elaborate mutational approaches have been undertaken to reduce the environmental sensitivity of GFP and GFP-based variants. So far, only Citrine, a yellow fluorescent protein (YFP) -based mutant, has been reported with superior chloride and pH stability (pK_a 5.7) compared to previous YFPs (Griesbeck et al., 2001). In comparison, our results indicate that δ-FlincG did not require mutational optimization to accomplish resistance to small changes in pH under physiological conditions (pK_a 6.1).

An important requirement for a biosensor is to have fast kinetics so that intracellular temporal and spatial changes can be accurately monitored. Stopped-flow experiments revealed a fast rate of cGMP association (k_{on} = 5.9 x 10^6 $s^{-1}M^{-1}$; $t_{1/2}$ = 0.12 s) (Figure 3 A, Table 3). The dissociation constant determined by protein dilution was equally rapid (k_{off} = 4.2 s^{-1}; $t_{1/2}$ = 0.16 s) (Figure 3 B, Table 3). These rate constants ensure that the rate limiting step for detecting $[cGMP]_i$ does not occur at the level of cGMP association to or dissociation from the biosensor. Equally advantageous, δ-FlincG should not act as a sink for $[cGMP]_i$, because its cGMP binding constant (170 nM) is not significantly different from its major endogenous receptors PKG I α and PDE 5 in vascular smooth muscle (Ruth et al., 1991; Zoraghi et al., 2005). Superior spectral characteristics, environmental stability and fast association/dissociation kinetics should enable δ-FlincG to capture the rapid rise and fall of $[cGMP]_i$ in living VSM cells.

Intracellular properties of δ-FlincG in vascular smooth muscle cells

Recently, we reported that primary, unpassaged VSM cells from rat aorta retain the expression of key cGMP-signaling enzymes, such as PKG I, sGC and PDE5 (Cawley et al., 2007). Transfection of VSM cells with δ-FlincG adenovirus resulted in an even cytosolic distribution and nuclear exclusion of the indicator, with a 90% efficiency (inset, Figure 4 A). To determine the apparent affinity of intracellular δ-FlincG for cGMP, VSM cells were permeabilized with β-escin and the cells were exposed to different levels of cGMP in Ca^{2+}-free imaging buffer. Half-maximal fluorescence increases occurred at 150 nM cGMP (Figure 4A), similar to the value obtained for the purified biosensor (170 nM; Figure 1 C). With this approach, the level of intracellular cGMP can be estimated from the fractional change in fluorescence.

An important criterion for intracellular cGMP sensors is that they exhibit appropriately high sensitivity to NO, as previously reported for sGC (half-maximal NO: 1.7 nM for the purified enzyme, 11 nM for intact platelets,10 nM for cerebellar cells) (Mo et al., 2004; Roy and Garthwaite, 2006). DEA-NO and PROLI-NO were used as NO-donors due to their overall favorable fast chemistry of NO-release (see Methods). DEA-NO (0.75 to 6.50 nM) induced concentration-dependent, transient increases in $[cGMP]_i$, corresponding to 10 nM to 1 μM (Figures 4 A, B). The corresponding half activation constant ($EC_{50,DEA-NO}$) was 4 nM (Figure 1 E; Table 2). Similarly, transient and highly reproducible $[cGMP]_i$ changes were observed with 25 nM PROLI-NO ($EC_{50,\ PROLI-NO}$ = 16 nM; Table 2; Figure 4 C). In contrast to NO-stimulated sGC, activation of the plasma membrane associated guanylyl cyclase pGC-A using atrial natriuretic peptide

(ANP) resulted in sustained levels of $[cGMP]_i$ (Figure 4 D), as demonstrated previously in VSM cells using radio-immunoassays (Hamet et al., 1989; Leitman et al., 1988; Winquist et al., 1984). These results promote δ-FlincG as exceptional biosensor for physiological (low-nanomolar) NO- and ANP-induced cGMP dynamics in VSM cells.

NO-induced elevation of $[cGMP]_i$ requires activation of sGC. ODQ (10 μM), a specific inhibitor of sGC activation (Brunner et al., 1995; Garthwaite et al., 1995; Schrammel et al., 1996), prevented the PROLI-NO (50 nM) induced increase of cGMP (Figure 4 E), indicating that the observed rise in $[cGMP]_i$ is indeed due to NO-induced activation of sGC. The $[cGMP]_i$ also depends on its hydrolysis by PDE-5. Sildenafil, a PDE-5 specific inhibitor (Corbin et al., 2003; Turko et al., 1999), greatly slowed the decay in $[cGMP]_i$ in response to PROLI-NO (12 to 200 nM), supporting the concept of a dynamic interplay between sGC production and PDE-5 mediated hydrolysis of cGMP (Figure 4 F).

Spatial and temporal dynamics of NO- and ANP- induced cGMP signaling in δ-FlincG transfected vascular smooth muscle cells

Our current understanding of the intracellular distribution of cGMP derives from the fact that the predominant soluble guanylyl cyclase isoform sGC-$\alpha_1\beta_1$ is largely cytosolic, hence $[cGMP]_i$ should be cytosolic as well (Mullershausen et al., 2005). The natriuretic peptides ANP, BNP and CNP, in contrast, specifically activate plasma membrane associated guanylyl cyclases pGC-A and pGC-B and thus, may give rise to a distinct spatial pattern of $[cGMP]_i$ (Fischmeister et al., 2006; Kass et al., 2007). However,

the spatial distribution of $[cGMP]_i$ in response to NO and ANP has never been studied by the means of high resolution confocal imaging techniques. FlincG-indicators should permit the measurement of cGMP patterns in living cells.

A physiological dose of 1.5 nM NO induced a global, but transient, elevation in $[cGMP]_i$ (Figures 5 A, B; supp. Movie 1), similar to measurements conducted with lower resolution, epi-fluorescence microscopy (Figure 4 B, C). The membrane-permeant cGMP analog (8-Br-cGMP, 50 µM) was applied to VSM cells and a uniform increase in fluorescence was observed (supp. Movie 2), indicating homogenous expression of δ-FlincG in VSM cells. Forskolin (100 nM), which specifically activates the cAMP signaling pathway, had no effect on fluorescence intensity (supp. Movie 3), consistent with δ-FlincG selectivity for cGMP over cAMP.

In contrast to the transient NO-evoked $[cGMP]_i$ patterns, application of ANP (10 nM) induced sustained synthesis of at least 1 µM $[cGMP]_i$ (Figures 5 C, D). This finding is in agreement with our results shown in Figure 4 D, although different imaging techniques (epi- versus confocal microscopy) give rise to variations in the onset of ANP response (mean lag time: 25 ± 4 sec, Figure 5C; 45 ± 10 sec, Figure 4D). ANP induced local, spatially segregated patterns of $[cGMP]_i$ at the plasma membrane of single VSM cells (Figure 5 D; supp. Movie 4). To address spatial patterning due to uneven indicator expression and cell movement, which may present potential problems in single wavelength intensity measurements, we analyzed three-dimensional surface plots (Supporting Figure 3) indicating uniform cellular distribution of δ-FlincG (from Figures

5 A and D). Supporting Figure 4 verifies that the cell morphology does not change over time after NO or ANP application and that the cells do not move.

Spatially-confined cGMP signaling may be a combination of both local cGMP synthesis and local degradation at the membrane. Recently, compartmentalized $[cGMP]_i$ was reported in cardiac myocytes through specific activation of pGC by natriuretic peptides (Castro et al., 2006; Mongillo et al., 2006; Takimoto et al., 2007). These studies also suggested that cGMP specific PDEs maintain these local patterns of $[cGMP]_i$ elicited through pGC. Our results indicate that ANP (10 nM) induced cGMP synthesis is sustained and spatially confined in VSM cells (Figures 5 C, D). This spatial localization in response to ANP was abolished, when VSM cells were preincubated with the PDE-5 inhibitor, sildenafil (Figure 5 E). Instead, a global increase in $[cGMP]_i$ was observed, indicating that degradation of cGMP by PDE-5 prevents the cell's interior from experiencing an elevation of cGMP. These ANP-produced sub-membrane cGMP elevations suggest local targeting of sub-membrane targets such as the calcium-sensitive (BK) channel and SERCA-regulatory protein, phospholamban (Porter et al., 1998; Robertson et al., 1993).

In conclusion, FlincG represents a previously undescribed generation of cGMP biosensors that excels in monitoring $[cGMP]_i$ in response to physiological (low-nanomolar) NO concentrations. FlincG should ultimately be suitable for development of tissue-specific generation of transgenic mice with endogenous cGMP indicators, as has been done recently for calcium sensing with GCaMP (Ji et al., 2004; Tallini et al., 2006). The ratiometric possibilities of FlincG should enhance its versatility. FlincG revealed the

differential role of PDE-5 in the modulation of global cGMP in response to NO donors, and the spatial spread of cGMP away from the cell membrane in response to ANP. FlincG holds the promise of unraveling the complex interplay between cGMP and calcium signaling near the cell membrane.

Materials and Methods

Fluorescence measurements in cultured vascular smooth muscle cells (P0)

VSM cells were harvested from rat aortic tissue and cultured as described previously (Cawley et al., 2007). For transfection, 100 µl of adenovirus (10^7 to 10^9 per ml titer) were applied to 50% confluent VSM cells (P0) and incubated 24 to 48h at 37°C, 5% CO_2 until a 90 % transfection efficiency in VSM cells was achieved. Epi-fluorescence imaging was performed by incubating cells in imaging buffer (10mM TES (pH 7.4), 1 g/L D-glucose, Hank's Balanced Salt Solution (HBSS, Mediatech, Inc., Herndon, VA) at 37°C using a Delta T4 open culture system (Bioptechs, Butler, PA). A Nikon Diaphot 200 microscope outfitted with a Nikon 40x/1.30 oil objective, a cooled charge-coupled device camera (ORCA ER; Hamamatsu, Japan), and a mercury-halide lamp, X-CITE 120 (EXFO Photonics, Toronto, ON), were used to image individual cells with 3 seconds acquisitions. Imaging of FlincG indicators was controlled by Metafluor 6.2 software (Universal Imaging, Media, PA) using a D480/20m excitation filter, 505drxr dichroic mirror and D535/30m emission. For confocal imaging, P0 VSM cells were imaged using a spinning disk confocal system (Andor) outfitted on a Nikon E600SN microscope with a 60x water dipping objective (NA 1.0), and iXon ENCCD DVB camera with 5 frames/sec acquisition speed and 64 msec exposure time exciting with a solid state laser at 488 nm, and collecting the emission at 510 nm. Data analysis was performed with custom written software developed by Dr. Adrian Bonev. For confocal microscopy, cGMP responses were investigated upon local application (5 to 50 µl) and subsequent diffusion of DEA/NONOate (Calbiochem), PROLI/NONOate (Cayman Chemicals), ANP (Sigma),

Sildenafil (Pfizer), ODQ (Sigma), 8-Br-cGMP (BioLog) and Forskolin (Sigma). Approximately 75% of the data collected were rejected due to cell movement and morphology changes during the course of the experiments. For epi-fluorescence microscopy, chemicals were distributed evenly by mixing with imaging buffer. Calibration of adenoviral transfected VSM cells was performed in Hepes-buffered, Ca^{2+}-free PSS pH 7.4. VSM cells were permeabilized with 20 µM β-escin, exposed to increasing cGMP concentrations (0 to 2 µM) and analyzed using the epi-fluorescence microscope facility. For NO-titration, δ-FlincG transfected VSM cells were exposed to 0.4 nM - 500 nM DEA-NO ($t_{1/2}$ = 2.4 min at 37°C, pH 7.4), or to 1.5 nM - 2 µM PROLI-NO ($t_{1/2}$ = 1.8 sec at 37°C, pH 7.4). Data were analyzed using the Metafluor software and dose-response curves were calculated with GraphPadPrism.

Further methods are provided in supporting information 1.

Acknowledgements

We thank Dr. Alan Howe (University of Vermont, Burlington, Vermont) for providing anti-GFP antibodies and Dr. Christopher Berger (University of Vermont, Burlington, Vermont) for assistance with the stopped-flow equipment. This work was supported by grants from the NIH (HL68891) and the NSF (MCB-9983097) to WRD, by grants from the NIH (HL44455, DK53832, DK65947, HL77378) to MTN, by the Canadian Institutes for Health Research and Fonds de Recherche en Santé du Québec and the Totman Trust for Medical Research.

Table 1: cGMP and cAMP selectivity of recombinant FlincG biosensors

FlincG isoform	$(F/F_0)_{max}$	$K_{D,cGMP}$ [µM]	$K_{D,cAMP}$ [µM]	cGMP/cAMP
Alpha[1]	1.55 ± 0.05 [4]	0.035 ± 0.010 [4]	40 ± 8 [3]	1140
Beta[1]	2.05 ± 0.03 [5]	1.100 ± 0.050 [5]	31 ± 10 [4]	30
Delta[1]	1.75 ± 0.03 [5]	0.170 ± 0.020 [5]	48 ± 10 [4]	280
Delta[2]	3.50 ± 0.06 [4]	0.488 ± 0.004 [4]	48 ± 10 [4]	100

[1]: single excitation at 480 nm, emission at 510 nm (Fig. 1C); [2]: ratiometric excitation at 410 and 480 nm, emission at 510 nm (Fig. 2D); the values represent the mean ± SEM of n Numbers of experiments (shown in brackets);0

Table 2: NO-titration and Calibration of FlincG biosensors in VSM cells

FlincG isoform	$EC_{50,\ DEA\text{-}NO}$ [nM]	$EC_{50,\ PROLI\text{-}NO}$ [nM]	$(F/F_0)_{max}$	$EC^1_{50,\ cGMP}$ [nM]
Alpha	0.3 ± 0.2 [6]	–	1.12 ± 0.08	–
Beta	12 ± 0.4 [6]	–	1.19 ± 0.06	–
Delta	4 ± 0.5 [8]	16 ± 2 [6]	1.75 ± 0.03	150 ± 12 [4]

[1]: calibration for cGMP in β-escin permeabilized VSM cells; the values represent the mean ± SEM of n Numbers of experiments (shown in brackets);

Table 3: cGMP association and dissociation kinetics

FlincG isoform	k_{on} [$s^{-1}M^{-1}$]	$t_{1/2}{}^1$ [s]	k_{off} [s^{-1}]	$t_{1/2}{}^2$ [s]
Delta	5.9×10^6 [4]	0.12 [4]	4.2 [3]	0.16 [3]

[1]: $t_{1/2}$ cGMP association; [2]: $t_{1/2}$ cGMP dissociation; the values represent the mean ± SEM of n Numbers of experiments (shown in brackets);

Figure legends:

Figure 1: Characterization of FlincG biosensors as recombinant proteins and in VSM cells. (A) Schematic architecture: fusion of regulatory fragments of PKG I to cpEGFP induces cGMP dependent changes in fluorescence emission intensity. (B) Domain structure: α-, β- and δ-FlincG utilize regulatory fragments of PKG I α and PKG I β. (C) cGMP dose response curves for α-, β- and δ-FlincG (Table 1); inset: cGMP dose-dependent increase in fluorescence intensity shown for α-FlincG. NO-titration of (D) α- and β-FlincG and (E) δ-FlincG in single VSM cells using epi-fluorescence microscopy (see Table 2).

Figure 2: Spectral analysis of δ-FlincG. (A) Excitation spectrum of δ-FlincG in presence and absence of 1 μM cGMP detected at 510 nm. Emission spectra excited at (B) 410 and (C) 480 nm in the presence and absence of 1 μM cGMP. (D) Ratiometric (480/410 nm) dose response curves for cGMP and cAMP detected at 510 nm.

Figure 3: cGMP binding kinetics of δ-FlincG. (A) cGMP association kinetics using stopped-flow fluorometry. Slopes represent the initial association velocities at different cGMP concentrations (inset). (B) cGMP dissociation kinetics using a dilution protocol (see Methods). Intensity changes were detected using a fluo-spectrophotometer.

Figure 4: Temporal dynamics of cGMP in VSM cells. (A) Calibration of δ-FlincG. Adenovirus-transfected VSM cells (inset) were permeabilized with β-escin and exposed

to increasing cGMP concentrations (25 nM - 2 μM). (B, C) Temporal cGMP dynamics in VSM cells were analyzed upon addition of 0.75 - 6.5 nM DEA-NO (B), 25 nM PROLI-NO (C) and 50 nM ANP (D) using epi-fluorescence microscopy . (E, F) Effects of ODQ and Sildenafil on δ-FlincG-transfected VSM cells. Cells were exposed repeatedly to 50 nM PROLI-NO in presence and absence of 10 μM ODQ (E) and to 12 to 200 nM PROLI-NO in presence of 50 μM Sildenafil (F). For each experimental series, n numbers are 4 to 10.

Figure 5: Spatial analysis of the NO and ANP pools of cGMP in δ-FlincG transfected VSM cells. $[cGMP]_i$ in response to (A, B) 1.5 nM DEA-NO and (C, D) 10 nM ANP using confocal microscopy. Regions of interest and their corresponding intensity traces are indicated with arrows and corresponding color boxes. Acquisition speed = 5 frames/sec; exposure time = 64 msec. (E) Application of 10 nM ANP after preincubation with 100 μM Sildenafil. For each experimental series, n numbers are 4 to 6.

Figure 1:

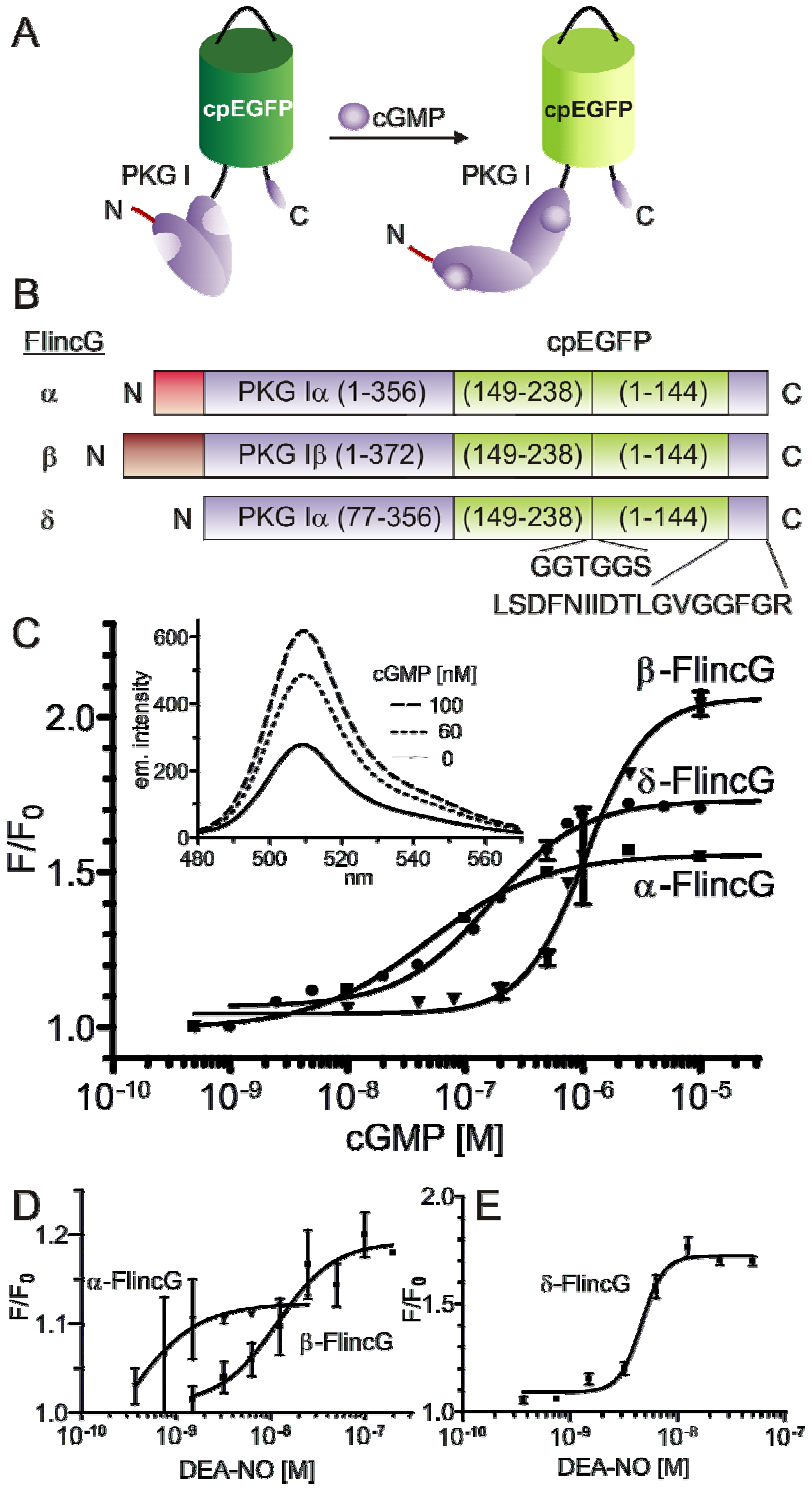
A
cpEGFP
cGMP
cpEGFP
PKG I
N
C
PKG I
N
C
B
FlincG
cpEGFP
α
N
PKG Iα (1-356)
(149-238)
(1-144)
C
β
N
PKG Iβ (1-372)
(149-238)
(1-144)
C
δ
N
PKG Iα (77-356)
(149-238)
(1-144)
C
GGTGGS
LSDFNIIDTLGVGGFGR
C
em. intensity
cGMP [nM]
100
60
0
nm
β-FlincG
δ-FlincG
α-FlincG
F/F0
cGMP [M]
D
α-FlincG
β-FlincG
F/F0
DEA-NO [M]
E
δ-FlincG
F/F0
DEA-NO [M]

Figure 2:

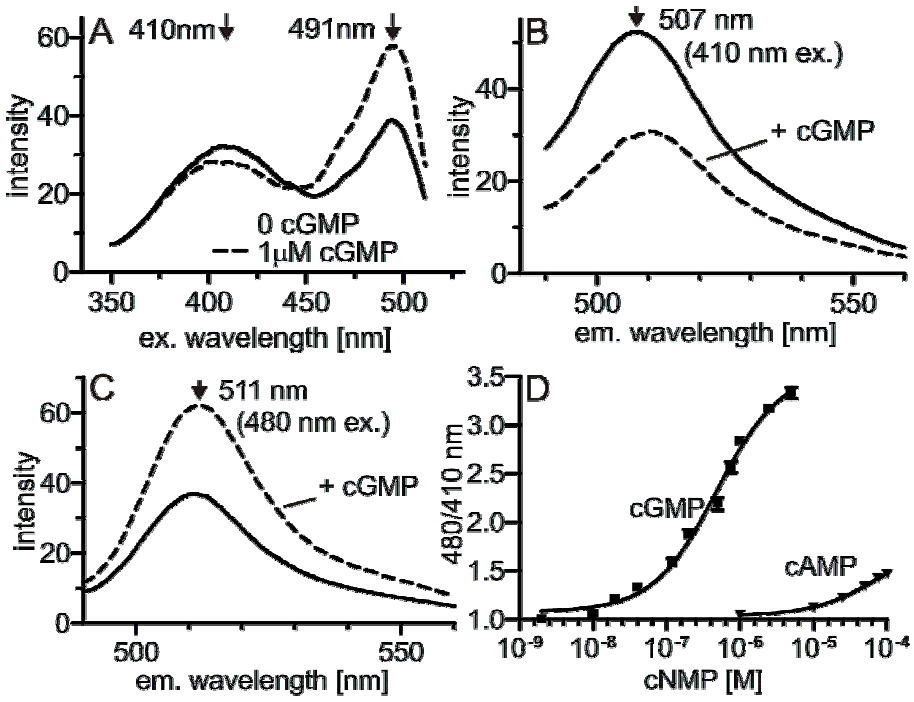
A
410nm
491nm
intensity
0 cGMP
1μM cGMP
ex. wavelength [nm]
B
507 nm
(410 nm ex.)
+ cGMP
intensity
em. wavelength [nm]
C
511 nm
(480 nm ex.)
+ cGMP
intensity
em. wavelength [nm]
D
480/410 nm
cGMP
cAMP
cNMP [M]

Figure 3:

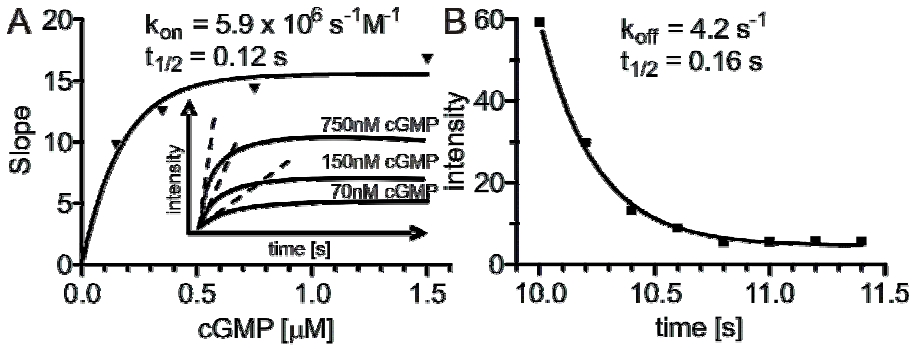
A
k_{on} = 5.9 x 10^6 $s^{-1}M^{-1}$
$t_{1/2}$ = 0.12 s
Slope
cGMP [µM]
750nM cGMP
150nM cGMP
70nM cGMP
intensity
time [s]
B
k_{off} = 4.2 s^{-1}
$t_{1/2}$ = 0.16 s
intensity
time [s]

Figure 4:

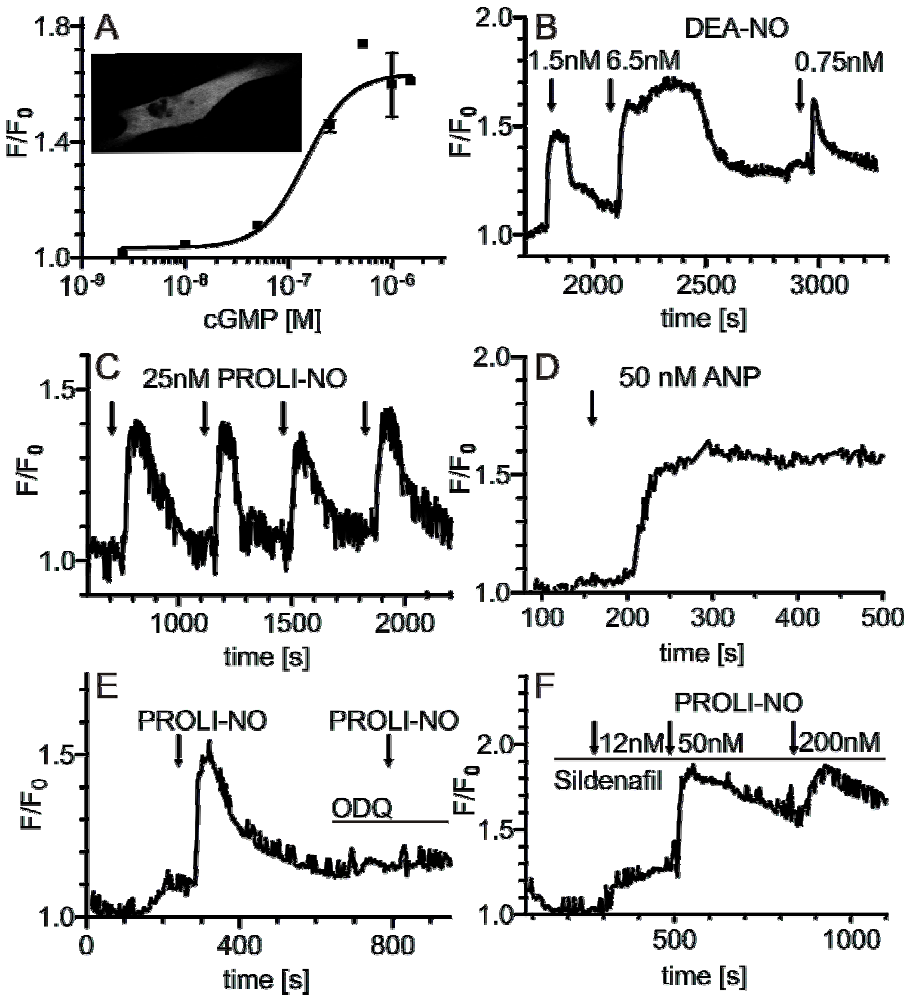
A
1.8
1.4
1.0
F/F0
10-9
10-8
10-7
10-6
cGMP [M]
B
DEA-NO
1.5nM 6.5nM
0.75nM
2.0
1.5
1.0
F/F0
2000
2500
3000
time [s]
C
25nM PROLI-NO
1.5
1.0
F/F0
1000
1500
2000
time [s]
D
50 nM ANP
2.0
1.5
1.0
F/F0
100
200
300
400
500
time [s]
E
PROLI-NO
PROLI-NO
ODQ
1.5
1.0
F/F0
0
400
800
time [s]
F
PROLI-NO
12nM
50nM
200nM
Sildenafil
2.0
1.5
1.0
F/F0
500
1000
time [s]

Figure 5:

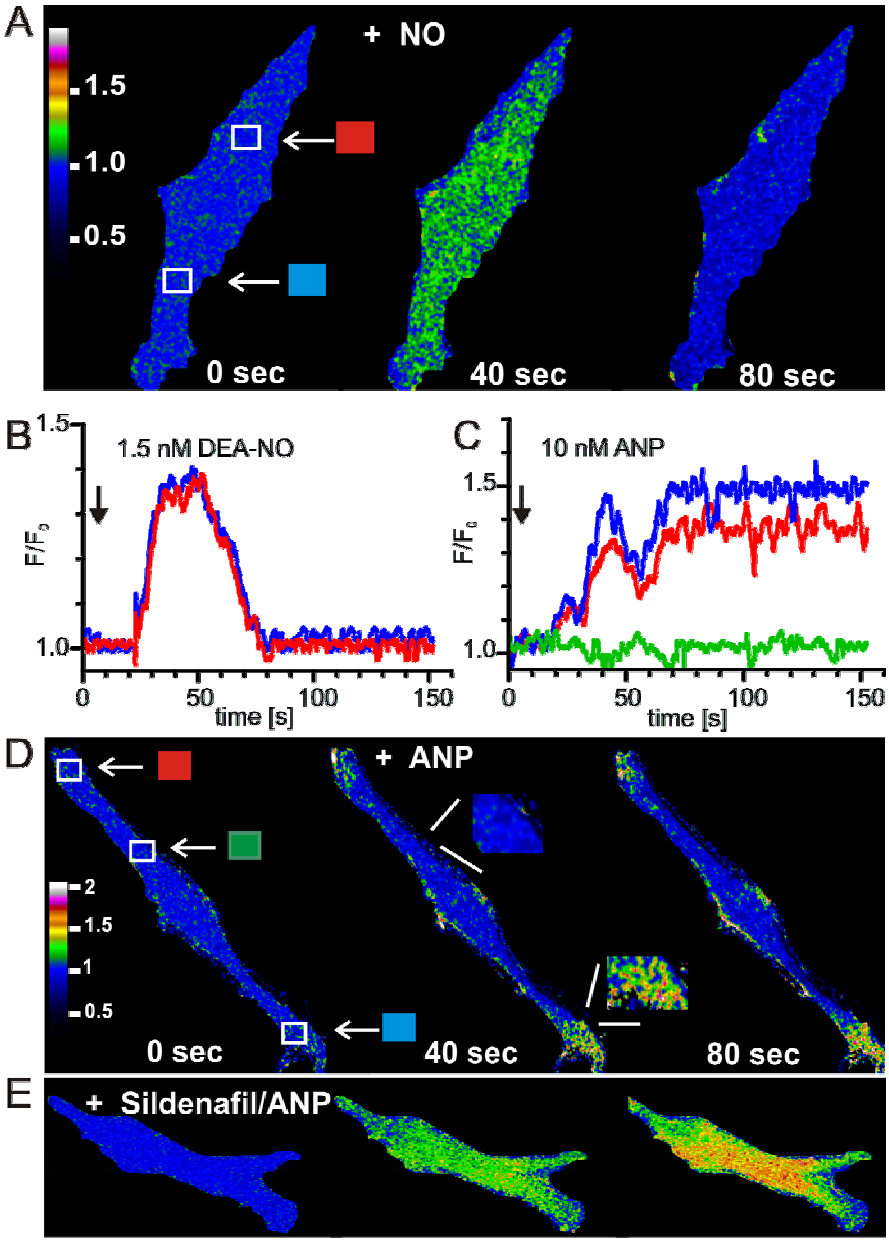
A
+ NO
1.5
1.0
0.5
0 sec
40 sec
80 sec
B
1.5 nM DEA-NO
F/F0
1.5
1.0
0
50
100
150
time [s]
C
10 nM ANP
F/F0
1.5
1.0
0
50
100
150
time [s]
D
+ ANP
2
1.5
1
0.5
0 sec
40 sec
80 sec
E
+ Sildenafil/ANP

Supporting Information 1:

Materials and Methods

Plasmid construction and bacterial expression

FlincG variants were constructed by fusing the regulatory domains of bovine PKG I α (1-356, α-FlincG), PKG I β (1-372, β-FlincG), or a deletion mutant of PKG I α (77-356, δ-FlincG) to the 5' end of circular permutated EGFP (cpEGFP 149-144, (Nakai et al., 2001)) by overlapping PCR. For bacterial expression, PKG regulatory domains were preceded by an *XhoI* site, and a start codon (ATG). cpEGFP 149-144 was connected at the 3' end to a 17 aminoacid sequence (LSDFNIIDTLGVGGFGR) by overlapping PCR and was followed by a stop codon and an *EcoRI* site. The entire FlincG coding sequence was inserted into the *XhoI* and *EcoRI* sites of pRSET-A, multiplied in *E.coli DH5α* and expressed in *E.coli BLR*. Similarly, mammalian adenoviral FlincG constructs were preceded at the 5'end by a *BamHI* site and a Kozak sequence (ACCATGG), inserted into the *BamHI* and *EcoRI* sites of pENTR vector and sub-cloned into pAd-DEST (ViraPower adenoviral expression system, invitrogen). For *in vitro* studies, *E.Coli BLR* transformed with FlincG-containing pRSET-A vectors were cultured at 25°C for 12h after protein induction with 0.4 mM isopropyl-β-D-thiogalactoside (IPTG). After centrifugation, FlincG variants were purified using cyclic nucleotide affinity chromatography as described previously (Dostmann et al., 2000; Feil et al., 1993).

In vitro characterization

Excitation spectra (detected at 510 nm) and emission spectra (excited at 410 or 480 nm) were taken using a fluorescence spectrophotometer F4500 (Hitachi, Tokyo, Japan). 200 nM purified FlincG was combined with increasing concentrations of cGMP (0-10 µM) or cAMP (0-100 µM) to generate cNMP dose response curves. For pH titration experiments at 200 nM protein concentration, phosphate buffer (for pH 6.5) was replaced with either citrate (for pH 5 to 6), Hepes-buffered HBSS (for pH 7 to 8), or with glycine (for pH 8.5 to 9). The pH-titration was calculated for each pH point by monitoring the baseline (F_0) in absence of cGMP, and by determining the increase in fluorescence (F) in presence of 1 µM cGMP. This approach represents the difference between zero-cGMP and saturating cGMP depending on various pH conditions. Kinetic measurements for cGMP association were performed utilizing a stopped-flow instrument (BioLogic Science Instruments µSFM-20, France). Typically, four independent mixing experiments (10 µM protein, 0 to 2 µM cGMP) were averaged before mono-exponential fitting with a Simplex routine in Bio-Kine (v. 3.0) proprietary software provided by BioLogic. cGMP dissociation kinetics were determined by mixing 500 nM FlincG protein and 150 nM cGMP, followed by subsequent > 5 fold dilution in Hepes-buffered HBSS pH 7.4 to final cGMP concentrations below 30 nM. The intensity changes indicative of cGMP dissociation were recorded using the fluorescent spectrophotometer F4500 (Hitachi, Tokyo, Japan). For immunoprecipitation studies, a mixture of 5 µg FlincG protein in PSS, 0.1 % NP-40 and 5 µg protein of the corresponding PKG isoform was combined with 2 µg rabbit anti-GFP antibody (Invitrogen, Molprobes) and incubated at 25°C for 30

minutes. The protein-protein complex was precipitated with Protein A/G beads and was washed > 3 times with PBS, 0.1% NP-40 buffer. Beads were resuspended in Laemmli buffer and subjected to 10 % SDS-PAGE.

Supporting Figure legends

Supporting Figure 1: 10 % SDS-PAGE showing the co-immunoprecipitation of FlincG variants with their corresponding PKG isoforms using a rabbit anti-GFP antibody.

Supporting Figure 2: pH titration of normalized fluorescence. For each pH point, the baseline (F_0) was monitored in absence of cGMP, and the increase in fluorescence (F) was determined in presence of 1 µM cGMP.

Supporting Figure 3:

Uniform distribution of fluorescence intensity of δ-FlincG in VSM cells. (A, C) Images showing the distribution of fluorescence intensity in VSM cells represented in Figures 5 A (NO) and D (ANP) at time points zero. (B, D) Three-dimensional surface plots. X- and Y-axes represent the orientation of the cells and the Z-axis shows the fluorescence intensities.

Supporting Figure 4:

Cell morphology of δ-FlincG transfected VSM cells. (A, B) Fluorescence images of VSM cells depicted in Figures 5 A and D. Dotted lines trace the cell shape over the time-course of the experiment. Arrows indicate the regions of interest in Figure 5. The insets in (B) magnify the region of interest and verify the absence of cellular movement and morphology changes over time.

Supporting Movie 1: Application of 1.5 nM DEA-NO to δ-FlincG transfected VSM cell

Supporting movie 2: Application of 50 μM 8-Br-cGMP to δ-FlincG transfected VSM cell

Supporting movie 3: Application of 100 nM Forskolin to δ-FlincG transfected VSM cell.

Supporting movie 4: Application of 10 nM ANP to δ-FlincG transfected VSM cells;

Supporting Figure 1:

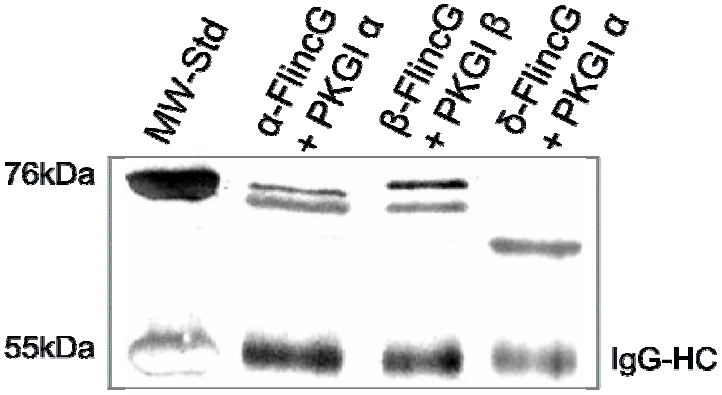

Supporting Figure 2:

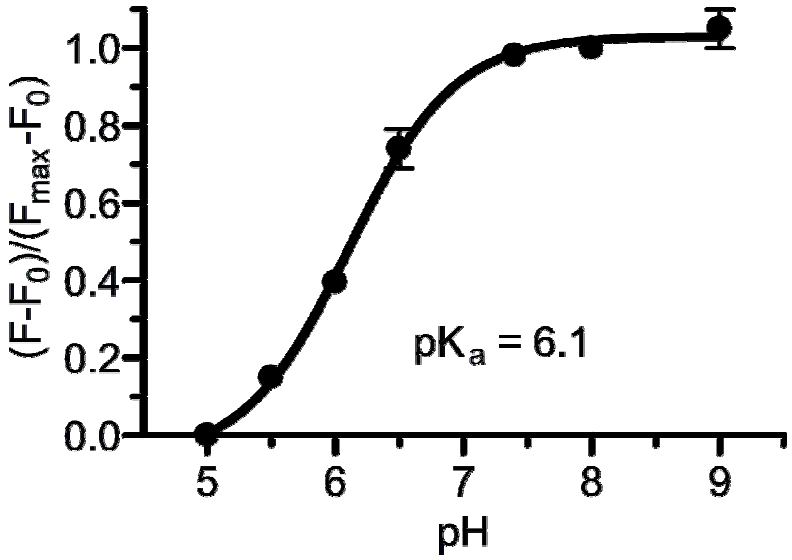

Supporting Figure 3:

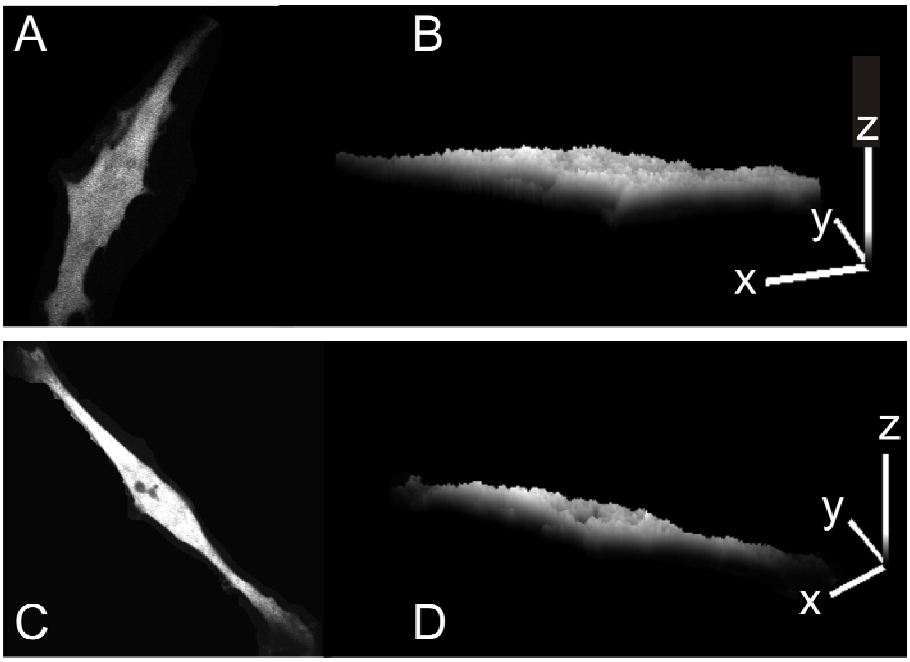

Supporting Figure 4:

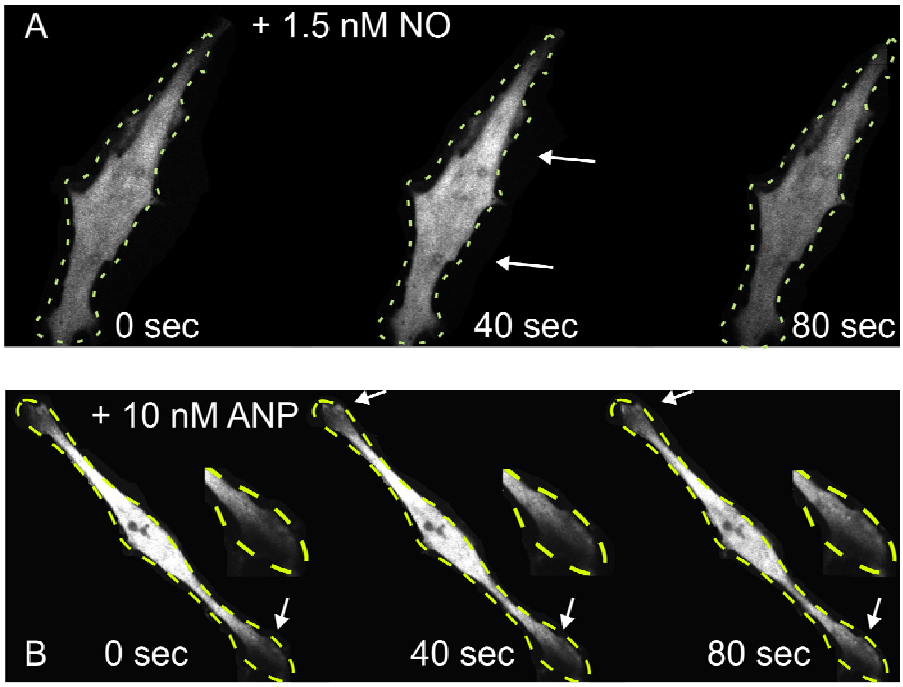

References

Baird GS, Zacharias DA and Tsien RY. Circular permutation and receptor insertion within green fluorescent proteins. *Proc Natl Acad Sci U S A* 96(20): 11241-6, 1999.

Brunner F, Stessel H and Kukovetz WR. Novel guanylyl cyclase inhibitor, ODQ reveals role of nitric oxide, but not of cyclic GMP in endothelin-1 secretion. *FEBS Lett* 376(3): 262-6, 1995.

Cary SP, Winger JA, Derbyshire ER and Marletta MA. Nitric oxide signaling: no longer simply on or off. *Trends Biochem Sci* 31(4): 231-9, 2006.

Castro LR, Verde I, Cooper DM and Fischmeister R. Cyclic guanosine monophosphate compartmentation in rat cardiac myocytes. *Circulation* 113(18): 2221-8, 2006.

Cawley SM, Sawyer CL, Brunelle KF, van der Vliet A and Dostmann WR. Nitric oxide-evoked transient kinetics of cyclic GMP in vascular smooth muscle cells. *Cell Signal* 19(5): 1023-33, 2007.

Conti M and Beavo J. Biochemistry and physiology of cyclic nucleotide phosphodiesterases: essential components in cyclic nucleotide signaling. *Annu Rev Biochem* 76: 481-511, 2007.

Corbin JD, Blount MA, Weeks JL, 2nd, Beasley A, Kuhn KP, Ho YS, Saidi LF, Hurley JH, Kotera J and Francis SH. [3H]sildenafil binding to phosphodiesterase-5 is specific, kinetically heterogeneous, and stimulated by cGMP. *Mol Pharmacol* 63(6): 1364-72, 2003.

Dostmann WR, Koep N and Endres R. The catalytic domain of the cGMP-dependent protein kinase Ialpha modulates the cGMP-binding characteristics of its regulatory domain. *FEBS Lett* 398(2-3): 206-10, 1996.

Dostmann WR, Taylor MS, Nickl CK, Brayden JE, Frank R and Tegge WJ. Highly specific, membrane-permeant peptide blockers of cGMP-dependent protein kinase Ialpha inhibit NO-induced cerebral dilation. *Proc Natl Acad Sci U S A* 97(26): 14772-7, 2000.

Feil R, Muller S and Hofmann F. High-level expression of functional cGMP-dependent protein kinase using the baculovirus system. *FEBS Lett* 336(1): 163-7, 1993.

Fischmeister R, Castro LR, Abi-Gerges A, Rochais F, Jurevicius J, Leroy J and Vandecasteele G. Compartmentation of cyclic nucleotide signaling in the heart: the role of cyclic nucleotide phosphodiesterases. *Circ Res* 99(8): 816-28, 2006.

Francis SH, Blount MA, Zoraghi R and Corbin JD. Molecular properties of mammalian proteins that interact with cGMP: protein kinases, cation channels, phosphodiesterases, and multi-drug anion transporters. *Front Biosci* 10: 2097-117, 2005.

Garthwaite J. Dynamics of cellular NO-cGMP signaling. *Front Biosci* 10: 1868-80, 2005.

Garthwaite J, Southam E, Boulton CL, Nielsen EB, Schmidt K and Mayer B. Potent and selective inhibition of nitric oxide-sensitive guanylyl cyclase by 1H-[1,2,4]oxadiazolo[4,3-a]quinoxalin-1-one. *Mol Pharmacol* 48(2): 184-8, 1995.

Griesbeck O, Baird GS, Campbell RE, Zacharias DA and Tsien RY. Reducing the environmental sensitivity of yellow fluorescent protein. Mechanism and applications. *J Biol Chem* 276(31): 29188-94, 2001.

Grynkiewicz G, Poenie M and Tsien RY. A new generation of Ca2+ indicators with greatly improved fluorescence properties. *J Biol Chem* 260(6): 3440-50, 1985.

Hamet P, Pang SC and Tremblay J. Atrial natriuretic factor-induced egression of cyclic guanosine 3':5'-monophosphate in cultured vascular smooth muscle and endothelial cells. *J Biol Chem* 264(21): 12364-9, 1989.

Hofmann F. The biology of cyclic GMP-dependent protein kinases. *J Biol Chem* 280(1): 1-4, 2005.

Hofmann F, Biel M and Kaupp UB. International Union of Pharmacology. LI. Nomenclature and structure-function relationships of cyclic nucleotide-regulated channels. *Pharmacol Rev* 57(4): 455-62, 2005.

Honda A, Adams SR, Sawyer CL, Lev-Ram V, Tsien RY and Dostmann WR. Spatiotemporal dynamics of guanosine 3',5'-cyclic monophosphate revealed by a genetically encoded, fluorescent indicator. *Proc Natl Acad Sci U S A* 98(5): 2437-42, 2001.

Honda A, Moosmeier MA and Dostmann WR. Membrane-permeable cygnets: rapid cellular internalization of fluorescent cGMP-indicators. *Front Biosci* 10: 1290-301, 2005.

Honda A, Sawyer CL, Cawley SM and Dostmann WR. Cygnets: in vivo characterization of novel cGMP indicators and in vivo imaging of intracellular cGMP. *Methods Mol Biol* 307: 27-43, 2005.

Ji G, Feldman ME, Deng KY, Greene KS, Wilson J, Lee JC, Johnston RC, Rishniw M, Tallini Y, Zhang J, Wier WG, Blaustein MP, Xin HB, Nakai J and Kotlikoff MI.

Ca2+-sensing transgenic mice: postsynaptic signaling in smooth muscle. *J Biol Chem* 279(20): 21461-8, 2004.

Kass DA, Takimoto E, Nagayama T and Champion HC. Phosphodiesterase regulation of nitric oxide signaling. *Cardiovasc Res* 75(2): 303-14, 2007.

Kuhn M. Cardiac and intestinal natriuretic peptides: insights from genetically modified mice. *Peptides* 26(6): 1078-85, 2005.

Leitman DC, Andresen JW, Catalano RM, Waldman SA, Tuan JJ and Murad F. Atrial natriuretic peptide binding, cross-linking, and stimulation of cyclic GMP accumulation and particulate guanylate cyclase activity in cultured cells. *J Biol Chem* 263(8): 3720-8, 1988.

Mo E, Amin H, Bianco IH and Garthwaite J. Kinetics of a cellular nitric oxide/cGMP/phosphodiesterase-5 pathway. *J Biol Chem* 279(25): 26149-58, 2004.

Mongillo M, Tocchetti CG, Terrin A, Lissandron V, Cheung YF, Dostmann WR, Pozzan T, Kass DA, Paolocci N, Houslay MD and Zaccolo M. Compartmentalized phosphodiesterase-2 activity blunts beta-adrenergic cardiac inotropy via an NO/cGMP-dependent pathway. *Circ Res* 98(2): 226-34, 2006.

Mullershausen F, Koesling D and Friebe A. NO-sensitive guanylyl cyclase and NO-induced feedback inhibition in cGMP signaling. *Front Biosci* 10: 1269-78, 2005.

Nakai J, Ohkura M and Imoto K. A high signal-to-noise Ca(2+) probe composed of a single green fluorescent protein. *Nat Biotechnol* 19(2): 137-41, 2001.

Nikolaev VO, Gambaryan S and Lohse MJ. Fluorescent sensors for rapid monitoring of intracellular cGMP. *Nat Methods* 3(1): 23-5, 2006.

Piggott LA, Hassell KA, Berkova Z, Morris AP, Silberbach M and Rich TC. Natriuretic peptides and nitric oxide stimulate cGMP synthesis in different cellular compartments. *J Gen Physiol* 128(1): 3-14, 2006.

Porter VA, Bonev AD, Knot HJ, Heppner TJ, Stevenson AS, Kleppisch T, Lederer WJ and Nelson MT. Frequency modulation of Ca2+ sparks is involved in regulation of arterial diameter by cyclic nucleotides. *Am J Physiol* 274(5 Pt 1): C1346-55, 1998.

Richie-Jannetta R, Busch JL, Higgins KA, Corbin JD and Francis SH. Isolated regulatory domains of cGMP-dependent protein kinase Ialpha and Ibeta retain dimerization and native cGMP-binding properties and undergo isoform-specific conformational changes. *J Biol Chem* 281(11): 6977-84, 2006.

Robertson BE, Schubert R, Hescheler J and Nelson MT. cGMP-dependent protein kinase activates Ca-activated K channels in cerebral artery smooth muscle cells. *Am J Physiol* 265(1 Pt 1): C299-303, 1993.

Roy B and Garthwaite J. Nitric oxide activation of guanylyl cyclase in cells revisited. *Proc Natl Acad Sci U S A* 103(32): 12185-90, 2006.

Russwurm M, Mullershausen F, Friebe A, Jager R, Russwurm C and Koesling D. Design of fluorescence resonance energy transfer (FRET)-based cGMP indicators: a systematic approach. *Biochem J* 407(1): 69-77, 2007.

Ruth P, Landgraf W, Keilbach A, May B, Egleme C and Hofmann F. The activation of expressed cGMP-dependent protein kinase isozymes I alpha and I beta is determined by the different amino-termini. *Eur J Biochem* 202(3): 1339-44, 1991.

Ruth P, Pfeifer A, Kamm S, Klatt P, Dostmann WR and Hofmann F. Identification of the amino acid sequences responsible for high affinity activation of cGMP kinase Ialpha. *J Biol Chem* 272(16): 10522-8, 1997.

Schrammel A, Behrends S, Schmidt K, Koesling D and Mayer B. Characterization of 1H-[1,2,4]oxadiazolo[4,3-a]quinoxalin-1-one as a heme-site inhibitor of nitric oxide-sensitive guanylyl cyclase. *Mol Pharmacol* 50(1): 1-5, 1996.

Takimoto E, Belardi D, Tocchetti CG, Vahebi S, Cormaci G, Ketner EA, Moens AL, Champion HC and Kass DA. Compartmentalization of cardiac beta-adrenergic inotropy modulation by phosphodiesterase type 5. *Circulation* 115(16): 2159-67, 2007.

Takimoto E, Champion HC, Belardi D, Moslehi J, Mongillo M, Mergia E, Montrose DC, Isoda T, Aufiero K, Zaccolo M, Dostmann WR, Smith CJ and Kass DA. cGMP catabolism by phosphodiesterase 5A regulates cardiac adrenergic stimulation by NOS3-dependent mechanism. *Circ Res* 96(1): 100-9, 2005.

Tallini YN, Ohkura M, Choi BR, Ji G, Imoto K, Doran R, Lee J, Plan P, Wilson J, Xin HB, Sanbe A, Gulick J, Mathai J, Robbins J, Salama G, Nakai J and Kotlikoff MI. Imaging cellular signals in the heart in vivo: Cardiac expression of the high-signal Ca2+ indicator GCaMP2. *Proc Natl Acad Sci U S A* 103(12): 4753-8, 2006.

Turko IV, Ballard SA, Francis SH and Corbin JD. Inhibition of cyclic GMP-binding cyclic GMP-specific phosphodiesterase (Type 5) by sildenafil and related compounds. *Mol Pharmacol* 56(1): 124-30, 1999.

Wall ME, Francis SH, Corbin JD, Grimes K, Richie-Jannetta R, Kotera J, Macdonald BA, Gibson RR and Trewhella J. Mechanisms associated with cGMP

binding and activation of cGMP-dependent protein kinase. *Proc Natl Acad Sci U S A* 100(5): 2380-5, 2003.

Winquist RJ, Faison EP, Waldman SA, Schwartz K, Murad F and Rapoport RM. Atrial natriuretic factor elicits an endothelium-independent relaxation and activates particulate guanylate cyclase in vascular smooth muscle. *Proc Natl Acad Sci U S A* 81(23): 7661-4, 1984.

Wolfe L, Corbin JD and Francis SH. Characterization of a novel isozyme of cGMP-dependent protein kinase from bovine aorta. *J Biol Chem* 264(13): 7734-41, 1989.

Zhao J, Trewhella J, Corbin J, Francis S, Mitchell R, Brushia R and Walsh D. Progressive cyclic nucleotide-induced conformational changes in the cGMP-dependent protein kinase studied by small angle X-ray scattering in solution. *J Biol Chem* 272(50): 31929-36, 1997.

Zoraghi R, Bessay EP, Corbin JD and Francis SH. Structural and functional features in human PDE5A1 regulatory domain that provide for allosteric cGMP binding, dimerization, and regulation. *J Biol Chem* 280(12): 12051-63, 2005.

CHAPTER FIVE: NON-GENETIC DELIVERY SYSTEM FOR NOVEL cGMP-BIOSENSORS INTO INTACT ARTERIES REVEALS cGMP DYNAMICS IN RESPONSE TO NITRIC OXIDE AND ATRIAL NATRIURETIC PEPTIDE.

Introduction

Nitric oxide (NO) and atrial natriuretic peptide (ANP) were first suggested to regulate vascular smooth muscle tone more than 25 years ago. In 1980, Furchgott & Zawadzki (Furchgott and Zawadzki, 1980) first described endothelium-dependent relaxation, a phenomenon whereby acetylcholine relaxes isolated preparations of blood vessels only if the vascular endothelium lining the vessels is present and intact. Subsequent studies revealed that acetylcholine and other agents (including bradykinin, histamine and 5-hydroxytryptamine) release a transferable factor (endothelium-derived relaxing factor, EDRF) which is unstable, acts via stimulation of the soluble guanylate cyclase and is inhibited by hemoglobin and methylene blue (Furchgott et al., 1984). Several years later, Furchgott as well as Ignarro proposed that EDRF might be nitric oxide (Furchgott, 1988; Ignarro et al., 1988). Since then, the vasodilatory effect of NO has been studied in great detail, and it is now known that it is caused by a soluble guanylyl cyclase-mediated increase in $[cGMP]_i$ (Mullershausen et al., 2005). Another regulatory factor for vascular smooth muscle tone was discovered in 1981, when Adolfo de Bold isolated a potent diuretic and natriuretic factor from rat atrial extracts (de Bold et al., 1981). Atrial natriuretic peptide (ANP) has been shown to bind to the membrane-bound, particulate gunalylyl cyclase A (GC-A), thereby increasing $[cGMP]_i$ (Garbers,

1991; Garbers and Lowe, 1994). Although several methods exist to detect cGMP in vitro, such as biosensors (Honda et al., 2001; Nikolaev et al., 2006; Russwurm et al., 2007), radio-immunoassays (Brooker et al., 1979), patch clamping (Castro et al., 2006) and patch cramming (Trivedi and Kramer, 1998), it has been challenging to follow $[cGMP]_i$ dynamics in intact tissue under near-physiological conditions. Commonly used myograph studies are suitable to monitor changes in vessel diameter in response to various stimuli, thereby indirectly predicting fluctuations in cGMP and calcium dynamics. However, there is growing demand for methods to directly detect $[cGMP]_i$ in intact arteries. Recently, FRET-based cGMP biosensors (Cygnets) were permanently fused to membrane permeable peptides (MPP) and shown to be fully functional in cultured VSM cells and in intact vessels (Honda et al., 2005). However, these FRET-based indicators have limited utility in studying spatio-temporal cGMP dynamics in intact tissue, since they display overall low FRET-ratio change in cells, low responsiveness to physiological NO and ANP concentrations, and have limited use for high-speed, real-time confocal microscopy. These restrictions prompted us to develop a non-genetic delivery system for our novel, non-FRET cGMP biosensors, FlincGs (Chapter 4), utilizing intact arteries as a model system. Here, we report for the first time a non-FRET based cGMP biosensor suitable to detect NO- and ANP-dependent $[cGMP]_i$ responses in cerebral arteries.

Results and discussion

Previously, several genetic methods, as well as viral delivery systems, have been reported to translocate small nucleotides or plasmids into intact tissue (Bolz and Pohl, 2003; Earley et al., 2005; Tang et al., 2003; Yao and Wang, 1995; Zhang et al., 2005). Since all these methods have limited use to translocate large-size plasmids into intact tissue and require long incubation times (several days) for successful delivery, we have used a different approach in this study. Npys-TAT, a 2,2'-(5-nitropyridine (Npys)) activated form of the membrane-permeable TAT-peptide (Rabanal, 2003), was mixed with purified α-FlincG protein in vitro and the activated TAT peptide bound reversibly to surface cysteines of α-FlincG (Figure 1 A). TAT-labeling of α-FlincG preserved overall cGMP (K_a = 40 ± 3 nM) over cAMP (K_a = 54 ± 8 μM) selectivity and maximal 1.35-fold fluorescence intensity change of the cGMP biosensor, indicating that the chemical labeling process does not interfere with critical FlincG folding to allow detection of $[cGMP]_i$ (Figure 1 B; see also Table 1 in chapter 4). This stable TAT-SS-FlincG complex translocated randomly and distributed uniformly into all cell types found in small resistance vessels, including VSM cells (Figures 2 A, B). Upon intracellular entry, the reducing environment cleaves the TAT peptide and releases α-FlincG. To verify cytosolic localization of α-FlincG, we applied 8-Br-cGMP (50 μM) to FlincG-labeled, cerebral arteries (Figure 2 C).

Recent studies in cultured VSM cells utilizing FlincG indicators revealed distinct spatio-temporal $[cGMP]_i$ kinetics depending on NO or ANP stimuli (Chapter 4, Figures 4 and 5). Interestingly, similar temporal cGMP dynamics were detected in intact cerebral

arteries utilizing α-FlincG. Application of NO induced transient cGMP responses (lag time = 25 sec) with a maximum 1.3 fold increase in fluorescence intensity (Figure 3 A). The spatial distribution of $[cGMP]_i$ in response to NO in cerebral arteries could not be determined due to the slow frame rate of the confocal imaging system utilized in these experiments. In contrast to NO-evoked, transient cGMP kinetics, application of ANP (100 nM) induced sustained cGMP synthesis (lag time = 40 sec) with maximum 1.3 fold increase in fluorescence intensity (Figure 3 B). The spatial distribution of ANP-evoked $[cGMP]_i$ could not be resolved because of low-resolution epi-fluorescence imaging techniques. The overall low increase in intensity for α-FlincG is consistent with previous observations showing that different FlincG indicators (α- and β- FlincGs) generate small changes in the maximal fold intensity increase in cells due to interactions with endogenous proteins (Chapter 4: Figure 1 D; Tables 1 and 2).

Although this novel, non-genetic delivery method for FlincG biosensors holds the potential to advance our understanding of the spatio-temporal dynamics of $[cGMP]_i$ in intact arteries, several complications still remain: relatively long incubation times (12-15h) of the arteries are required to successfully deliver TAT-FlincG into VSM cells. This may result in precipitation of TAT-FlincG protein, as well as downregulation of key enzymes of the cGMP signaling cascade over time in arteries (Boerth et al., 1997; Browner et al., 2004). Furthermore, FlincG-loading efficiency is only modest (10-20%) and transient, since intracellular FlincG is degraded over time by proteases. Thus, future studies on $[cGMP]_i$ dynamics in intact tissue may greatly benefit from the development of FlincG transgenic mice. This transgenic approach is advantageous over current

methods, because $[cGMP]_i$ dynamics can be studied directly in freshly isolated arteries. Furthermore, tissue-specific expression of FlincG may reveal distinct cGMP patterns in various cell types such as vascular smooth muscle, cardiac myocytes or endothelial cells.

Methods

Protein expression and purification

To express α-FlincG, E.Coli BLR were transformed with α-FlincG-containing pRSET-A vectors and were cultured at 25°C for 12h after protein induction with 0.4 mM isopropyl-β-D-thiogalactoside (IPTG). After centrifugation, α-FlincG was purified using cyclic nucleotide affinity chromatography as described previously (Feil et al., 1993).

Cross-linking of α-FlincG with TAT and *in vitro* characterization

To cross-label α-FlincG with TAT, purified protein (0.5 mg/ml) was mixed with a 50-fold molar excess of Npys-TAT under nitrogen atmosphere. 200 nM recombinant TAT-α-FlincG was combined with increasing concentrations of cGMP (0-10 µM) or cAMP (0-100 µM) to generate cNMP dose response curves. Excitation spectra (detected at 510 nm) and emission spectra (excited at 410 or 480 nm) were taken using a fluorescence spectrophotometer F4500 (Hitachi, Tokyo, Japan).

TAT-α-FlincG in intact cerebral arteries

TAT-α-FlincG (50 µl) was then added to a canulated, pressurized, freshly isolated anterior, cerebral artery (~80-130um diameter) and incubated 12-15h at 37°C. Imaging for NO application was performed using the Noran OZ (Middleton, WI) laser scanning confocal system (10 second acquisitions; 60 x magnification). Epi-fluorescence imaging was performed to follow 8-Br-cGMP and ANP-evoked cGMP responses (10 sec acquisitions; 40 x magnification).

Figure legends:

Figure 1: (A) Non-genetic delivery of TAT-FlincG into intact tissue. Surface accessible Cys residues of FlincG were labeled with an NPys-activated form of TAT. Following translocation into VSM cells within intact arteries, the carrier is cleaved and the biosensor is liberated. (B) cGMP and cAMP selectivity of recombinant TAT-α-FlincG.

Figure 2: Rat cerebral arteries incubated with (A) TAT-α-FlincG and nuclear stain or (B) without any treatment. Confocal images were taken at 60 x magnification (see Methods). (C) Application of 50 µM 8-Br-cGMP.

Figure 3: cGMP signaling in intact cerebral arteries upon application of (A) 5 µM DEA-NO and (B) 100 nM ANP.

Figure 1

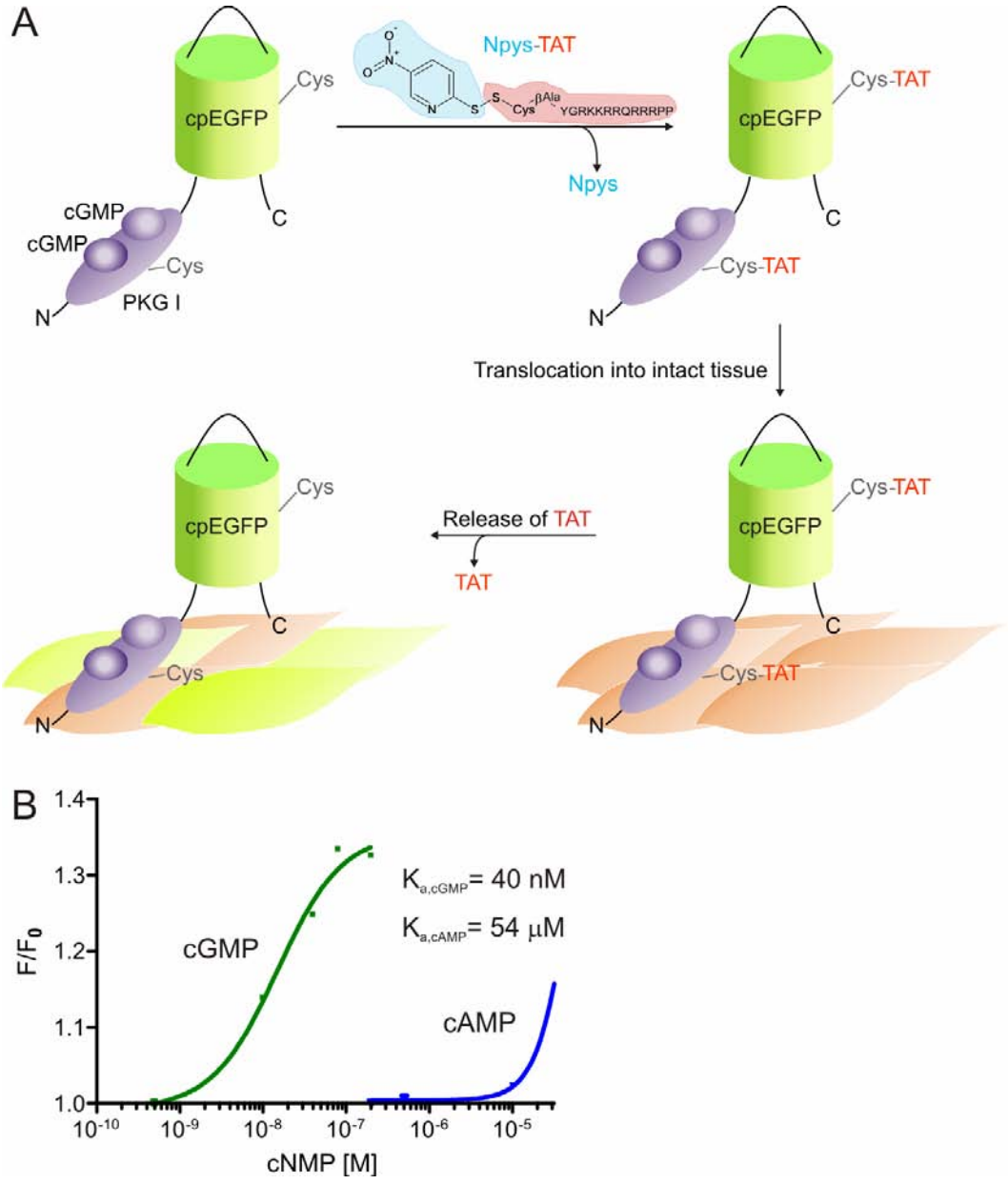
A
cpEGFP
Cys
C
cGMP
cGMP
Cys
PKG I
N
Npys-TAT
Cys
βAla
YGRKKRRQRRRPP
Npys
cpEGFP
Cys-TAT
C
Cys-TAT
N
Translocation into intact tissue
cpEGFP
Cys
C
Cys
N
Release of TAT
TAT
cpEGFP
Cys-TAT
C
Cys-TAT
N
B
1.4
1.3
1.2
1.1
1.0
F/F0
cGMP
cAMP
Ka,cGMP= 40 nM
Ka,cAMP= 54 µM
10-10
10-9
10-8
10-7
10-6
10-5
cNMP [M]

Figure 2

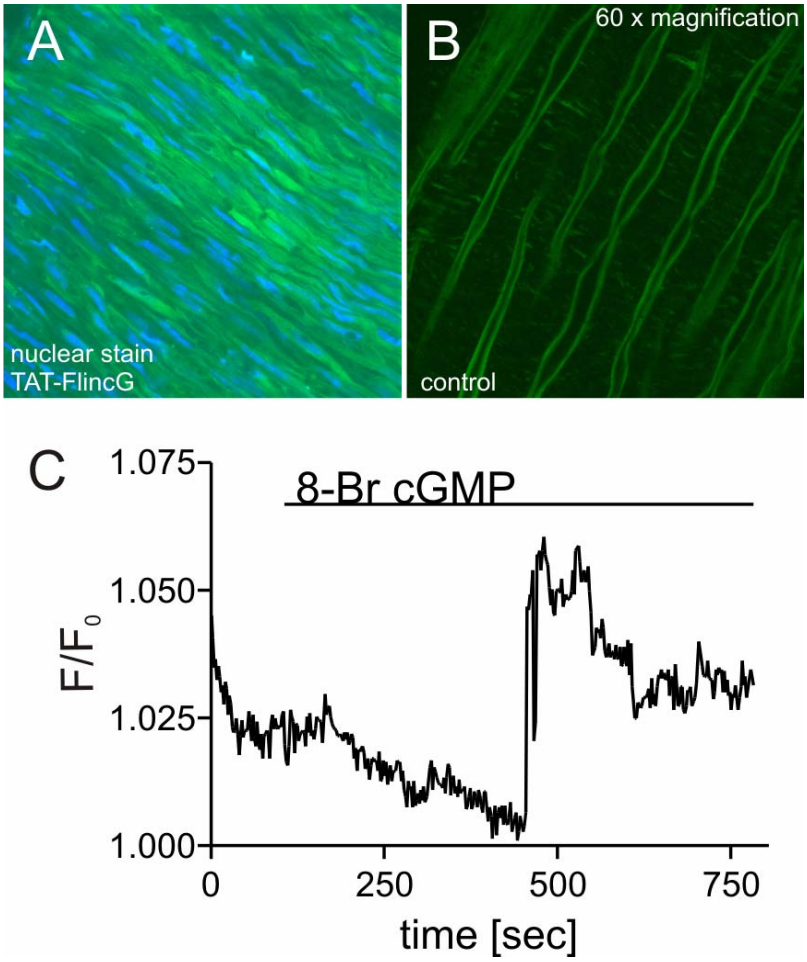
A
nuclear stain
TAT-FlincG
B
60 x magnification
control
C
8-Br cGMP
F/F0
1.075
1.050
1.025
1.000
0
250
500
750
time [sec]

Figure 3

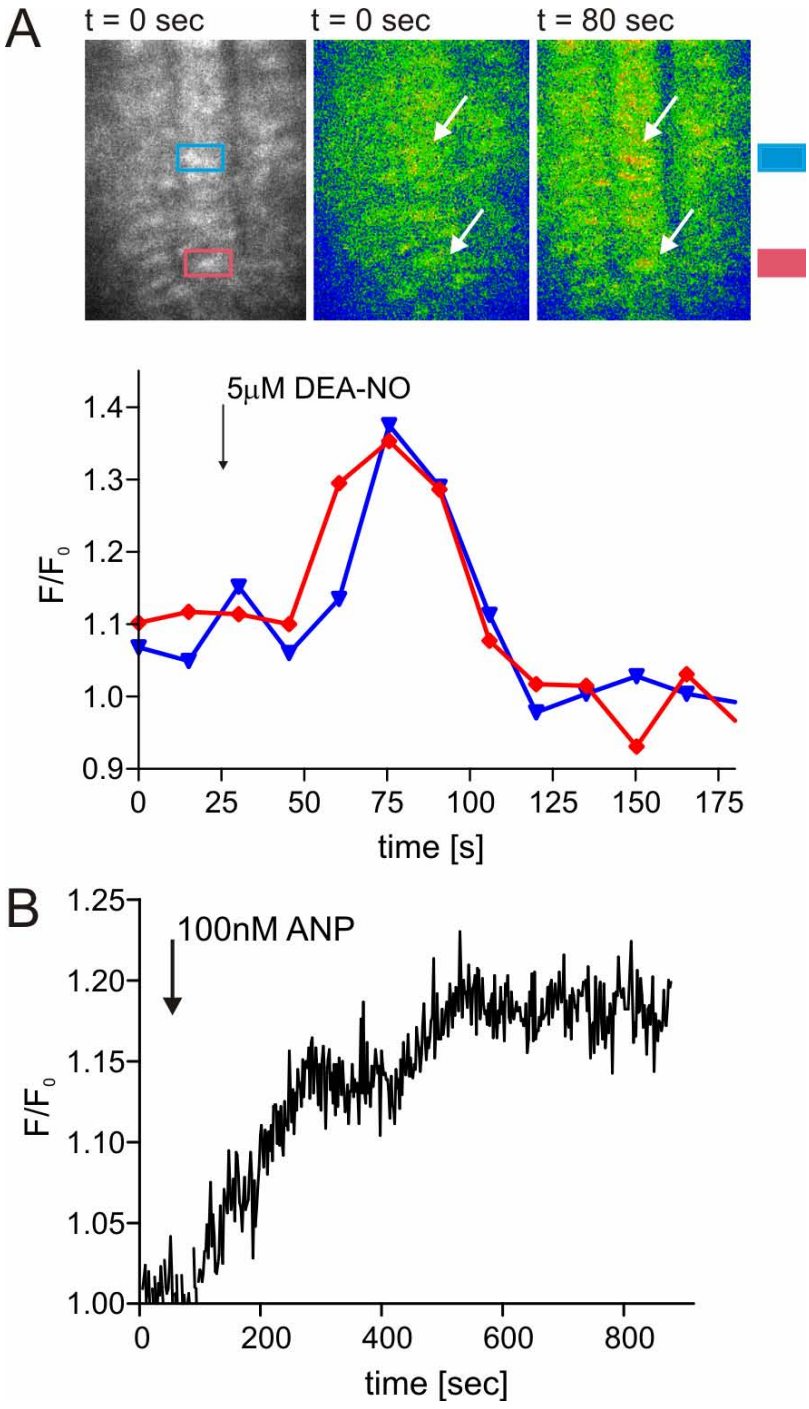
A
t = 0 sec
t = 0 sec
t = 80 sec
5μM DEA-NO
F/F0
1.4
1.3
1.2
1.1
1.0
0.9
0
25
50
75
100
125
150
175
time [s]
B
100nM ANP
F/F0
1.25
1.20
1.15
1.10
1.05
1.00
0
200
400
600
800
time [sec]

References

Boerth NJ, Dey NB, Cornwell TL and Lincoln TM. Cyclic GMP-dependent protein kinase regulates vascular smooth muscle cell phenotype. *J Vasc Res* 34(4): 245-59, 1997.

Bolz SS and Pohl U. Highly effective non-viral gene transfer into vascular smooth muscle cells of cultured resistance arteries demonstrated by genetic inhibition of sphingosine-1-phosphate-induced vasoconstriction. *J Vasc Res* 40(4): 399-405, 2003.

Brooker G, Harper JF, Terasaki WL and Moylan RD. Radioimmunoassay of cyclic AMP and cyclic GMP. *Adv Cyclic Nucleotide Res* 10: 1-33, 1979.

Browner NC, Dey NB, Bloch KD and Lincoln TM. Regulation of cGMP-dependent protein kinase expression by soluble guanylyl cyclase in vascular smooth muscle cells. *J Biol Chem* 279(45): 46631-6, 2004.

Castro LR, Verde I, Cooper DM and Fischmeister R. Cyclic guanosine monophosphate compartmentation in rat cardiac myocytes. *Circulation* 113(18): 2221-8, 2006.

de Bold AJ, Borenstein HB, Veress AT and Sonnenberg H. A rapid and potent natriuretic response to intravenous injection of atrial myocardial extract in rats. *Life Sci* 28(1): 89-94, 1981.

Earley S, Heppner TJ, Nelson MT and Brayden JE. TRPV4 forms a novel Ca2+ signaling complex with ryanodine receptors and BKCa channels. *Circ Res* 97(12): 1270-9, 2005.

Feil R, Muller S and Hofmann F. High-level expression of functional cGMP-dependent protein kinase using the baculovirus system. *FEBS Lett* 336(1): 163-7, 1993.

Furchgott RF. Studies on relaxation of rabbit aorta by sodium nitrite: the basis for the proposal that the acid-activatable inhibitory factor from retractor penis is inorganic nitrite and the endothelium-derived relaxing factor is nitric oxide. Vasodilatation: Vascular Smooth Muscle, Peptides, Autonomic Nerves and Endothelium, ed. Vanhoutte, P.M. New York, Raven Press. 1988

Furchgott RF, Cherry PD, Zawadzki JV and Jothianandan D. Endothelial cells as mediators of vasodilation of arteries. *J Cardiovasc Pharmacol* 6 Suppl 2: S336-43, 1984.

Furchgott RF and Zawadzki JV. The obligatory role of endothelial cells in the relaxation of arterial smooth muscle by acetylcholine. *Nature* 288(5789): 373-6, 1980.

Garbers DL. Guanylyl cyclase-linked receptors. *Pharmacol Ther* 50(3): 337-45, 1991.

Garbers DL and Lowe DG. Guanylyl cyclase receptors. *J Biol Chem* 269(49): 30741-4, 1994.

Honda A, Adams SR, Sawyer CL, Lev-Ram V, Tsien RY and Dostmann WR. Spatiotemporal dynamics of guanosine 3',5'-cyclic monophosphate revealed by a genetically encoded, fluorescent indicator. *Proc Natl Acad Sci U S A* 98(5): 2437-42, 2001.

Honda A, Moosmeier MA and Dostmann WR. Membrane-permeable cygnets: rapid cellular internalization of fluorescent cGMP-indicators. *Front Biosci* 10: 1290-301, 2005.

Ignarro LJ, Byrns RE and Wood KS. Biochemical and pharmacological properties of endothelium-derived relaxing factor and its similarity to nitric oxide radical. Vasodilatation: Vascular Smooth Muscle, Peptide, Autonomic Nerves and Endothelium, ed. Vanhoutte, P.M. New York, Raven Press. 1988

Mullershausen F, Koesling D and Friebe A. NO-sensitive guanylyl cyclase and NO-induced feedback inhibition in cGMP signaling. *Front Biosci* 10: 1269-78, 2005.

Nikolaev VO, Gambaryan S and Lohse MJ. Fluorescent sensors for rapid monitoring of intracellular cGMP. *Nat Methods* 3(1): 23-5, 2006.

Rabanal F. Use of 2,2'-(5-nirtopyridine) for the Heterodimerization of Cystein Containing Peptides. Introduction of the 5-nitro-2- pyridinesulfenyl Group. *Tetrahedron Lett* 37: 1347-1350, 2003.

Russwurm M, Mullershausen F, Friebe A, Jager R, Russwurm C and Koesling D. Design of fluorescence resonance energy transfer (FRET)-based cGMP indicators: a systematic approach. *Biochem J* 407(1): 69-77, 2007.

Tang DD, Turner CE and Gunst SJ. Expression of non-phosphorylatable paxillin mutants in canine tracheal smooth muscle inhibits tension development. *J Physiol* 553(Pt 1): 21-35, 2003.

Trivedi B and Kramer RH. Real-time patch-cram detection of intracellular cGMP reveals long-term suppression of responses to NO and muscarinic agonists. *Neuron* 21(4): 895-906, 1998.

Yao A and Wang DH. Heterogeneity of adenovirus-mediated gene transfer in cultured thoracic aorta and renal artery of rats. *Hypertension* 26(6 Pt 2): 1046-50, 1995.

Zhang W, Wu Y, Du L, Tang DD and Gunst SJ. Activation of the Arp2/3 complex by N-WASp is required for actin polymerization and contraction in smooth muscle. *Am J Physiol Cell Physiol* 288(5): C1145-60, 2005.

CONCLUSIONS AND FUTURE DIRECTIONS

In this dissertation, we investigated in detail the mechanism of PKG activation using site-specific mutagenesis, electrospray ionization mass spectrometry, kinase activity assays, cGMP binding and dissociation studies (chapter two) as well as crystallography (chapter three). Based on the specific cGMP binding characteristics of PKG, we developed a new generation of cGMP biosensors to examine the spatial distribution of $[cGMP]_i$ in response to NO and ANP in VSM cells (chapter four) and in intact tissue (chapter five).

In chapter two, we mutated several conserved aminoacids in the cGMP binding pockets of PKG regulatory domain to investigate the molecular mechanism of PKG activation. Based on site A and site B knock-out mutants (G167E, E168G, G291E, E292G), we suggest an overall concerted mechanism of activation for PKG I α that is significantly different form the sequential mechanism of PKA activation. Our results support coupling between both cGMP binding sites A and B, as well as coupling between cGMP binding site A and the catalytic domain. Furthermore, cGMP binding site B seems to play a pivotal role in modulating responsiveness of PKG to a broader range of $[cGMP]_i$. In addition, the structural order of high and low affinity binding sites for PKG I α have been determined as sites A and B, respectively. We further investigated the roles of aminoacids arginine 177 and arginine 301, that are highly conserved among protein kinases, and that coordinate the phosphate backbone of cAMP in PKA (Bubis et al., 1988; Zawadzki and Taylor, 2004). In contrast, our studies have shown that these highly conserved arginines are not essential for stabilizing cGMP in PKG. That raises the

question, what the functional role of the conserved arginine in the cGMP binding pocket is. It could still be involved in coordinating cGMP, but it might also be the discriminating factor for distinguishing between cGMP and cAMP binding. In addition to cGMP, binding and activation assays should be performed for cAMP to test the hypothesis that the conserved arginine plays a role in cGMP selectivity. PKA-selective inhibitors such as Rp-cAMPs have been shown to bind to the cAMP binding pocket in a certain steric conformation (Dostmann and Taylor, 1991). Therefore, the effect of PKG-selective inhibitors (Rp-cGMPs) on the arginine mutants should be examined. In particular, the crystal structure of PKG, or the regulatory domain, would be of great benefit to decipher molecular interactions between cGMP and the cGMP binding pockets and to unravel the molecular details essential for PKG activation.

In general, crystallization studies require large quantities of protein, in order to screen as many conditions as possible for successful crystallization. PKG wildtype can only be expressed in a soluble form in (SF9-) insect cells (Feil et al., 1993), thereby demanding long expression times (>72 hours) and generally resulting in protein yields (< 5mg/l) too low for crystallization. In chapter three, we developed successfully a bacterial expression and purification protocol for deletion fragments of the regulatory domain of PKG, resulting in protein quantities sufficient for crystallization (> 5 mg/ 50 ml). We attempted to crystallize these deletion fragments of the regulatory cGMP binding domain, as well as full-length, wildtype PKG utilizing Hampton Screens #1 and #2, and were able to obtain crystals and crystal-like structures (Figures 3 and 5, chapter 3). These preliminary crystallization conditions need to be refined in future studies by varying pH,

incubation temperature, salt- and precipitant concentrations. Fine-tuning these conditions and utilizing macro- or micro- seeding may result in enlarged PKG crystals that qualify for high diffraction and ultimately reveal a structural model for PKG. Although crystal structures will provide invaluable insights into PKG structure and function, they are static and limited in their use to study the dynamics of PKG in a physiologically-relevant environment.

To meet this challenge, we developed a new generation of cGMP biosensors (FlincG) to monitor cGMP signaling in living cells and in intact tissue (Chapters 4 and 5). FlincG excels in monitoring $[cGMP]_i$ in response to physiological (low-nanomolar) NO concentrations and is suitable for high-resolution, real-time confocal microscopy. FlincG revealed the differential role of PDE-5 in the modulation of global cGMP in response to NO donors, and the spatial spread of cGMP away from the cell membrane in response to ANP. FlincG holds the promise of unraveling the complex interplay between cGMP and calcium signaling near the cell membrane and should ultimately be suitable for development of tissue-specific generation of transgenic mice with endogenous cGMP indicators, as has been done recently for calcium sensing with GCaMP (Ji et al., 2004; Tallini et al., 2006). One of the most important criteria for developing a transgenic mouse is the maximal signal-to-noise ratio of the biosensor. For GCaMP, the recombinant protein displayed 4-fold maximal fluorescence intensity change upon stimulation (Nakai et al., 2001), but in the transgenic GCaMP-mouse, the change in fluorescence intensity was decreased to approximately 1.6 fold (Ji et al., 2004; Tallini et al., 2006). GCaMP is composed of cpEGFP sandwiched between calmodulin and M13. The reduction in

fluorescence intensity in transgenic mice is most likely due to interactions of calmodulin and M13 with endogenous proteins. Our FlincG indicators, however, were specifically designed to prevent interactions with endogenous PKG, by deleting the N-terminal dimerization domain. Therefore, the overall maximal 1.75 fold increase in fluorescence intensity should not vary between recombinant δ-FlincG and the biosensor in transgenic mice. Furthermore, overall signal strength of the biosensor should be verified, by comparing the basal fluorescence of EGFP-transfected cells with δ-FlincG transfected cells. This is important, since a very 'dim' indicator could not be distinguished from auto-fluorescent cells in a transgenic mouse.

To study in greater detail the role of compartmentalized cGMP signaling, FlincG should be fused to the GC-A receptor to co-localize the biosensor to the cell membrane. Similarly, FlincG can be tethered to phosphodiesterases, G-protein kinase anchoring proteins, or to cyclic nucleotide gated ion channels to force the biosensor into close proximity to target molecules and to study cGMP dynamics together with calcium in spatially distinct compartments in cells. Currently, FlincG offers the exciting possibility to study calcium and cGMP dynamics simultaneously, by utilizing Fura- or Rhodamine-calcium dyes. To expand the variety of imaging options, cpEGFP in FlincG may be replaced by other circular permutated fluorophores (e.g. tangerine). The concept of this new generation of cGMP indicators may also set the stage for the development of non-FRET based cAMP biosensors. This approach holds the exciting potential to investigate not only the cross-talk between cGMP and calcium, but also between cGMP and cAMP, by utilizing modified FlincG and FRET-based cAMP indicators simultaneously.

In the future, FlincG can be used as a tool not only to address physiologically relevant questions, but also to study the structure and function of PKG. FlincG biosensors are composed of the regulatory domain of PKG fused to the N-terminus of cpEGFP. Since FlincG biosensors can be expressed in bacteria and purified to reasonable yield (> 7 mg/l), they are prime candidates for crystallization studies. Screening for FlincG-crystals should be facilitated by the fact that the presence of green fluorescent protein (GFP) 'stains' the crystals green. Furthermore, the structure-solving process of FlincG should be fairly straight forward, since the crystal structure of GFP (Ormo et al., 1996) can be utilized for molecular replacement. The structural characterization would allow us to gain insight into the regulatory domain of PKG as well as into the folding properties that define cGMP biosensors. In addition, the overall change in fluorescence intensity of FlincG can be used as read-out system to screen for novel PKG inhibitors and activators.

COMPREHENSIVE BIBLIOGRAPHY

Albrecht EW, Stegeman CA, Heeringa P, Henning RH and van Goor H. Protective role of endothelial nitric oxide synthase. *J Pathol* 199(1): 8-17, 2003.

Ammendola A, Geiselhoringer A, Hofmann F and Schlossmann J. Molecular determinants of the interaction between the inositol 1,4,5-trisphosphate receptor-associated cGMP kinase substrate (IRAG) and cGMP kinase Ibeta. *J Biol Chem* 276(26): 24153-9, 2001.

Aszodi A, Pfeifer A, Ahmad M, Glauner M, Zhou XH, Ny L, Andersson KE, Kehrel B, Offermanns S and Fassler R. The vasodilator-stimulated phosphoprotein (VASP) is involved in cGMP- and cAMP-mediated inhibition of agonist-induced platelet aggregation, but is dispensable for smooth muscle function. *Embo J* 18(1): 37-48, 1999.

Baird GS, Zacharias DA and Tsien RY. Circular permutation and receptor insertion within green fluorescent proteins. *Proc Natl Acad Sci U S A* 96(20): 11241-6, 1999.

Ballou DP, Zhao Y, Brandish PE and Marletta MA. Revisiting the kinetics of nitric oxide (NO) binding to soluble guanylate cyclase: the simple NO-binding model is incorrect. *Proc Natl Acad Sci U S A* 99(19): 12097-101, 2002.

Berman HM, Ten Eyck LF, Goodsell DS, Haste NM, Kornev A and Taylor SS. The cAMP binding domain: an ancient signaling module. *Proc Natl Acad Sci U S A* 102(1): 45-50, 2005.

Boerth NJ, Dey NB, Cornwell TL and Lincoln TM. Cyclic GMP-dependent protein kinase regulates vascular smooth muscle cell phenotype. *J Vasc Res* 34(4): 245-59, 1997.

Bolz SS and Pohl U. Highly effective non-viral gene transfer into vascular smooth muscle cells of cultured resistance arteries demonstrated by genetic inhibition of sphingosine-1-phosphate-induced vasoconstriction. *J Vasc Res* 40(4): 399-405, 2003.

Brooker G, Harper JF, Terasaki WL and Moylan RD. Radioimmunoassay of cyclic AMP and cyclic GMP. *Adv Cyclic Nucleotide Res* 10: 1-33, 1979.

Brostrom CO, Corbin JD, King CA and Krebs EG. Interaction of the subunits of adenosine 3':5'-cyclic monophosphate-dependent protein kinase of muscle. *Proc Natl Acad Sci U S A* 68(10): 2444-7, 1971.

Browner NC, Dey NB, Bloch KD and Lincoln TM. Regulation of cGMP-dependent protein kinase expression by soluble guanylyl cyclase in vascular smooth muscle cells. *J Biol Chem* 279(45): 46631-6, 2004.

Brunner F, Stessel H and Kukovetz WR. Novel guanylyl cyclase inhibitor, ODQ reveals role of nitric oxide, but not of cyclic GMP in endothelin-1 secretion. *FEBS Lett* 376(3): 262-6, 1995.

Bubis J, Neitzel JJ, Saraswat LD and Taylor SS. A point mutation abolishes binding of cAMP to site A in the regulatory subunit of cAMP-dependent protein kinase. *J Biol Chem* 263(20): 9668-73, 1988.

Bubis J and Taylor SS. Correlation of photolabeling with occupancy of cAMP binding sites in the regulatory subunit of cAMP-dependent protein kinase I. *Biochemistry* 26(12): 3478-86, 1987.

Burgoyne JR, Madhani M, Cuello F, Charles RL, Brennan JP, Schroder E, Browning DD and Eaton P. Cysteine redox sensor in PKGIa enables oxidant-induced activation. *Science* 317(5843): 1393-7, 2007.

Calderone A, Thaik CM, Takahashi N, Chang DL and Colucci WS. Nitric oxide, atrial natriuretic peptide, and cyclic GMP inhibit the growth-promoting effects of norepinephrine in cardiac myocytes and fibroblasts. *J Clin Invest* 101(4): 812-8, 1998.

Cary SP, Winger JA, Derbyshire ER and Marletta MA. Nitric oxide signaling: no longer simply on or off. *Trends Biochem Sci* 31(4): 231-9, 2006.

Castro LR, Verde I, Cooper DM and Fischmeister R. Cyclic guanosine monophosphate compartmentation in rat cardiac myocytes. *Circulation* 113(18): 2221-8, 2006.

Cawley SM, Sawyer CL, Brunelle KF, van der Vliet A and Dostmann WR. Nitric oxide-evoked transient kinetics of cyclic GMP in vascular smooth muscle cells. *Cell Signal* 19(5): 1023-33, 2007.

Cha B, Kim JH, Hut H, Hogema BM, Nadarja J, Zizak M, Cavet M, Lee-Kwon W, Lohmann SM, Smolenski A, Tse CM, Yun C, de Jonge HR and Donowitz M. cGMP inhibition of Na+/H+ antiporter 3 (NHE3) requires PDZ domain adapter NHERF2, a broad specificity protein kinase G-anchoring protein. *J Biol Chem* 280(17): 16642-50, 2005.

Chen L, Daum G, Chitaley K, Coats SA, Bowen-Pope DF, Eigenthaler M, Thumati NR, Walter U and Clowes AW. Vasodilator-stimulated phosphoprotein regulates proliferation and growth inhibition by nitric oxide in vascular smooth muscle cells. *Arterioscler Thromb Vasc Biol* 24(8): 1403-8, 2004.

Chinkers M and Garbers DL. The protein kinase domain of the ANP receptor is required for signaling. *Science* 245(4924): 1392-4, 1989.

Chu DM, Francis SH, Thomas JW, Maksymovitch EA, Fosler M and Corbin JD. Activation by autophosphorylation or cGMP binding produces a similar apparent conformational change in cGMP-dependent protein kinase. *J Biol Chem* 273(23): 14649-56, 1998.

Chusho H, Tamura N, Ogawa Y, Yasoda A, Suda M, Miyazawa T, Nakamura K, Nakao K, Kurihara T, Komatsu Y, Itoh H, Tanaka K, Saito Y, Katsuki M and Nakao K. Dwarfism and early death in mice lacking C-type natriuretic peptide. *Proc Natl Acad Sci U S A* 98(7): 4016-21, 2001.

Conti M and Beavo J. Biochemistry and physiology of cyclic nucleotide phosphodiesterases: essential components in cyclic nucleotide signaling. *Annu Rev Biochem* 76: 481-511, 2007.

Corbin JD, Blount MA, Weeks JL, 2nd, Beasley A, Kuhn KP, Ho YS, Saidi LF, Hurley JH, Kotera J and Francis SH. [3H]sildenafil binding to phosphodiesterase-5 is specific, kinetically heterogeneous, and stimulated by cGMP. *Mol Pharmacol* 63(6): 1364-72, 2003.

Corbin JD and Rannels SR. Perturbation and structural organization of the two intrachain cAMP binding sites of cAMP-dependent protein kinase II. *J Biol Chem* 256(22): 11671-6, 1981.

Corbin JD, Turko IV, Beasley A and Francis SH. Phosphorylation of phosphodiesterase-5 by cyclic nucleotide-dependent protein kinase alters its catalytic and allosteric cGMP-binding activities. *Eur J Biochem* 267(9): 2760-7, 2000.

de Bold AJ, Borenstein HB, Veress AT and Sonnenberg H. A rapid and potent natriuretic response to intravenous injection of atrial myocardial extract in rats. *Life Sci* 28(1): 89-94, 1981.

de Bold AJ, Ma KK, Zhang Y, de Bold ML, Bensimon M and Khoshbaten A. The physiological and pathophysiological modulation of the endocrine function of the heart. *Can J Physiol Pharmacol* 79(8): 705-14, 2001.

de Vente J, Asan E, Gambaryan S, Markerink-van Ittersum M, Axer H, Gallatz K, Lohmann SM and Palkovits M. Localization of cGMP-dependent protein kinase type II in rat brain. *Neuroscience* 108(1): 27-49, 2001.

Dietz JR. Mechanisms of atrial natriuretic peptide secretion from the atrium. *Cardiovasc Res* 68(1): 8-17, 2005.

Diller TC, Madhusudan, Xuong NH and Taylor SS. Molecular basis for regulatory subunit diversity in cAMP-dependent protein kinase: crystal structure of the type II beta regulatory subunit. *Structure* 9(1): 73-82, 2001.

Dimmeler S, Fleming I, Fisslthaler B, Hermann C, Busse R and Zeiher AM. Activation of nitric oxide synthase in endothelial cells by Akt-dependent phosphorylation. *Nature* 399(6736): 601-5, 1999.

Domino SE, Tubb DJ and Garbers DL. Assay of guanylyl cyclase catalytic activity. *Methods Enzymol* 195: 345-55, 1991.

Doskeland SO and Ogreid D. Ammonium sulfate precipitation assay for the study of cyclic nucleotide binding to proteins. *Methods Enzymol* 159: 147-50, 1988.

Doskeland SO, Vintermyr OK, Corbin JD and Ogreid D. Studies on the interactions between the cyclic nucleotide-binding sites of cGMP-dependent protein kinase. *J Biol Chem* 262(8): 3534-40, 1987.

Dostmann WR, Koep N and Endres R. The catalytic domain of the cGMP-dependent protein kinase Ialpha modulates the cGMP-binding characteristics of its regulatory domain. *FEBS Lett* 398(2-3): 206-10, 1996.

Dostmann WR, Taylor MS, Nickl CK, Brayden JE, Frank R and Tegge WJ. Highly specific, membrane-permeant peptide blockers of cGMP-dependent protein kinase Ialpha inhibit NO-induced cerebral dilation. *Proc Natl Acad Sci U S A* 97(26): 14772-7, 2000.

Dostmann WR and Taylor SS. Identifying the molecular switches that determine whether (Rp)-cAMPS functions as an antagonist or an agonist in the activation of cAMP-dependent protein kinase I. *Biochemistry* 30(35): 8710-6, 1991.

Dostmann WR, Taylor SS, Genieser HG, Jastorff B, Doskeland SO and Ogreid D. Probing the cyclic nucleotide binding sites of cAMP-dependent protein kinases I and II with analogs of adenosine 3',5'-cyclic phosphorothioates. *J Biol Chem* 265(18): 10484-91, 1990.

Earley S, Heppner TJ, Nelson MT and Brayden JE. TRPV4 forms a novel Ca2+ signaling complex with ryanodine receptors and BKCa channels. *Circ Res* 97(12): 1270-9, 2005.

el-Husseini AE, Bladen C and Vincent SR. Molecular characterization of a type II cyclic GMP-dependent protein kinase expressed in the rat brain. *J Neurochem* 64(6): 2814-7, 1995.

Erlichman J, Rubin CS and Rosen OM. Physical properties of a purified cyclic adenosine 3':5'-monophosphate-dependent protein kinase from bovine heart muscle. *J Biol Chem* 248(21): 7607-9, 1973.

Erwin PA, Lin AJ, Golan DE and Michel T. Receptor-regulated dynamic S-nitrosylation of endothelial nitric-oxide synthase in vascular endothelial cells. *J Biol Chem* 280(20): 19888-94, 2005.

Etter EF, Eto M, Wardle RL, Brautigan DL and Murphy RA. Activation of myosin light chain phosphatase in intact arterial smooth muscle during nitric oxide-induced relaxation. *J Biol Chem* 276(37): 34681-5, 2001.

Evgenov OV, Pacher P, Schmidt PM, Hasko G, Schmidt HH and Stasch JP. NO-independent stimulators and activators of soluble guanylate cyclase: discovery and therapeutic potential. *Nat Rev Drug Discov* 5(9): 755-68, 2006.

Feil R, Muller S and Hofmann F. High-level expression of functional cGMP-dependent protein kinase using the baculovirus system. *FEBS Lett* 336(1): 163-7, 1993.

Fischmeister R, Castro LR, Abi-Gerges A, Rochais F, Jurevicius J, Leroy J and Vandecasteele G. Compartmentation of cyclic nucleotide signaling in the heart: the role of cyclic nucleotide phosphodiesterases. *Circ Res* 99(8): 816-28, 2006.

Fitzpatrick DA, O'Halloran DM and Burnell AM. Multiple lineage specific expansions within the guanylyl cyclase gene family. *BMC Evol Biol* 6: 26, 2006.

Francis SH, Blount MA, Zoraghi R and Corbin JD. Molecular properties of mammalian proteins that interact with cGMP: protein kinases, cation channels, phosphodiesterases, and multi-drug anion transporters. *Front Biosci* 10: 2097-117, 2005.

Francis SH and Corbin JD. Structure and function of cyclic nucleotide-dependent protein kinases. *Annu Rev Physiol* 56: 237-72, 1994.

Francis SH and Corbin JD. Cyclic nucleotide-dependent protein kinases: intracellular receptors for cAMP and cGMP action. *Crit Rev Clin Lab Sci* 36(4): 275-328, 1999.

Francis SH, Noblett BD, Todd BW, Wells JN and Corbin JD. Relaxation of vascular and tracheal smooth muscle by cyclic nucleotide analogs that preferentially activate purified cGMP-dependent protein kinase. *Mol Pharmacol* 34(4): 506-17, 1988.

Friebe A, Mergia E, Dangel O, Lange A and Koesling D. Fatal gastrointestinal obstruction and hypertension in mice lacking nitric oxide-sensitive guanylyl cyclase. *Proc Natl Acad Sci U S A* 104(18): 7699-704, 2007.

Furchgott RF. Studies on relaxation of rabbit aorta by sodium nitrite: the basis for the proposal that the acid-activatable inhibitory factor from retractor penis is inorganic nitrite and the endothelium-derived relaxing factor is nitric oxide. Vasodilatation: Vascular Smooth Muscle, Peptides, Autonomic Nerves and Endothelium, ed. Vanhoutte, P.M. New York, Raven Press. 1988

Furchgott RF, Cherry PD, Zawadzki JV and Jothianandan D. Endothelial cells as mediators of vasodilation of arteries. *J Cardiovasc Pharmacol* 6 Suppl 2: S336-43, 1984.

Furchgott RF and Zawadzki JV. The obligatory role of endothelial cells in the relaxation of arterial smooth muscle by acetylcholine. *Nature* 288(5789): 373-6, 1980.

Gambaryan S, Geiger J, Schwarz UR, Butt E, Begonja A, Obergfell A and Walter U. Potent inhibition of human platelets by cGMP analogs independent of cGMP-dependent protein kinase. *Blood* 103(7): 2593-600, 2004.

Garbers DL. Guanylyl cyclase-linked receptors. *Pharmacol Ther* 50(3): 337-45, 1991.

Garbers DL and Lowe DG. Guanylyl cyclase receptors. *J Biol Chem* 269(49): 30741-4, 1994.

Gardner DG, Chen S, Glenn DJ and Grigsby CL. Molecular biology of the natriuretic peptide system: implications for physiology and hypertension. *Hypertension* 49(3): 419-26, 2007.

Garg UC and Hassid A. Nitric oxide-generating vasodilators and 8-bromo-cyclic guanosine monophosphate inhibit mitogenesis and proliferation of cultured rat vascular smooth muscle cells. *J Clin Invest* 83(5): 1774-7, 1989.

Garthwaite J. Dynamics of cellular NO-cGMP signaling. *Front Biosci* 10: 1868-80, 2005.

Garthwaite J, Southam E, Boulton CL, Nielsen EB, Schmidt K and Mayer B. Potent and selective inhibition of nitric oxide-sensitive guanylyl cyclase by 1H-[1,2,4]oxadiazolo[4,3-a]quinoxalin-1-one. *Mol Pharmacol* 48(2): 184-8, 1995.

Geiselhoringer A, Gaisa M, Hofmann F and Schlossmann J. Distribution of IRAG and cGKI-isoforms in murine tissues. *FEBS Lett* 575(1-3): 19-22, 2004.

Geiselhoringer A, Werner M, Sigl K, Smital P, Worner R, Acheo L, Stieber J, Weinmeister P, Feil R, Feil S, Wegener J, Hofmann F and Schlossmann J. IRAG is essential for relaxation of receptor-triggered smooth muscle contraction by cGMP kinase. *Embo J* 23(21): 4222-31, 2004.

Gill GN and Garren LD. Role of the receptor in the mechanism of action of adenosine 3':5'-cyclic monophosphate. *Proc Natl Acad Sci U S A* 68(4): 786-90, 1971.

Gill GN, Holdy KE, Walton GM and Kanstein CB. Purification and characterization of 3':5'-cyclic GMP-dependent protein kinase. *Proc Natl Acad Sci U S A* 73(11): 3918-22, 1976.

Gopal VK, Francis SH and Corbin JD. Allosteric sites of phosphodiesterase-5 (PDE5). A potential role in negative feedback regulation of cGMP signaling in corpus cavernosum. *Eur J Biochem* 268(11): 3304-12, 2001.

Gorman KB and Steinberg RA. Spectrum of spontaneous missense mutations causing cyclic AMP-resistance phenotypes in cultured S49 mouse lymphoma cells differs markedly from those of mutations induced by alkylating mutagens. *Somat Cell Mol Genet* 20(4): 301-11, 1994.

Griesbeck O, Baird GS, Campbell RE, Zacharias DA and Tsien RY. Reducing the environmental sensitivity of yellow fluorescent protein. Mechanism and applications. *J Biol Chem* 276(31): 29188-94, 2001.

Grynkiewicz G, Poenie M and Tsien RY. A new generation of Ca2+ indicators with greatly improved fluorescence properties. *J Biol Chem* 260(6): 3440-50, 1985.

Hamet P, Pang SC and Tremblay J. Atrial natriuretic factor-induced egression of cyclic guanosine 3':5'-monophosphate in cultured vascular smooth muscle and endothelial cells. *J Biol Chem* 264(21): 12364-9, 1989.

Hauser W, Knobeloch KP, Eigenthaler M, Gambaryan S, Krenn V, Geiger J, Glazova M, Rohde E, Horak I, Walter U and Zimmer M. Megakaryocyte hyperplasia and enhanced agonist-induced platelet activation in vasodilator-stimulated phosphoprotein knockout mice. *Proc Natl Acad Sci U S A* 96(14): 8120-5, 1999.

Herberg FW, Taylor SS and Dostmann WR. Active site mutations define the pathway for the cooperative activation of cAMP-dependent protein kinase. *Biochemistry* 35(9): 2934-42, 1996.

Hofmann F. The biology of cyclic GMP-dependent protein kinases. *J Biol Chem* 280(1): 1-4, 2005.

Hofmann F, Biel M and Kaupp UB. International Union of Pharmacology. LI. Nomenclature and structure-function relationships of cyclic nucleotide-regulated channels. *Pharmacol Rev* 57(4): 455-62, 2005.

Hofmann F, Gensheimer HP and Gobel C. cGMP-dependent protein kinase. Autophosphorylation changes the characteristics of binding site 1. *Eur J Biochem* 147(2): 361-5, 1985.

Honda A, Adams SR, Sawyer CL, Lev-Ram V, Tsien RY and Dostmann WR. Spatiotemporal dynamics of guanosine 3',5'-cyclic monophosphate revealed by a genetically encoded, fluorescent indicator. *Proc Natl Acad Sci U S A* 98(5): 2437-42, 2001.

Honda A, Moosmeier MA and Dostmann WR. Membrane-permeable cygnets: rapid cellular internalization of fluorescent cGMP-indicators. *Front Biosci* 10: 1290-301, 2005.

Honda A, Sawyer CL, Cawley SM and Dostmann WR. Cygnets: in vivo characterization of novel cGMP indicators and in vivo imaging of intracellular cGMP. *Methods Mol Biol* 307: 27-43, 2005.

Hwang TL, Wu CC and Teng CM. Comparison of two soluble guanylyl cyclase inhibitors, methylene blue and ODQ, on sodium nitroprusside-induced relaxation in guinea-pig trachea. *Br J Pharmacol* 125(6): 1158-63, 1998.

Ignarro LJ, Adams JB, Horwitz PM and Wood KS. Activation of soluble guanylate cyclase by NO-hemoproteins involves NO-heme exchange. Comparison of heme-containing and heme-deficient enzyme forms. *J Biol Chem* 261(11): 4997-5002, 1986.

Ignarro LJ, Byrns RE and Wood KS. Biochemical and pharmacological properties of endothelium-derived relaxing factor and its similarity to nitric oxide radical. Vasodilatation: Vascular Smooth Muscle, Peptide, Autonomic Nerves and Endothelium, ed. Vanhoutte, P.M. New York, Raven Press. 1988

Ignarro LJ, Wood KS and Wolin MS. Activation of purified soluble guanylate cyclase by protoporphyrin IX. *Proc Natl Acad Sci U S A* 79(9): 2870-3, 1982.

Iyer LM, Anantharaman V and Aravind L. Ancient conserved domains shared by animal soluble guanylyl cyclases and bacterial signaling proteins. *BMC Genomics* 4(1): 5, 2003.

Jancarik J and Kim SH. Sparse matrix sampling: a screening method for crystallization of proteins. *J Appl Cryst* 24: 409-411, 1991.

Ji G, Feldman ME, Deng KY, Greene KS, Wilson J, Lee JC, Johnston RC, Rishniw M, Tallini Y, Zhang J, Wier WG, Blaustein MP, Xin HB, Nakai J and Kotlikoff MI. Ca2+-sensing transgenic mice: postsynaptic signaling in smooth muscle. *J Biol Chem* 279(20): 21461-8, 2004.

John SW, Veress AT, Honrath U, Chong CK, Peng L, Smithies O and Sonnenberg H. Blood pressure and fluid-electrolyte balance in mice with reduced or absent ANP. *Am J Physiol* 271(1 Pt 2): R109-14, 1996.

Joubert S, McNicoll N and De Lean A. Biochemical and pharmacological characterization of P-site inhibitors on homodimeric guanylyl cyclase domain from natriuretic peptide receptor-A. *Biochem Pharmacol* 73(7): 954-63, 2007.

Kangawa K and Matsuo H. Purification and complete amino acid sequence of alpha-human atrial natriuretic polypeptide (alpha-hANP). *Biochem Biophys Res Commun* 118(1): 131-9, 1984.

Kass DA, Takimoto E, Nagayama T and Champion HC. Phosphodiesterase regulation of nitric oxide signaling. *Cardiovasc Res* 75(2): 303-14, 2007.

Kemp BE, Bylund DB, Huang TS and Krebs EG. Substrate specificity of the cyclic AMP-dependent protein kinase. *Proc Natl Acad Sci U S A* 72(9): 3448-52, 1975.

Kim C, Cheng CY, Saldanha SA and Taylor SS. PKA-I holoenzyme structure reveals a mechanism for cAMP-dependent activation. *Cell* 130(6): 1032-43, 2007.

Kim C, Xuong NH and Taylor SS. Crystal structure of a complex between the catalytic and regulatory (RIalpha) subunits of PKA. *Science* 307(5710): 690-6, 2005.

Kinderman FS, Kim C, von Daake S, Ma Y, Pham BQ, Spraggon G, Xuong NH, Jennings PA and Taylor SS. A dynamic mechanism for AKAP binding to RII isoforms of cAMP-dependent protein kinase. *Mol Cell* 24(3): 397-408, 2006.

Knighton DR, Zheng JH, Ten Eyck LF, Ashford VA, Xuong NH, Taylor SS and Sowadski JM. Crystal structure of the catalytic subunit of cyclic adenosine monophosphate-dependent protein kinase. *Science* 253(5018): 407-14, 1991.

Koller A, Schlossmann J, Ashman K, Uttenweiler-Joseph S, Ruth P and Hofmann F. Association of phospholamban with a cGMP kinase signaling complex. *Biochem Biophys Res Commun* 300(1): 155-60, 2003.

Koller KJ, de Sauvage FJ, Lowe DG and Goeddel DV. Conservation of the kinaselike regulatory domain is essential for activation of the natriuretic peptide receptor guanylyl cyclases. *Mol Cell Biol* 12(6): 2581-90, 1992.

Kotera J, Grimes KA, Corbin JD and Francis SH. cGMP-dependent protein kinase protects cGMP from hydrolysis by phosphodiesterase-5. *Biochem J* 372(Pt 2): 419-26, 2003.

Kou R, Greif D and Michel T. Dephosphorylation of endothelial nitric-oxide synthase by vascular endothelial growth factor. Implications for the vascular responses to cyclosporin A. *J Biol Chem* 277(33): 29669-73, 2002.

Kuhn M. Cardiac and intestinal natriuretic peptides: insights from genetically modified mice. *Peptides* 26(6): 1078-85, 2005.

Landgraf W and Hofmann F. The amino terminus regulates binding to and activation of cGMP-dependent protein kinase. *Eur J Biochem* 181(3): 643-50, 1989.

Landgraf W, Hofmann F, Pelton JT and Huggins JP. Effects of cyclic GMP on the secondary structure of cyclic GMP dependent protein kinase and analysis of the enzyme's amino-terminal domain by far-ultraviolet circular dichroism. *Biochemistry* 29(42): 9921-8, 1990.

Landgraf W, Regulla S, Meyer HE and Hofmann F. Oxidation of cysteines activates cGMP-dependent protein kinase. *J Biol Chem* 266(25): 16305-11, 1991.

Leitman DC, Andresen JW, Catalano RM, Waldman SA, Tuan JJ and Murad F. Atrial natriuretic peptide binding, cross-linking, and stimulation of cyclic GMP accumulation and particulate guanylate cyclase activity in cultured cells. *J Biol Chem* 263(8): 3720-8, 1988.

Leroy MJ, Degerman E, Taira M, Murata T, Wang LH, Movsesian MA, Meacci E and Manganiello VC. Characterization of two recombinant PDE3 (cGMP-inhibited cyclic nucleotide phosphodiesterase) isoforms, RcGIP1 and HcGIP2, expressed in NIH 3006 murine fibroblasts and Sf9 insect cells. *Biochemistry* 35(31): 10194-202, 1996.

Lin CS, Lin G, Xin ZC and Lue TF. Expression, distribution and regulation of phosphodiesterase 5. *Curr Pharm Des* 12(27): 3439-57, 2006.

Lincoln TM, Dills WL, Jr. and Corbin JD. Purification and subunit composition of guanosine 3':5'-monophosphate-dependent protein kinase from bovine lung. *J Biol Chem* 252(12): 4269-75, 1977.

Liu Y, Ruoho AE, Rao VD and Hurley JH. Catalytic mechanism of the adenylyl and guanylyl cyclases: modeling and mutational analysis. *Proc Natl Acad Sci U S A* 94(25): 13414-9, 1997.

Lopez MJ, Wong SK, Kishimoto I, Dubois S, Mach V, Friesen J, Garbers DL and Beuve A. Salt-resistant hypertension in mice lacking the guanylyl cyclase-A receptor for atrial natriuretic peptide. *Nature* 378(6552): 65-8, 1995.

Ma X, Sayed N, Beuve A and van den Akker F. NO and CO differentially activate soluble guanylyl cyclase via a heme pivot-bend mechanism. *Embo J* 26(2): 578-88, 2007.

MacMillan-Crow LA and Lincoln TM. High-affinity binding and localization of the cyclic GMP-dependent protein kinase with the intermediate filament protein vimentin. *Biochemistry* 33(26): 8035-43, 1994.

Marshall SJ, Senis YA, Auger JM, Feil R, Hofmann F, Salmon G, Peterson JT, Burslem F and Watson SP. GPIb-dependent platelet activation is dependent on Src kinases but not MAP kinase or cGMP-dependent kinase. *Blood* 103(7): 2601-9, 2004.

Massberg S, Gruner S, Konrad I, Garcia Arguinzonis MI, Eigenthaler M, Hemler K, Kersting J, Schulz C, Muller I, Besta F, Nieswandt B, Heinzmann U, Walter U and Gawaz M. Enhanced in vivo platelet adhesion in vasodilator-stimulated phosphoprotein (VASP)-deficient mice. *Blood* 103(1): 136-42, 2004.

Massberg S, Sausbier M, Klatt P, Bauer M, Pfeifer A, Siess W, Fassler R, Ruth P, Krombach F and Hofmann F. Increased adhesion and aggregation of platelets lacking cyclic guanosine 3',5'-monophosphate kinase I. *J Exp Med* 189(8): 1255-64, 1999.

Mayer B and Koesling D. cGMP signalling beyond nitric oxide. *Trends Pharmacol Sci* 22(11): 546-8, 2001.

Mergia E, Friebe A, Dangel O, Russwurm M and Koesling D. Spare guanylyl cyclase NO receptors ensure high NO sensitivity in the vascular system. *J Clin Invest* 116(6): 1731-7, 2006.

Miyazawa T, Ogawa Y, Chusho H, Yasoda A, Tamura N, Komatsu Y, Pfeifer A, Hofmann F and Nakao K. Cyclic GMP-dependent protein kinase II plays a critical role in C-type natriuretic peptide-mediated endochondral ossification. *Endocrinology* 143(9): 3604-10, 2002.

Mo E, Amin H, Bianco IH and Garthwaite J. Kinetics of a cellular nitric oxide/cGMP/phosphodiesterase-5 pathway. *J Biol Chem* 279(25): 26149-58, 2004.

Moncada S, Palmer RM and Higgs EA. Nitric oxide: physiology, pathophysiology, and pharmacology. *Pharmacol Rev* 43(2): 109-42, 1991.

Mongillo M, Tocchetti CG, Terrin A, Lissandron V, Cheung YF, Dostmann WR, Pozzan T, Kass DA, Paolocci N, Houslay MD and Zaccolo M. Compartmentalized phosphodiesterase-2 activity blunts beta-adrenergic cardiac inotropy via an NO/cGMP-dependent pathway. *Circ Res* 98(2): 226-34, 2006.

Monken CE and Gill GN. Structural analysis of cGMP-dependent protein kinase using limited proteolysis. *J Biol Chem* 255(15): 7067-70, 1980.

Moosmang S, Schulla V, Welling A, Feil R, Feil S, Wegener JW, Hofmann F and Klugbauer N. Dominant role of smooth muscle L-type calcium channel Cav1.2 for blood pressure regulation. *Embo J* 22(22): 6027-34, 2003.

Mullershausen F, Koesling D and Friebe A. NO-sensitive guanylyl cyclase and NO-induced feedback inhibition in cGMP signaling. *Front Biosci* 10: 1269-78, 2005.

Mullershausen F, Russwurm M, Thompson WJ, Liu L, Koesling D and Friebe A. Rapid nitric oxide-induced desensitization of the cGMP response is caused by increased activity of phosphodiesterase type 5 paralleled by phosphorylation of the enzyme. *J Cell Biol* 155(2): 271-8, 2001.

Murphy CS and Steinberg RA. Hotspots for spontaneous and mutagen-induced lesions in regulatory subunit of cyclic AMP-dependent protein kinase in S49 mouse lymphoma cells. *Somat Cell Mol Genet* 11(6): 605-15, 1985.

Nakai J, Ohkura M and Imoto K. A high signal-to-noise Ca(2+) probe composed of a single green fluorescent protein. *Nat Biotechnol* 19(2): 137-41, 2001.

Neitzel JJ, Dostmann WR and Taylor SS. Role of MgATP in the activation and reassociation of cAMP-dependent protein kinase I: consequences of replacing the essential arginine in cAMP binding site A. *Biochemistry* 30(3): 733-9, 1991.

Newlon MG, Roy M, Morikis D, Carr DW, Westphal R, Scott JD and Jennings PA. A novel mechanism of PKA anchoring revealed by solution structures of anchoring complexes. *Embo J* 20(7): 1651-62, 2001.

Nikolaev VO, Gambaryan S and Lohse MJ. Fluorescent sensors for rapid monitoring of intracellular cGMP. *Nat Methods* 3(1): 23-5, 2006.

Ogreid D and Doskeland SO. Protein kinase II has two distinct binding sites for cyclic AMP, only one of which is detectable by the conventional membrane-filtration method. *FEBS Lett* 121(2): 340-4, 1980.

Ogreid D and Doskeland SO. The kinetics of association of cyclic AMP to the two types of binding sites associated with protein kinase II from bovine myocardium. *FEBS Lett* 129(2): 287-92, 1981.

Ogreid D and Doskeland SO. Cyclic nucleotides modulate the release of [3H] adenosine cyclic 3',5'-phosphate bound to the regulatory moiety of protein kinase I by the catalytic subunit of the kinase. *Biochemistry* 22(7): 1686-96, 1983.

Ogreid D, Doskeland SO, Gorman KB and Steinberg RA. Mutations that prevent cyclic nucleotide binding to binding sites A or B of type I cyclic AMP-dependent protein kinase. *J Biol Chem* 263(33): 17397-404, 1988.

Ogreid D, Doskeland SO and Miller JP. Evidence that cyclic nucleotides activating rabbit muscle protein kinase I interact with both types of cAMP binding sites associated with the enzyme. *J Biol Chem* 258(2): 1041-9, 1983.

Okada D and Asakawa S. Allosteric activation of cGMP-specific, cGMP-binding phosphodiesterase (PDE5) by cGMP. *Biochemistry* 41(30): 9672-9, 2002.

Olesen SP, Drejer J, Axelsson O, Moldt P, Bang L, Nielsen-Kudsk JE, Busse R and Mulsch A. Characterization of NS 2028 as a specific inhibitor of soluble guanylyl cyclase. *Br J Pharmacol* 123(2): 299-309, 1998.

Olivera A and Spiegel S. Sphingosine-1-phosphate as second messenger in cell proliferation induced by PDGF and FCS mitogens. *Nature* 365(6446): 557-60, 1993.

Ormo M, Cubitt AB, Kallio K, Gross LA, Tsien RY and Remington SJ. Crystal structure of the Aequorea victoria green fluorescent protein. *Science* 273(5280): 1392-5, 1996.

Palmer RM, Ashton DS and Moncada S. Vascular endothelial cells synthesize nitric oxide from L-arginine. *Nature* 333(6174): 664-6, 1988.

Pellicena P, Karow DS, Boon EM, Marletta MA and Kuriyan J. Crystal structure of an oxygen-binding heme domain related to soluble guanylate cyclases. *Proc Natl Acad Sci U S A* 101(35): 12854-9, 2004.

Pfeifer A, Aszodi A, Seidler U, Ruth P, Hofmann F and Fassler R. Intestinal secretory defects and dwarfism in mice lacking cGMP-dependent protein kinase II. *Science* 274(5295): 2082-6, 1996.

Pfeifer A, Ruth P, Dostmann W, Sausbier M, Klatt P and Hofmann F. Structure and function of cGMP-dependent protein kinases. *Rev Physiol Biochem Pharmacol* 135: 105-49, 1999.

Piggott LA, Hassell KA, Berkova Z, Morris AP, Silberbach M and Rich TC. Natriuretic peptides and nitric oxide stimulate cGMP synthesis in different cellular compartments. *J Gen Physiol* 128(1): 3-14, 2006.

Pilz RB and Casteel DE. Regulation of gene expression by cyclic GMP. *Circ Res* 93(11): 1034-46, 2003.

Pinkse MW, Heck AJ, Rumpel K and Pullen F. Probing noncovalent protein-ligand interactions of the cGMP-dependent protein kinase using electrospray ionization time of flight mass spectrometry. *J Am Soc Mass Spectrom* 15(10): 1392-9, 2004.

Porter VA, Bonev AD, Knot HJ, Heppner TJ, Stevenson AS, Kleppisch T, Lederer WJ and Nelson MT. Frequency modulation of Ca2+ sparks is involved in regulation of arterial diameter by cyclic nucleotides. *Am J Physiol* 274(5 Pt 1): C1346-55, 1998.

Rabanal F. Use of 2,2'-(5-nirtopyridine) for the Heterodimerization of Cystein Containing Peptides. Introduction of the 5-nitro-2- pyridinesulfenyl Group. *Tetrahedron Lett* 37: 1347-1350, 2003.

Rannels SR and Corbin JD. Two different intrachain cAMP binding sites of cAMP-dependent protein kinases. *J Biol Chem* 255(15): 7085-8, 1980.

Reed RB, Sandberg M, Jahnsen T, Lohmann SM, Francis SH and Corbin JD. Fast and slow cyclic nucleotide-dissociation sites in cAMP-dependent protein kinase are transposed in type Ibeta cGMP-dependent protein kinase. *J Biol Chem* 271(29): 17570-5, 1996.

Reimann EM, Brostrom CO, Corbin JD, King CA and Krebs EG. Separation of regulatory and catalytic subunits of the cyclic 3',5'-adenosine monophosphate-dependent protein kinase(s) of rabbit skeletal muscle. *Biochem Biophys Res Commun* 42(2): 187-94, 1971.

Richie-Jannetta R, Busch JL, Higgins KA, Corbin JD and Francis SH. Isolated regulatory domains of cGMP-dependent protein kinase Ialpha and Ibeta retain dimerization and native cGMP-binding properties and undergo isoform-specific conformational changes. *J Biol Chem* 281(11): 6977-84, 2006.

Robertson BE, Schubert R, Hescheler J and Nelson MT. cGMP-dependent protein kinase activates Ca-activated K channels in cerebral artery smooth muscle cells. *Am J Physiol* 265(1 Pt 1): C299-303, 1993.

Roy B and Garthwaite J. Nitric oxide activation of guanylyl cyclase in cells revisited. *Proc Natl Acad Sci U S A* 103(32): 12185-90, 2006.

Ruskoaho H. Atrial natriuretic peptide: synthesis, release, and metabolism. *Pharmacol Rev* 44(4): 479-602, 1992.

Russwurm M, Mullershausen F, Friebe A, Jager R, Russwurm C and Koesling D. Design of fluorescence resonance energy transfer (FRET)-based cGMP indicators: a systematic approach. *Biochem J* 407(1): 69-77, 2007.

Ruth P, Landgraf W, Keilbach A, May B, Egleme C and Hofmann F. The activation of expressed cGMP-dependent protein kinase isozymes I alpha and I beta is determined by the different amino-termini. *Eur J Biochem* 202(3): 1339-44, 1991.

Ruth P, Pfeifer A, Kamm S, Klatt P, Dostmann WR and Hofmann F. Identification of the amino acid sequences responsible for high affinity activation of cGMP kinase Ialpha. *J Biol Chem* 272(16): 10522-8, 1997.

Rybalkin SD, Rybalkina IG, Shimizu-Albergine M, Tang XB and Beavo JA. PDE5 is converted to an activated state upon cGMP binding to the GAF A domain. *Embo J* 22(3): 469-78, 2003.

Sausbier M, Schubert R, Voigt V, Hirneiss C, Pfeifer A, Korth M, Kleppisch T, Ruth P and Hofmann F. Mechanisms of NO/cGMP-dependent vasorelaxation. *Circ Res* 87(9): 825-30, 2000.

Schindler U, Strobel H, Schonafinger K, Linz W, Lohn M, Martorana PA, Rutten H, Schindler PW, Busch AE, Sohn M, Topfer A, Pistorius A, Jannek C and Mulsch A. Biochemistry and pharmacology of novel anthranilic acid derivatives activating heme-oxidized soluble guanylyl cyclase. *Mol Pharmacol* 69(4): 1260-8, 2006.

Schnell JR, Zhou GP, Zweckstetter M, Rigby AC and Chou JJ. Rapid and accurate structure determination of coiled-coil domains using NMR dipolar couplings: application to cGMP-dependent protein kinase Ialpha. *Protein Sci* 14(9): 2421-8, 2005.

Scholten A, Fuss H, Heck AJ and Dostmann WR. The hinge region operates as a stability switch in cGMP-dependent protein kinase I alpha. *Febs J* 274(9): 2274-86, 2007.

Schrammel A, Behrends S, Schmidt K, Koesling D and Mayer B. Characterization of 1H-[1,2,4]oxadiazolo[4,3-a]quinoxalin-1-one as a heme-site inhibitor of nitric oxide-sensitive guanylyl cyclase. *Mol Pharmacol* 50(1): 1-5, 1996.

Scott JD. Cyclic nucleotide-dependent protein kinases. *Pharmacol Ther* 50(1): 123-45, 1991.

Smith JA, Francis SH, Walsh KA, Kumar S and Corbin JD. Autophosphorylation of type Ibeta cGMP-dependent protein kinase increases basal catalytic activity and enhances allosteric activation by cGMP or cAMP. *J Biol Chem* 271(34): 20756-62, 1996.

Somlyo AP and Somlyo AV. Ca2+ sensitivity of smooth muscle and nonmuscle myosin II: modulated by G proteins, kinases, and myosin phosphatase. *Physiol Rev* 83(4): 1325-58, 2003.

Stasch JP, Schmidt PM, Nedvetsky PI, Nedvetskaya TY, H SA, Meurer S, Deile M, Taye A, Knorr A, Lapp H, Muller H, Turgay Y, Rothkegel C, Tersteegen A, Kemp-Harper B, Muller-Esterl W and Schmidt HH. Targeting the heme-oxidized nitric oxide receptor for selective vasodilatation of diseased blood vessels. *J Clin Invest* 116(9): 2552-61, 2006.

Steinberg RA, Gorman KB, Ogreid D, Doskeland SO and Weber IT. Mutations that alter the charge of type I regulatory subunit and modify activation properties of cyclic AMP-dependent protein kinase from S49 mouse lymphoma cells. *J Biol Chem* 266(6): 3547-53, 1991.

Steinberg RA, Russell JL, Murphy CS and Yphantis DA. Activation of type I cyclic AMP-dependent protein kinases with defective cyclic AMP-binding sites. *J Biol Chem* 262(6): 2664-71, 1987.

Steinhelper ME, Cochrane KL and Field LJ. Hypotension in transgenic mice expressing atrial natriuretic factor fusion genes. *Hypertension* 16(3): 301-7, 1990.

Su Y, Dostmann WR, Herberg FW, Durick K, Xuong NH, Ten Eyck L, Taylor SS and Varughese KI. Regulatory subunit of protein kinase A: structure of deletion mutant with cAMP binding domains. *Science* 269(5225): 807-13, 1995.

Sudoh T, Kangawa K, Minamino N and Matsuo H. A new natriuretic peptide in porcine brain. *Nature* 332(6159): 78-81, 1988.

Surks HK, Mochizuki N, Kasai Y, Georgescu SP, Tang KM, Ito M, Lincoln TM and Mendelsohn ME. Regulation of myosin phosphatase by a specific interaction with cGMP- dependent protein kinase Ialpha. *Science* 286(5444): 1583-7, 1999.

Tahallah N, Pinkse M, Maier CS and Heck AJ. The effect of the source pressure on the abundance of ions of noncovalent protein assemblies in an electrospray ionization orthogonal time-of-flight instrument. *Rapid Commun Mass Spectrom* 15(8): 596-601, 2001.

Takimoto E, Belardi D, Tocchetti CG, Vahebi S, Cormaci G, Ketner EA, Moens AL, Champion HC and Kass DA. Compartmentalization of cardiac beta-adrenergic inotropy modulation by phosphodiesterase type 5. *Circulation* 115(16): 2159-67, 2007.

Takimoto E, Champion HC, Belardi D, Moslehi J, Mongillo M, Mergia E, Montrose DC, Isoda T, Aufiero K, Zaccolo M, Dostmann WR, Smith CJ and Kass DA. cGMP catabolism by phosphodiesterase 5A regulates cardiac adrenergic stimulation by NOS3-dependent mechanism. *Circ Res* 96(1): 100-9, 2005.

Takio K, Wade RD, Smith SB, Krebs EG, Walsh KA and Titani K. Guanosine cyclic 3',5'-phosphate dependent protein kinase, a chimeric protein homologous with two separate protein families. *Biochemistry* 23(18): 4207-18, 1984.

Tallini YN, Ohkura M, Choi BR, Ji G, Imoto K, Doran R, Lee J, Plan P, Wilson J, Xin HB, Sanbe A, Gulick J, Mathai J, Robbins J, Salama G, Nakai J and Kotlikoff MI. Imaging cellular signals in the heart in vivo: Cardiac expression of the high-signal Ca2+ indicator GCaMP2. *Proc Natl Acad Sci U S A* 103(12): 4753-8, 2006.

Tamura N, Doolittle LK, Hammer RE, Shelton JM, Richardson JA and Garbers DL. Critical roles of the guanylyl cyclase B receptor in endochondral ossification and development of female reproductive organs. *Proc Natl Acad Sci U S A* 101(49): 17300-5, 2004.

Tang DD, Turner CE and Gunst SJ. Expression of non-phosphorylatable paxillin mutants in canine tracheal smooth muscle inhibits tension development. *J Physiol* 553(Pt 1): 21-35, 2003.

Taylor MK and Uhler MD. The amino-terminal cyclic nucleotide binding site of the type II cGMP-dependent protein kinase is essential for full cyclic nucleotide-dependent activation. *J Biol Chem* 275(36): 28053-62, 2000.

Taylor MS, Okwuchukwuasanya C, Nickl CK, Tegge W, Brayden JE and Dostmann WR. Inhibition of cGMP-dependent protein kinase by the cell-permeable peptide DT-2 reveals a novel mechanism of vasoregulation. *Mol Pharmacol* 65(5): 1111-9, 2004.

Taylor SS, Kim C, Vigil D, Haste NM, Yang J, Wu J and Anand GS. Dynamics of signaling by PKA. *Biochim Biophys Acta* 1754(1-2): 25-37, 2005.

Taylor SS and Stafford PH. Characterization of adenosine 3':5'-monophosphate-dependent protein kinase and its dissociated subunits from porcine skeletal muscle. *J Biol Chem* 253(7): 2284-7, 1978.

Thomas MK, Francis SH and Corbin JD. Substrate- and kinase-directed regulation of phosphorylation of a cGMP-binding phosphodiesterase by cGMP. *J Biol Chem* 265(25): 14971-8, 1990.

Tischkau SA, Weber ET, Abbott SM, Mitchell JW and Gillette MU. Circadian clock-controlled regulation of cGMP-protein kinase G in the nocturnal domain. *J Neurosci* 23(20): 7543-50, 2003.

Trivedi B and Kramer RH. Real-time patch-cram detection of intracellular cGMP reveals long-term suppression of responses to NO and muscarinic agonists. *Neuron* 21(4): 895-906, 1998.

Turko IV, Ballard SA, Francis SH and Corbin JD. Inhibition of cyclic GMP-binding cyclic GMP-specific phosphodiesterase (Type 5) by sildenafil and related compounds. *Mol Pharmacol* 56(1): 124-30, 1999.

Turko IV, Francis SH and Corbin JD. Binding of cGMP to both allosteric sites of cGMP-binding cGMP-specific phosphodiesterase (PDE5) is required for its phosphorylation. *Biochem J* 329 (Pt 3): 505-10, 1998.

Vaandrager AB, Bot AG, Ruth P, Pfeifer A, Hofmann F and De Jonge HR. Differential role of cyclic GMP-dependent protein kinase II in ion transport in murine small intestine and colon. *Gastroenterology* 118(1): 108-14, 2000.

Vaandrager AB, Smolenski A, Tilly BC, Houtsmuller AB, Ehlert EM, Bot AG, Edixhoven M, Boomaars WE, Lohmann SM and de Jonge HR. Membrane targeting of cGMP-dependent protein kinase is required for cystic fibrosis transmembrane conductance regulator Cl- channel activation. *Proc Natl Acad Sci U S A* 95(4): 1466-71, 1998.

Vaandrager AB, Tilly BC, Smolenski A, Schneider-Rasp S, Bot AG, Edixhoven M, Scholte BJ, Jarchau T, Walter U, Lohmann SM, Poller WC and de Jonge HR. cGMP stimulation of cystic fibrosis transmembrane conductance regulator Cl- channels co-expressed with cGMP-dependent protein kinase type II but not type Ibeta. *J Biol Chem* 272(7): 4195-200, 1997.

Wall ME, Francis SH, Corbin JD, Grimes K, Richie-Jannetta R, Kotera J, Macdonald BA, Gibson RR and Trewhella J. Mechanisms associated with cGMP binding and activation of cGMP-dependent protein kinase. *Proc Natl Acad Sci U S A* 100(5): 2380-5, 2003.

Weber IT, Shabb JB and Corbin JD. Predicted structures of the cGMP binding domains of the cGMP-dependent protein kinase: a key alanine/threonine difference in evolutionary divergence of cAMP and cGMP binding sites. *Biochemistry* 28(14): 6122-7, 1989.

Weber IT, Steitz TA, Bubis J and Taylor SS. Predicted structures of cAMP binding domains of type I and II regulatory subunits of cAMP-dependent protein kinase. *Biochemistry* 26(2): 343-51, 1987.

Werner C, Raivich G, Cowen M, Strekalova T, Sillaber I, Buters JT, Spanagel R and Hofmann F. Importance of NO/cGMP signalling via cGMP-dependent protein kinase II for controlling emotionality and neurobehavioural effects of alcohol. *Eur J Neurosci* 20(12): 3498-506, 2004.

Wilson EM and Chinkers M. Identification of sequences mediating guanylyl cyclase dimerization. *Biochemistry* 34(14): 4696-701, 1995.

Winger JA and Marletta MA. Expression and characterization of the catalytic domains of soluble guanylate cyclase: interaction with the heme domain. *Biochemistry* 44(10): 4083-90, 2005.

Winquist RJ, Faison EP, Waldman SA, Schwartz K, Murad F and Rapoport RM. Atrial natriuretic factor elicits an endothelium-independent relaxation and activates particulate guanylate cyclase in vascular smooth muscle. *Proc Natl Acad Sci U S A* 81(23): 7661-4, 1984.

Wolfe L, Corbin JD and Francis SH. Characterization of a novel isozyme of cGMP-dependent protein kinase from bovine aorta. *J Biol Chem* 264(13): 7734-41, 1989.

Wolfe L, Francis SH and Corbin JD. Properties of a cGMP-dependent monomeric protein kinase from bovine aorta. *J Biol Chem* 264(7): 4157-62, 1989.

Woodford TA, Correll LA, McKnight GS and Corbin JD. Expression and characterization of mutant forms of the type I regulatory subunit of cAMP-dependent protein kinase. The effect of defective cAMP binding on holoenzyme activation. *J Biol Chem* 264(22): 13321-8, 1989.

Wu J, Jones JM, Nguyen-Huu X, Ten Eyck LF and Taylor SS. Crystal structures of RIalpha subunit of cyclic adenosine 5'-monophosphate (cAMP)-dependent protein kinase complexed with (Rp)-adenosine 3',5'-cyclic monophosphothioate and (Sp)-adenosine 3',5'-cyclic monophosphothioate, the phosphothioate analogues of cAMP. *Biochemistry* 43(21): 6620-9, 2004.

Yamahara K, Itoh H, Chun TH, Ogawa Y, Yamashita J, Sawada N, Fukunaga Y, Sone M, Yurugi-Kobayashi T, Miyashita K, Tsujimoto H, Kook H, Feil R, Garbers DL, Hofmann F and Nakao K. Significance and therapeutic potential of the natriuretic peptides/cGMP/cGMP-dependent protein kinase pathway in vascular regeneration. *Proc Natl Acad Sci U S A* 100(6): 3404-9, 2003.

Yao A and Wang DH. Heterogeneity of adenovirus-mediated gene transfer in cultured thoracic aorta and renal artery of rats. *Hypertension* 26(6 Pt 2): 1046-50, 1995.

Zabel U, Weeger M, La M and Schmidt HH. Human soluble guanylate cyclase: functional expression and revised isoenzyme family. *Biochem J* 335 (Pt 1): 51-7, 1998.

Zawadzki KM and Taylor SS. cAMP-dependent protein kinase regulatory subunit type IIbeta: active site mutations define an isoform-specific network for allosteric signaling by cAMP. *J Biol Chem* 279(8): 7029-36, 2004.

Zhang W, Wu Y, Du L, Tang DD and Gunst SJ. Activation of the Arp2/3 complex by N-WASp is required for actin polymerization and contraction in smooth muscle. *Am J Physiol Cell Physiol* 288(5): C1145-60, 2005.

Zhao J, Trewhella J, Corbin J, Francis S, Mitchell R, Brushia R and Walsh D. Progressive cyclic nucleotide-induced conformational changes in the cGMP-dependent protein kinase studied by small angle X-ray scattering in solution. *J Biol Chem* 272(50): 31929-36, 1997.

Zhao Y, Brandish PE, Ballou DP and Marletta MA. A molecular basis for nitric oxide sensing by soluble guanylate cyclase. *Proc Natl Acad Sci U S A* 96(26): 14753-8, 1999.

Zhao Y, Brandish PE, DiValentin M, Schelvis JP, Babcock GT and Marletta MA. Inhibition of soluble guanylate cyclase by ODQ. *Biochemistry* 39(35): 10848-54, 2000.

Zoraghi R, Bessay EP, Corbin JD and Francis SH. Structural and functional features in human PDE5A1 regulatory domain that provide for allosteric cGMP binding, dimerization, and regulation. *J Biol Chem* 280(12): 12051-63, 2005.